Journal of Medicinal Chemistry

Article

A Conformational Restriction Strategy for the Identification of a Highly Selective Pyrimido-Pyrrolo-Oxazine mTOR Inhibitor

Chiara Borsari, Denise Rageot, Alix Dall'Asen, Thomas Bohnacker, Anna Melone, Alexander Markus Sele, Eileen Jackson, Jean-Baptiste Langlois, Florent Beaufils, Paul Hebeisen, Doriano Fabbro, Petra Hillmann, and Matthias P. Wymann

J. Med. Chem., **Just Accepted Manuscript** • DOI: 10.1021/acs.jmedchem.9b00972 • Publication Date (Web): 29 Aug 2019

A Conformational Restriction Strategy for the Identification of a Highly Selective Pyrimido-Pyrrolo-Oxazine mTOR Inhibitor

Chiara Borsari,[†] Denise Rageot,[†] Alix Dall'Asen,[‡] Thomas Bohnacker,[†] Anna Melone,[†] Alexander M. Sele,[†] Eileen Jackson,[†] Jean-Baptiste Langlois,[†] Florent Beaufils,[‡] Paul Hebeisen,[‡] Doriano Fabbro,[‡] Petra Hillmann,[‡] Matthias P. Wymann[†*]

[†]Department of Biomedicine, University of Basel, Mattenstrasse 28, 4058 Basel, Switzerland

[‡]PIQUR Therapeutics AG, Hochbergerstrasse 60, 4057 Basel, Switzerland

*Correspondence to: matthias.wymann@unibas.ch, Dept. Biomedicine, University of Basel, Mattenstrasse 28, 4058 Basel, Switzerland; Tel. +41 61 207 5046; Fax. +41 61 207 3566

KEYWORDS

Conformational restriction strategy; tricyclic pyrimido-pyrrolo-oxazines; mammalian or mechanistic target of rapamycin (mTOR); mTOR kinase inhibitors; ATP-competitive; pharmacokinetic studies; cancer.

ABSTRACT

The mechanistic target of rapamycin (mTOR) plays a pivotal role in growth and tumor progression and is an attractive target for cancer treatment. ATP-competitive mTOR kinase inhibitors (TORKi) have the potential to overcome limitations of rapamycin-derivatives in a wide range of malignancies. Herein, we exploit a conformational restriction approach to explore a novel chemical space for the generation of TORKi. Structure Activity Relationship (SAR) studies led to the identification of compound **12b** with a ~450-fold selectivity for mTOR over class I PI3K isoforms. Pharmacokinetic studies in male Sprague Dawley rats highlighted a good exposure after oral dosing and a minimum brain penetration. CYP450 reactive phenotyping pointed out the high metabolic stability of **12b**. These results identify the tricyclic pyrimido-pyrrolo-oxazine moiety as a novel scaffold for the development of highly selective mTOR inhibitors for cancer treatment.

INTRODUCTION

The mechanistic target of rapamycin (mTOR, also mammalian TOR) is a key signaling node in the phosphoinositide 3-kinase (PI3K)/mTOR signaling pathway and operates downstream of PI3K. mTOR is a serine/threonine protein kinase and is part of two functionally distinct multiprotein complexes, mammalian target of rapamycin complex 1 (mTORC1) and mammalian target of rapamycin complex 2 (mTORC2).[1,2] TORC1 integrates inputs from cell surface receptors, cellular energy, stress levels, availability of oxygen and amino acids. Cell surface receptors activate PI3K to produce PtdIns(3,4,5)P_3, which serves as a docking site for protein kinase B (PKB/Akt) and phosphoinositide-dependent protein kinase 1 (PDK1). This results in phosphorylation of PKB/Akt at two regulatory sites, Thr308 by PDK1 and Ser473 by mTORC2, and other hydrophobic motif kinases.[3-6]

Through the activation of S6 kinase (S6K), TORC1 promotes phosphorylation of ribosomal protein S6, which is a key regulator of protein and lipid synthesis.[7] TORC1 also regulates lysosome function and autophagy, while TORC2 promotes cytoskeletal rearrangement, cell survival, and cell cycle entry.[8] The PI3K/mTOR axis is involved in many cellular processes including cell growth, proliferation and metabolism, and it has been found to be dysregulated in fatal diseases, such as cancer, metabolic, cardiovascular, and neurological disorders.[5,9-12]

The pivotal role of mTOR in numerous human cancers has made this Ser/Thr -kinase a therapeutic target for cancer treatment.

Rapamycin and its analogs (rapalogs) are allosteric inhibitors of TORC1 (Figure 1) and form a TORC1/rapalog/FK506 binding protein 12 (FKBP12) complex.[13] Rapalogs have been extensively investigated in clinical trials in oncology[14-17] and have been approved for a number of cancer treatments such as lung, gastrointestinal neuroendocrine, noncancerous kidney, and advanced pancreatic tumors, advanced ER+/HER2-negative breast and endometrial cancer, mantle cell lymphoma, tuberous sclerosis complex (TSC), and pediatric subependymal giant cell astrocytoma (SEGA).[16,18,19]

Their efficacy as single agents in major solid tumors, however, has turned out to be limited.[20] This might be explained by the selective allosteric inhibition of TORC1, which i) leaves mTORC2 intact; and (ii) suppresses TORC1-dependent feedback loops.[21-24] Small molecule ATP-competitive TORKi target both mTORC1 and mTORC2. Hence, these inhibitors efficiently block two branches of PI3K downstream signaling: i) one via PKB/Akt to tuberous sclerosis complex (TSC) and Ras homolog enriched in brain (Rheb1) controlling TORC1, and ii) the PtdIns(3,4,5)P_3-medited Sin1-dependent TORC2 activation,[25] explaining their robust antitumor efficacy.[26] However, by targeting the ATP-binding site of mTOR, TORKi potentially inhibit other protein and lipid kinases at elevated doses, especially the structurally related PI3Ks. Thus, the development of highly selective TORKi is an ongoing challenge. Structurally distinct mTOR-selective inhibitors have been reported and evaluated in a wide range of malignancies. Among the most noteworthy examples, CC-223 (**55**)[27], Sapanisertib (INK128, MLN0128, **56**)[28], and Vistusertib (AZD2014, **57**)[29] have been explored in clinical trials, and were found superior to rapalogs in terms of cytostatic and cytotoxic potential (see Figure 1 for chemical structures).[30]

Very recently, we have reported on PQR620 (**58**) (Figure 1), a highly selective and potent ATP-competitive mTOR inhibitor, targeting both mTORC1 and mTORC2 kinase activities.[31] PQR620 (**58**) had been discovered through chemical modification of PQR309 (**1**), a pan-PI3K and moderate mTOR inhibitor currently in clinical trials for the treatment of lymphoma and solid tumors.[32-35]

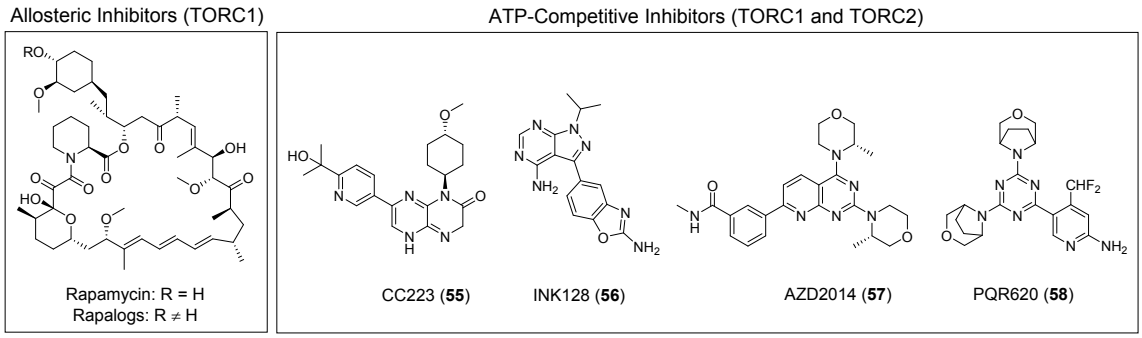

Figure 1. Chemical structures of rapamycin and rapalogs, and a selection of ATP-competitive mTOR kinase inhibitors (TORKi).

Here, we report the discovery of conformationally restricted compounds as a novel scaffold for the development of highly selective TORKIs. The design of conformationally constrained analogs is often used to minimize the entropic loss associated to target binding, to enhance the potency for the target and to increase the selectivity.[36] This conformational restriction approach explores a novel chemical space and secured intellectual property.[37] An extensive Structure Activity Relationship (SAR) study led us to the identification of a highly selective and potent ATP-competitive inhibitor **12b**. Compound **12b** is orally bioavailable, metabolically stable and has a minimal brain permeability, an advantage in the treatment of systemic tumors. Our results disclose the tricyclic pyrimido-pyrrolo-oxazine moiety as an innovative scaffold for selectively targeting mTOR kinase.

RESULTS AND DISCUSSION

Rigidification Strategy.

In our rigidification strategy, we started from PQR309 (**1**) and introduced a methylene bridge between one of the morpholines and the aromatic core (Figure 2). This led to the conversion of the triazine ring into a pyrimidine core. Moreover, we have removed the trifluoromethyl group from the 2-aminopyridine moiety (Figure 2) to alter lipophilicity, increase solubility and change electronic and steric parameters.[38]

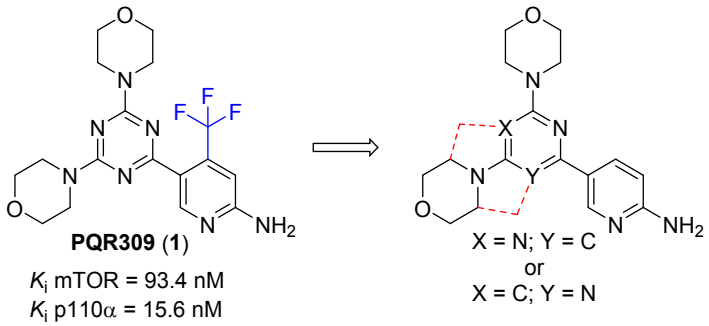

Figure 2. Strategy for the development of mTOR selective inhibitors starting from PQR309 (**1**): rigidification strategy (red dotted lines) and removal of trifluoromethyl group from the 2-aminopyridine moiety (blue).

For the designed compounds, two different regioisomers exist, each with two enantiomers (Table 1, **2a**/**2b** and **2c**/**2d**). To evaluate the rigidification effect on compounds activity, compounds **2a-d** were evaluated for *in vitro* binding [K_i for mTOR and PI3Kα (p110α)] and for PI3K/mTOR signaling in A2058 cells (IC_{50} for phosphorylated S6 to detect mTORC1 activity, and protein kinase B (PKB/Akt) phosphorylation on Ser473 to detect mTORC2 activity). One regioisomer is more potent both in cells and *in vitro*, as highlighted by comparing **2a** with **2c** and **2b** with **2d**. Compound **2a** was >9-fold more potent in cells and >11-fold more potent *in vitro* than **2c** (Table 1).

Table 1. Conformationally restricted regioisomers **2a**/**2b** and **2c**/**2d**.

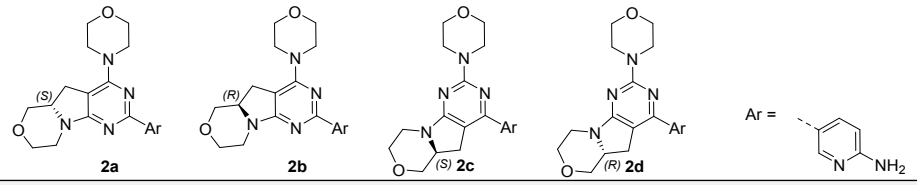

2a **2b** (S) **2c** (R) **2d**

Comp. Name	Cellular Assays IC_{50} [nM][a]		*in vitro* Binding Assays K_i [nM][b]		Selectivity Ki(p110α)/Ki(mTOR)	clogP[c]
	pPKB S473	pS6 S235/236	p110α	mTOR		
PQR309 (1)	139	205	17	62	0.27	3.11
2a	194	164	76	69	1.1	2.65
2b	118	96	432	24	18.3	2.65
2c	1871	1790	867	812	1.1	2.65
2d	1560	1857	541	1279	0.4	2.65

[a]PKB phosphorylation on Ser473 and ribosomal S6 phosphorylation on Ser235/236 were analyzed in A2058 cells exposed to the indicated inhibitors and subsequent detection of phosphoproteins in an in-cell Western assay. Each experiment performed n = 2. LogIC_{50}s and Standard Errors are reported in Table S7 in the Supporting Information. [b]Compounds were tested for the *in vitro* binding to the ATP-binding site of p110α and mTOR using a commercially available time-resolved FRET (TR-FRET) displacement assay (LanthaScreen). Each experiment performed n = 2. IC_{50}s, LogIC_{50}s and Standard Errors are reported in Table S7 in the Supporting Information. [c]Marvin/JChem 16.10.17 was used for calculation of logP (partition coefficient) values.

Elucidation of Binding Modes to PI3K and mTOR.

To explain activity differences of the regioisomers, we considered the possible interactions of the inhibitors within the ATP-binding site of the kinases. As previously reported for PQR309 (**1**)[33] and other morpholino-substituted PI3K inhibitors,[32,39] a crucial interaction for PI3K binding is the hydrogen bond formation in the hinge region between the backbone amide of Val882 residue in PI3Kγ (Val851 in PI3Kα) and the morpholine oxygen atom. Herein, we started from the conformationally restricted PQR309 (**1**) analogs (**3a** and **3b**, Table 2) and replaced the morpholine with a piperidine (**4a-4b** and **5a-5b**, Table 2) to investigate whether the methylene-bridged morpholine or the unrestricted morpholine points towards and interacts with the hinge region Val of the ATP-binding pocket. The obtained K_i values for PI3Kα suggested that the methylene-bridged morpholine locates to the solvent exposed region, since only the compounds with a methylene-bridged piperidine (**4a** and **4b**) displayed a strong affinity for PI3Kα (K_i = 22 and 48 nM, respectively). The *in vitro* potency of **4a** and **4b** is comparable

to that of the dimorpholine-substituted parental compounds (**3a** and **3b**). On the contrary, replacement of the unrestricted morpholine with a piperidine (**5a** and **5b**) led to a drop in PI3K binding affinity.

Table 2. Binding mode: morpholine vs. piperidine in unrestricted and restricted positions.

Name	Structure (Ar = 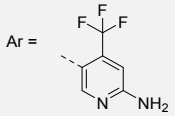)	Cellular Assays, IC_{50} [nM][a]		*in vitro* Binding Assays, K_i [nM][b]
		pPKB S473	pS6 S235/236	p110α
3a	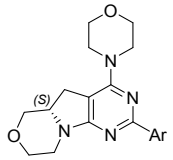	353	751	21
3b	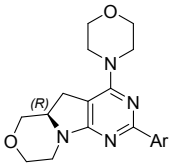	355	524	56
4b	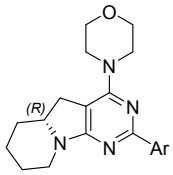	321	1239	22
4a	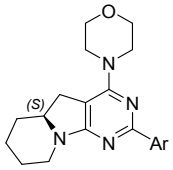	407	938	48
5a	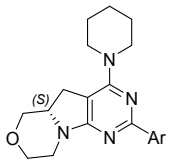	21893	43317	2835
5b	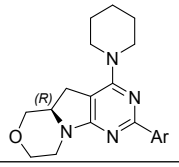	2075	2655	138

[a]PKB phosphorylation on Ser473 and ribosomal S6 phosphorylation on Ser235/236 were analyzed in A2058 cells exposed to the indicated inhibitors and subsequent detection of phosphoproteins in an in-cell Western assay. Each experiment performed n = 2. LogIC_{50}s and Standard Errors are reported in Table S8. [b]Compounds were tested for the in vitro binding to the ATP-binding site of p110α and mTOR using a commercially available time-resolved FRET (TR-FRET) displacement assay (LanthaScreen). Each experiment performed n = 2. IC_{50}s, LogIC_{50}s and Standard Errors are reported in Table S8.

We thus concluded that the unrestricted morpholine binds to the hinge region and establishes a H-bond with the Val backbone amide. We exploited the 2.48 Å resolution X-ray structure of PIKiN3 in PI3Kγ (see Ref. 32; PDB code 5JHB), and substituted PIKiN3 for compound **3a** to confirm its binding mode. Energy minimization calculations of the resulting PI3Kγ-**3a** complex maintained important

interactions such as H-bonds between the aminopyridine and Asp836/964 as well as the interaction of the oxygen atom of the unrestricted morpholine and the backbone amide of Val882 (as present in the parental structure with PIKiN3; Figure 3A). Moreover, the interaction of the core nitrogen of compound **3a** with the structured water molecule allows to stabilize the inhibitor binding through a H-bond network. In PI3Kγ, this interaction had been proved to play a pivotal role in inhibitor binding (see Ref. 32; PDB code: 5JHB).

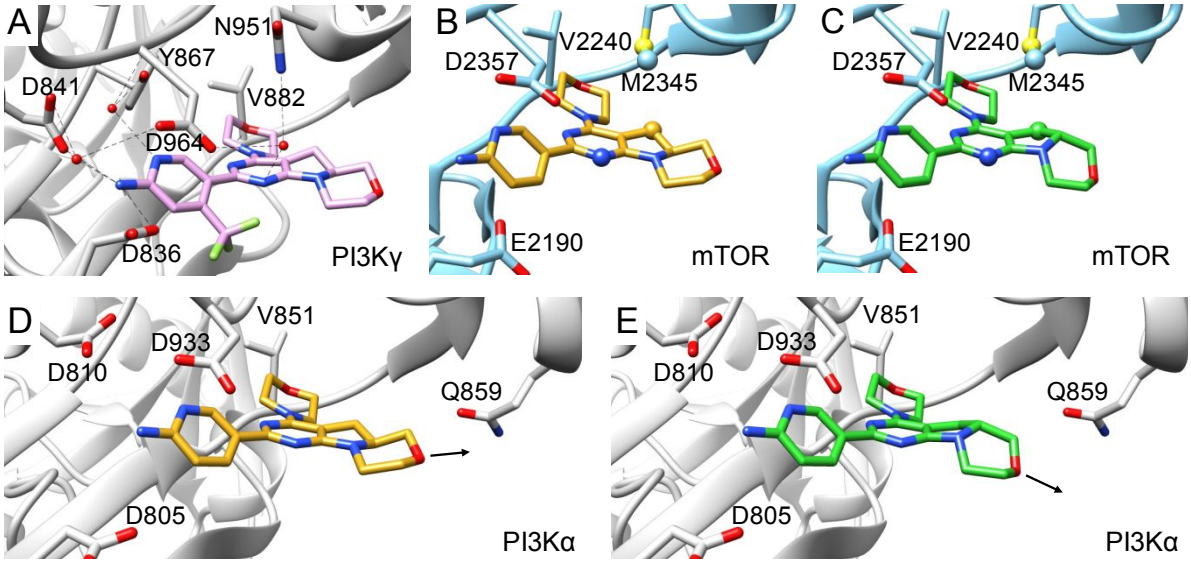

Figure 3. A) Docking of compound **3a** (plum) into PI3Kγ (gray) starting from PDB 5JHB (see Ref. 32). Structural water molecules are shown in red and water-mediated H-bonds are depicted as dashed black lines. **B)** Docking of compound **2a** (gold) and **C)** compound **2b** (green) into mTOR (turquoise) starting from PDB 4JT6. The important features for mTOR selectivity are depicted in a ball and stick representation. **D)** Docking of compound **2a** (gold) and **E)** compound **2b** (green) into PI3Kα (gray) starting from PDB 3ZIM. The exit vector from the restricted morpholine oxygen is shown as a black arrow.

Given the high homology of the ATP-binding pocket of class I PI3Ks and mTOR, a similar binding mode and orientation in mTOR and all PI3K isoforms can be assumed. Computational modeling studies were performed to elucidate the binding mode of the conformationally restricted compounds **2a** and **2b** in mTOR starting from the PI103-mTOR complex (PDB code: 4JT6). In analogy to PI3K, the higher mTOR potency of the compounds bearing the unrestricted morpholine in the 4-position of the pyrimidine core (**2a** and **2b**, Scheme 1B) could be derived from the interaction of a pyrimidine core nitrogen with a putative structured water molecule, even though the 3.6 Å structural resolution of mTOR did not reveal such structured water molecules. Thus, the position of N-1 of the pyrimidine core (see

Scheme 1 for numbering) in the ATP-binding pocket is an essential parameter for mTOR affinity. The binding affinity data of compounds **2a-d** suggests a similar structured water network in mTOR, which is only maintained by binding of regioisomer **2a** and **2b**, but not with **2c** and **2d** (K_i **2a**, **2b** = 69, 24 nM Vs K_i **2c**, **2d** = 812, 1279 nM). An additional stabilization of **2a**/**2b**-mTOR complex is provided by hydrophobic interactions between the methylene bridge and Met2345 (Figure 3B and 3C). The important features for mTOR selectivity are depicted in Figure 3B and 3C in a ball and stick representation.

Within one regioisomer pair (**2a** and **2b**), the (*R*)-enantiomer **2b** displayed a stronger affinity for mTOR, together with an 18-fold selectivity for mTOR kinase over PI3Kα (K_i for mTOR = 24 nM and K_i for PI3Kα = 432 nM). In contrast, the (*S*)-enantiomer **2a** is a dual mTOR/PI3Kα inhibitor (Table 1). The 6-fold difference in PI3K inhibitory activity between compound **2a** and **2b** (K_i for PI3Kα = 76 and 432 nM, respectively) might be related to the different orientation of the morpholine due to scaffold rigidification. In the (*S*)-configured compound **2a**, the oxygen of the restricted morpholine points towards the amide side-chain of Gln859 (4 Å) and a weak H-bond could stabilize the binding of **2a** in PI3Kα (see exit vector in Figure 3D). In the (*R*)-tricyclic pyrimido-pyrrolo-oxazine **2b** the morpholine oxygen is rotated by 1 Å with respect to the oxygen atom of **2a** and the exit vector does not point towards Gln859 (see Figure 3E). Therefore, no H-bond can be established.

Chemistry.

Procedures for library synthesis are depicted in Scheme 1. First, sulfamidates **33a** and **33b** were prepared (Scheme 1A). Typically, sulfamidates are made from chiral amino alcohols in several steps.[40] The 3-hydroxymethyl morpholines (**34a** and **34b**) were synthesized by a chiral synthesis starting from serine enantiomers. As for **34a**, the amino group of (*R*)-serine was protected with a benzyl group (compound **37b**) since the ring closure has been described to proceed in higher yields when a protecting group is present.[41] *N*-Benzyl-(*R*)-serine (**37b**) underwent ring closure in presence of chloroacetyl chloride to give (*R*)-4-benzyl-5-oxomorpholine-3-carboxylic acid (**36b**) in 71% yield. Reduction of **36b** using borane-dimethyl sulphide complex in tetrahydrofuran (THF) gave intermediate **35a** with an 82% yield. Hydrogenolysis of *N*-benzyl derivative (**35a**) over palladium on charcoal (Pd/C, H_2) yielded (*S*)-

morpholin-3-ylmethanol (**34a**). Subsequent two-step cyclic sulfamidate formation was performed by treating the amino alcohol (**34a**) with thionyl chloride, to give the corresponding cyclic sulfamidite, followed by oxidation using $NaIO_4$ and catalytic amounts of ruthenium(IV) oxide hydrate to give sulfamidate **33b** in 52% yield. The (*S*)-enantiomer (**33a**) was synthesized from (*S*)-serine following the procedure described for **33b** (Scheme 1A). The dichloropyrimidines (**26-31**) were prepared according to Scheme 1B starting from the commercially available 2,4,6-trichloropyrimidine. Morpholines M_0-M_5 were introduced as M_n substituents by nucleophilic aromatic substitution reaction. Following this procedure, both regioisomers were generated and separated by column chromatography. The desired regioisomers (**27-31**) were isolated in moderate to high yields (46-86%). The (*S*)-tricyclic intermediates (**20a-25a**) were synthesized by sequential alkylation and nucleophilic aromatic substitution reactions of dichloropyrimidines (**26-31**) with (*R*)-sulfamidate **33b** using *n*-BuLi in THF at -78 °C and a catalytic amount of copper(I) iodide followed by acidic hydrolysis of the intermediary sulfaminic acid and ring closure mediated by base treatment.[42] The same procedure was followed for the preparation of (*R*)-tricyclic intermediates (**20b-25b**), starting from (*S*)-sulfamidate **33a**. A subsequent palladium catalyzed Suzuki coupling between choloropyrimidine intermediates (**20a-25a** and **20b-25b**) and protected 2-aminopyridine-5-boronic acid pinacol ester (**38**, see Supporting Information) afforded compounds **2a**, **6a-10a** and **2b**, **6b-10b** in moderate to high yields (49-88%; Scheme 1B). In addition, the chlorine of intermediate **22b** was displaced by heteroaryl moieties using Suzuki cross-coupling reaction with boronic acid pinacol esters to give compounds **11b-17b** (Scheme 1B). For not commercially available boronic acid pinacol esters or corresponding bromo derivatives, the synthesis is reported in Scheme S1 and S2 in Supporting Information. The regioisomer bearing the unrestricted morpholine in the 2-position of the pyrimidine core (enantiomers **2c** and **2d**) was synthesized starting from dichloropyrimidine **32** (Scheme 1C) following the procedure described for **2a** and **2b**. The synthesis of the conformationally restricted PQR309 (**1**) analog **3a** and **3b** (Table 2) is depicted in Scheme S3A in Supporting Information and the synthetic procedure is analogous to that described for **2a** and **2b**. The procedure for the preparation of the compounds bearing a piperidine instead of a morpholine (**4a-4b** and **5a-5b**, Table 2) is reported in Scheme S3B and S3C in Supporting Information.

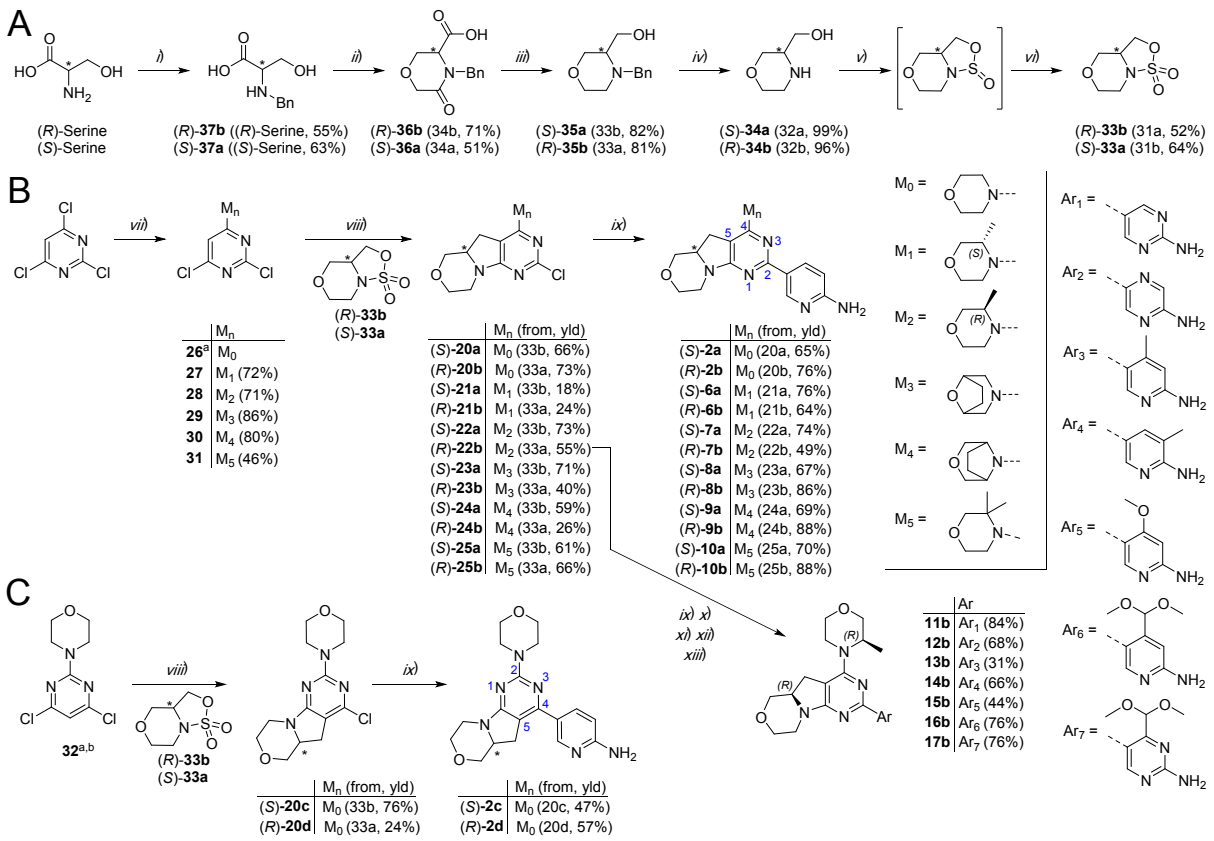

	M_n
26[a]	M_0
27	M_1 (72%)
28	M_2 (71%)
29	M_3 (86%)
30	M_4 (80%)
31	M_5 (46%)

	M_n (from, yld)
(*S*)-**20a**	M_0 (33b, 66%)
(*R*)-**20b**	M_0 (33a, 73%)
(*S*)-**21a**	M_1 (33b, 18%)
(*R*)-**21b**	M_1 (33a, 24%)
(*S*)-**22a**	M_2 (33b, 73%)
(*R*)-**22b**	M_2 (33a, 55%)
(*S*)-**23a**	M_3 (33b, 71%)
(*R*)-**23b**	M_3 (33a, 40%)
(*S*)-**24a**	M_4 (33b, 59%)
(*R*)-**24b**	M_4 (33a, 26%)
(*S*)-**25a**	M_5 (33b, 61%)
(*R*)-**25b**	M_5 (33a, 66%)

	M_n (from, yld)
(*S*)-**2a**	M_0 (20a, 65%)
(*R*)-**2b**	M_0 (20b, 76%)
(*S*)-**6a**	M_1 (21a, 76%)
(*R*)-**6b**	M_1 (21b, 64%)
(*S*)-**7a**	M_2 (22a, 74%)
(*R*)-**7b**	M_2 (22b, 49%)
(*S*)-**8a**	M_3 (23a, 67%)
(*R*)-**8b**	M_3 (23b, 86%)
(*S*)-**9a**	M_4 (24a, 69%)
(*R*)-**9b**	M_4 (24b, 88%)
(*S*)-**10a**	M_5 (25a, 70%)
(*R*)-**10b**	M_5 (25b, 88%)

	Ar
11b	Ar_1 (84%)
12b	Ar_2 (68%)
13b	Ar_3 (31%)
14b	Ar_4 (66%)
15b	Ar_5 (44%)
16b	Ar_6 (76%)
17b	Ar_7 (76%)

Scheme 1. A) Reagents and conditions: (i) 1) benzaldehyde, 2M NaOH, r.t, 30 min; 2) $NaBH_4$, 5 °C → r.t., 1 hr; (ii) 1) chloroacetyl chloride, K_2CO_3, THF / H_2O, 0 °C, 1 hr; 2) NaOH, 5 °C, 2 hrs; (iii) borane-dimethylsulfide complex, Et_3N, THF, 0 °C → 65 °C, 5 hrs; (iv) Pd/C, H_2, 2.8 bar, 48 hrs; (v) thionyl chloride, imidazole, DCM, -5 °C → r.t. → 0 °C, 2 hrs; (vi) ruthenium(IV) oxide hydrate, $NaIO_4$, r.t., o/n. **B)** Reagents and conditions: (vii) morpholine derivative (M_n-H), DIPEA, DCM, 0 °C → rt, o/n; (viii) 1) n-BuLi, CuI, -78 °C → r.t., o/n; 2) HCl conc., MeOH, 45 °C, 4-6 hrs; 3) NaOH, H_2O, r.t., 1-16 hrs; (ix) 1) boronic ester **38** or **41**, XPhosPdG2 (cat.), K_3PO_4, dioxane / H_2O, 95 °C, 2-16 hrs; 2) HCl, dioxane / H_2O, 60 °C, 3-16 hrs (for **2a**, **2b**, **2c**, **2d**, **6a**, **6b**, **7a**, **7b**, **8a**, **8b**, **9a**, **9b**, **10a**, **10b** and **14b**); (x) 2-aminopyridine-5-boronic acid pinacol ester, XPhosPdG2 (cat.), K_3PO_4, dioxane / H_2O, 95 °C (for **11b**), o/n; (xi) boronic ester **39**, Pd(dppf)Cl_2 (cat.), $CsCO_3$, THF, Δ, o/n (for **12b**); (xii) 1) Boronic ester generated *in situ*, XPhosPdG2 (cat.), K_3PO_4, dioxane / H_2O, 95 °C, 3-3.5 hrs; 2) HCl, 80 °C, o/n (for **13b** and **15b**); (xiii) 1) Boronic ester generated *in situ*, XPhosPdG2 (cat.), K_3PO_4, dioxane / H_2O, 95 °C, 2-16 hrs (isolated intermediates: **18b** and **19b**); 2) **18b** or **19b**, TFA, DCM, 0 °C → r.t., 1-3 hrs (for **16b** and **17b**). [a]prepared according to Ref. 32. [b]prepared according to procedure (vii). After the reaction, the two regioisomers (**26** and **32**) were separated by column chromatography.

Determination of Cellular Potency and PI3K vs mTOR Kinase Activities.

In the search for novel mTOR inhibitors, we selected the regioisomer bearing the unrestricted morpholine in the 4-position of the pyrimidine core (Scheme 1B), and built up a Structure Activity Relationship (SAR) study to investigate (i) the influence of the stereogenic center on mTOR selectivity and (ii) the effect of substitution on the unrestricted morpholine. We prepared a series of compounds introducing different morpholine derivatives (M_n substituents, Scheme 1B), such as 3-methylmorpholine [M_1: (*S*) and M_2: (*R*)], 8-oxa-3-azabicyclo[3.2.1]octane (M_3), 3-oxa-8-azabicyclo[3.2.1]octane (M_4) and 3,3-dimethylmorpholine (M_5). Morpholines with increased steric demand had already been shown to increase selectivity for mTOR over PI3K.[31,43] For each conformationally restricted compound both (*S*)- (**2a**, **6a-10a**) and (*R*)-enantiomers (**2b**, **6b-10b**) were synthesized and tested in kinase binding and cellular assays. For all the regioisomer pairs, the (*R*)-enantiomer had higher affinity for mTOR than the (*S*)-configured compound (Table 3), confirming the results of compounds **2a** and **2b**. Also the cellular potency of the (*R*)-configured compounds was 2-7 fold higher than that of their corresponding enantiomers (see Table 3). The introduction of sterically hindered morpholines in the hinge region of (*R*)-configured tricyclic pyrimido-pyrrolo-oxazines (**6b-10b**) did not affect the potency for mTOR, but led to a significant improvement in mTOR selectivity. With the exception of compound **10b**, the selectivity of (*R*)-configured tricyclic compounds for mTOR versus PI3Kα was higher than 35-fold [K_i(p110α)/K_i(mTOR) **6b** = 43; **7b** = 165; **8b** = 53 and **9b** = 36]. The (*S*)-3-methylmorpholine (M_1) only slightly increased the compound potency and selectivity for mTOR if compared with the morpholine (M_0) [K_i for mTOR **2b** = 24 nM; **6b** = 9.1 nM; Selectivity K_i(p110α)/K_i(mTOR) for **2b** was 18-fold, and for **6b** 43-fold]. On the contrary, the presence of a (*R*)-3-methylmorpholine (M_2) on the (*R*)-configured tricyclic pyrimido-pyrrolo-oxazine scaffold yielded the highest selectivity of the series [K_i(p110α)/K_i(mTOR) for **7b** was 165-fold]. In cells, compound **7b** displayed good activity (IC_{50} for phosphorylated PKB/Akt = 133 nM and for phosphorylated S6 = 61 nM) and was therefore selected for further optimization.

Table 3. SAR study on the unrestricted morpholine of tricyclic pyrimido-pyrrolo-oxazines.

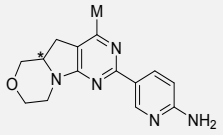

Name	Conf.	M_n	Cellular Assays IC_{50} [nM][a] pPKB S473	Cellular Assays IC_{50} [nM][a] pS6 S235/236	*in vitro* Binding Assays K_i [nM][b] p110α	*in vitro* Binding Assays K_i [nM][b] mTOR	Selectivity K_i(p110α)/ K_i(mTOR)	clogP[c]
2a	(*S*)	M_0	194	164	76	69	1.1	2.65
2b	(*R*)		116	96	432	24	18	2.65
6a	(*S*)	M_1	416	432	98	104	0.9	3.06
6b	(*R*)		194	149	386	9.1	43	3.06
7a	(*S*)	M_2	363	230	923	31	30	3.06
7b	(*R*)		133	61	2147	13	165	3.06
8a	(*S*)	M_3	403	245	1219	96	13	3.11
8b	(*R*)		207	160	1412	27	53	3.11
9a	(*S*)	M_4	389	354	3230	60	54	3.11
9b	(*R*)		152	132	1108	31	36	3.11
10a	(*S*)	M_5	1329	991	7187	121	59	3.14
10b	(*R*)		409	136	376	24	16	3.14

Chemical structures of M_0-M_5 are depicted in Scheme 1. [a]PKB phosphorylation on Ser473 and ribosomal S6 phosphorylation on Ser235/236 were analyzed in A2058 cells exposed to the indicated inhibitors and subsequent detection of phosphoproteins in an in-cell Western assay. Each experiment performed n = 2. $LogIC_{50}$s and Standard Errors are reported in Table S7 in the Supporting Information. [b]Compounds were tested for the *in vitro* binding to the ATP-binding site of p110α and mTOR using a commercially available time-resolved FRET (TR-FRET) displacement assay (LanthaScreen). Each experiment performed n = 2. IC_{50}s, $LogIC_{50}$s and Standard Errors are reported in Table S7 in the Supporting Information. [c]Marvin/JChem 16.10.17 was used for calculation of logP (partition coefficient) values.

To further improve the potency and selectivity for mTOR, and to modulate the physico-chemical properties of compound **7b**, we investigated the role of the aryl moiety (Table 4). First, we replaced the pyridine ring with a pyrimidine (**11b**) and a pyrazine (**12b**) to assess the effect of the polarity of the heteroaromatic ring. Afterwards, we introduced a methyl (**13b** and **14b**), a methoxy (**15b**) or a dimethoxymethyl substituent (**16b** and **17b**) on the 2-amino-substituted aryl group. The presence of a pyrimidine or a pyrazine ring slightly increased mTOR potency, selectivity and cellular activity (see comparison between **11b**/**12b** and **7b**, Table 4). Compound **13b**, bearing a methyl substituent in position 4 of the 2-aminopyridine ring, had a moderate activity towards mTOR (K_i = 85 nM), and was poorly active in cells (IC_{50} for phosphorylated PKB/Akt and for phosphorylated S6 > 800 nM, Table 4). In

contrast, compound **14b**, with a 3-methyl-substituted aminopyridine, maintained a moderate activity in cells (IC_{50} for phosphorylated PKB/Akt was 488 nM and 289 nM for phosphorylated S6). The introduction of a methoxy (**15b**) and a dimethoxymethyl substituent (**16b**) on the pyridine ring reduced cellular potency and binding to both PI3Kα and mTOR. Compound **17b**, bearing a dimethoxymethyl substituent on the pyrimidine ring, is a dual PI3Kα/mTOR inhibitor (K_i for p110α = 66 nM; K_i for mTOR = 34 nM), but showed a limited potency in cells (IC_{50} pPKB > 500 nM and pS6 > 300 nM, Table 4). With respect to compound **7b**, the introduction of an additional nitrogen on the heteroaromatic ring decreased the clogP value (compound **11b** = 2.22 and **12b** = 2.15), leading to compounds with predicted optimal physicochemical and ADME properties for oral drugs.[44] Moreover, the Polar Surface Area (PSA) > 90 Å of compounds **11b** and **12b** is indicative that they might not cross the Blood Brain Barrier (BBB). Limited brain uptake of mTOR inhibitors, normally used to treat systemic tumors, is an advantage because inhibition of the mTOR pathway in the brain could lead to neurological side effects.

Table 4. SAR study on the aryl moiety of tricyclic pyrimido-pyrrolo-oxazines.

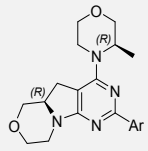

Name	Ar_n	Cellular Assays IC_{50} [nM][a] pPKB S473	Cellular Assays IC_{50} [nM][a] pS6 S235/236	in vitro Binding Assays K_i [nM][b] p110α	in vitro Binding Assays K_i [nM][b] mTOR	Selectivity K_i(p110α/ K_i(mTOR)	clogP[c]	PSA[c]
7b	Ar_0	133	61	2147	13	165	3.06	89.6
11b	Ar_1	77	55	536	2.5	214	2.22	102.5
12b	Ar_2	94	60	1695	8.0	212	2.15	102.5
13b	Ar_3	1544	826	2759	85	33	3.53	89.63
14b	Ar_4	488	289	9627	56	172	3.53	89.63
15b	Ar_5	3755	2520	15970	208	77	2.81	98.86
16b	Ar_6	6522	2425	1122	300	3.7	2.97	108.1
17b	Ar_7	534	377	66	34	2.0	2.43	121.0
PQR620 (**58**)*	Fig. 1	190	85.2	4203	10.8	389	3.06	102.5

Chemical structures of Ar_0-Ar_7 are depicted in Scheme 1. *PQR620 data are reprinted from Ref. 31 for comparison. [a]PKB phosphorylation on Ser473 and ribosomal S6 phosphorylation on Ser235/236 were analyzed in A2058 cells exposed to the indicated inhibitors and subsequent detection of phosphoproteins in an in-cell Western assay. Each experiment performed n = 2. LogIC_{50}s and Standard Errors are reported in Table S7 in the Supporting Information. [b]Compounds were tested for the *in*

vitro binding to the ATP-binding site of p110α and mTOR using a commercially available time-resolved FRET (TR-FRET) displacement assay (LanthaScreen). Each experiment performed n = 2. IC_{50}s, $LogIC_{50}$s and Standard Errors are reported in Table S7 in the Supporting Information. [c]Marvin/JChem 16.10.17 was used for calculation of logP (partition coefficient) values.

Pharmacological Parameters.

To assess the oral availability and to determine BBB permeability, pharmacokinetic studies (PK) were carried out for compounds **7b** and **12b**. Compounds **7b** and **12b** were administered orally (5 mg/kg p.o.) in male Sprague Dawley rats, and compound concentrations in plasma and brain were determined after a single dose (Figure 4A and 4B, respectively. See also Table S1-S4 in Supporting Information). Both compounds showed plasma exposure sufficient to efficiently inhibit mTOR kinase, and brain levels remined minimal. After 8 h, the total exposure AUC_{0-8} was 5730 ng·h/mL in plasma and 104 ng·h/g in brain for compound **12b**.

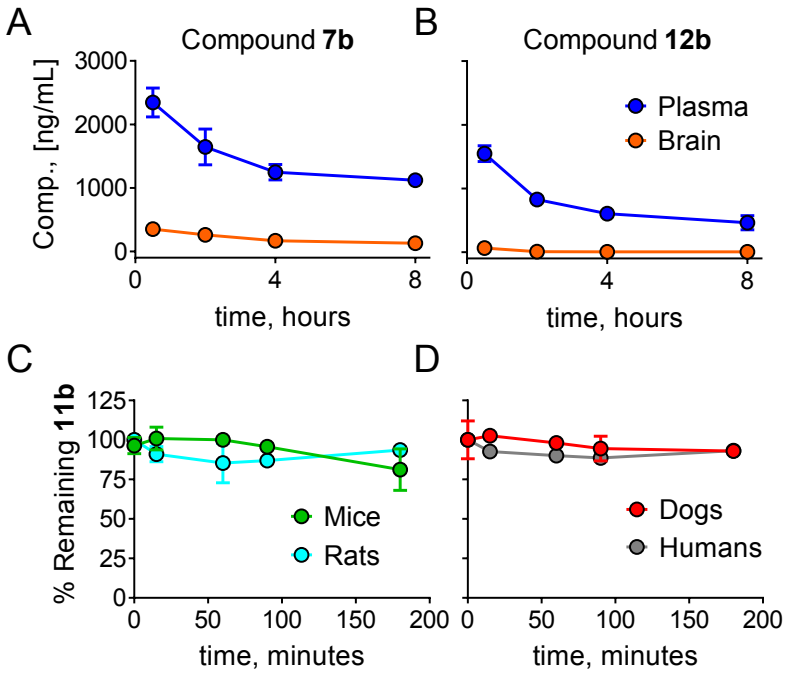

Figure 4. Plasma and brain concentration of **A)** compound **7b** and **B)** compound **12b** after p.o. dosing at 5 mg/kg in male Sprague Dawley rats. Stability of compound **11b** (5 μM) with primary hepatocytes from **C)** mice (green) and rats (turquoise) **D)** dogs (red) and humans (black) (n = 2). All values mean ± SEM. Error bars not shown when smaller than the symbols.

To predict the metabolic stability of our restricted scaffold, *in vitro* assays were performed for compound **11b**, using hepatocyte cultures of different origin (CD-1 mice, Sprague Dawley rats, Beagle dogs and humans). Compound **11b** was only minimally metabolized when incubated with mouse, rat, dog and human hepatocytes, as indicated by 81.2%, 93.6%, 93.0% and 93.2% remaining compound after 3 hours of incubation (Figure 3C, Figure 3D and Table S5 in Supporting Information). As compound **11b** was highly stable across species, neither half-lives nor intrinsic clearance could be determined under the experimental conditions.

CYP450 Reactive Phenotyping for Compounds **7b**, **11b** and **12b**.

CYP450 reactive phenotyping was performed to evaluate the involvement of different human hepatic CYP isoenzymes (CYP1A1 and CYP1A2) in the metabolism of compounds **7b**, **11b** and **12b**. All three compounds turned out to be moderate CYP1A1 substrates, as indicated by < 77% parental compound remaining after 60 minutes of incubation (Table 5). Compounds **7b** and **11b** were partially stable towards CYP1A1 (44% and 51% compound remaining, respectively), while the lowest turnover was observed with compound **12b** (77% remaining). A low metabolization by CYP1A2 was observed with **11b** (73% remaining). On the other hand, compounds **7b** and **12b** remained stable (Table 5), indicating that they are no substrates of CYP1A2.

Table 5. CYP1A1 and CYP1A2 Reactive Phenotyping of **7b**, **11b** and **12b** (1 μM).

Test item	remaining test item w/ cofactors		% remaining in corresponding negative control w/o cofactors		Mean (%) corr*
	mean %	SD	mean	SD	
CYP1A1					
7b	44	2.0	109	3.7	35
11b	51	0.3	93	2.9	58
12b	77	0.08	96	4.5	81
CYP1A2					
7b	98	0.6	94	0.1	104
11b	73	0.4	91	2.4	83
12b	92	0.2	91	0.8	101

Compounds remaining after 60 min of incubation with Supersomes™ at 25 pmol/ml (n=2), calculation based on absolute amounts (nM). *Mean $(\%)_{corr}$ = (100-% remaining negative control)+% remaining sample.

Based on these results, compound **11b** was further investigated to identify metabolites formed *in vitro* by CYP1A1 (Figure 5A) and CYP1A2 (Figure 5B). Upon incubation of **11b** with human recombinant CYP1A1, the highest peak areas were observed for metabolite M2 (9.3% of total peak areas, hydrolysis of the 3*R*-methyl-morpholinyl residue and oxidation to corresponding aldehyde) and its secondary products M5 (7.5%, introduction of a C-C double bond (desaturation) at the tricyclic backbone of M2; Figure 5C). Other minor metabolites were observed, highlighting that the preferred site of oxidative metabolism of compound **11b** was the 3*R*-methyl-substituted morpholinyl moiety (Table S6 and Figure S1-S5 in Supporting Information). In CYP1A2 incubates, M2 was the only metabolite (0.3%) suggesting that compound **11b** is not a substrate of CYP1A2.

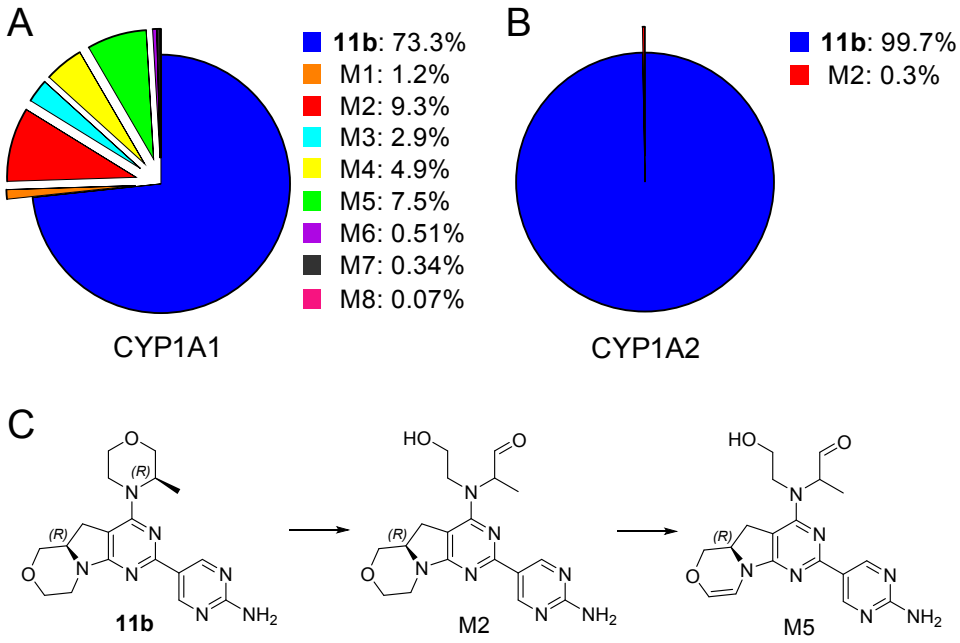

Figure 5. Pie chart showing the percentage of compound **11b** and its metabolites after 60 min of incubation with human recombinant **A)** CYP1A1 and **B)** CYP1A2. **C)** Major metabolites observed upon incubation of **11b** with CYP1A1.

Enzymatic Profiling and Determination of Selectivity.

According to our SAR studies, compounds **7b**, **11b** and **12b** were the most potent and selective mTOR inhibitors showing high potency in cellular assays and good pharmacokinetic profile. Therefore, **7b**, **11b** and **12b** were chosen for further characterization using the KINOMEScan platform of DiscoverX (Table 6). DiscoverX KdELECT assays confirmed the excellent mTOR selectivity of

compound **12b** over class I and III PI3K and PI4K: **12b** was ~450-fold more potent for mTOR than for class I PI3K isoforms. The selectivity of **12b** for mTOR over PI3K exceeds competitor compounds such as CC223 (**55**)[45] (~80×), INK128 (**56**) (~40×) and AZD2104 (**57**) (~230×) (Table 6). Moreover, compound **12b** showed negligible off-target effects when screened against a DiscoverX scanMAX kinase assay panel containing a set of 468 protein and lipid kinases (Supporting Information, Figure S6 an Table S10). At a concentration of 10 μM, compound **12b** and PQR620 (**58**) reached outstanding selectivity scores [S(10) was 0.005 for both compounds; see Supporting Information, Table S9], while the same value for INK128 (**56**) reached 0.14 (corresponding to 55 hits, Table S9).

Table 6. mTOR and lipid kinase binding constants of **7b**, **11b**, **12b** and reference compounds.

	Inhibitor binding constants [a]K_d, [nM]							*Most sensitive PI3K/mTOR
Kinase →	mTOR	PI3Kα	PI3Kβ	PI3Kδ	PI3Kγ	PI4Kβ	VPS34	Fold selectivity
7b	34	**610**	4100	6200	8700	>30000	2100	17.9
11b	14	**120**	1400	1900	1800	>30000	980	8.6
12b	3.5	**1600**	7500	12000	11000	>30000	3200	457
CC223 (**55**)[b]	28	**2300**	18000	6200	7100	39	2500	>80x
INK128 (**56**)[b]	0.092	15	81	30	**3.7**	n.d.	8200	>40x
AZD2014 (**57**)[b]	0.14	**33**	3300	1500	8400	>30000	23000	>230x
PQR620 (**58**)	0.27	**1000**	22000	23000	18000	>30000	2750	>3700x

[a]Dissociation constants (K_d) were determined using ScanMax technology (DiscoveRx) with 11 point 3-fold serial dilutions of the indicated compounds. K_d is the mean value from experiments performed in duplicate and were calculated from standard dose response curves using the Hill equation. n.d. = not determined. [b]Dissociation constants (K_d) of CC223 (**55**), INK128 (**56**), AZD2014 (**57**) and PQR620 (**58**) are reprinted from Ref. 31. n.d. = not determined. *Fold selectivity: ratio of K_d of most sensitive class I PI3K isoform (displayed in bold type) over K_d for mTOR.

CONCLUSION

In summary, we have exploited a conformational restriction strategy to enlarge the chemical space around PQR309 (**1**), a pan-PI3K and moderate mTOR inhibitor. Our rigidification strategy allowed to enhance potency and selectivity for mTOR. Molecular modeling elucidated interactions of the tricyclic pyrimido-pyrrolo-oxazine scaffold in the ATP-binding pocket of PI3Ks and mTOR, and explained the difference in potency between the regioisomers. An extensive SAR study led to the discovery of

compound **12b**, with a selectivity for mTOR higher than competitor compounds such as CC223 (**55**), INK128 (**56**) and AZD2104 (**57**). The selectivity of PQR620 (**58**) for mTOR over PI3Ks exceeds that of **12b**, however **12b** explores a novel chemical space and paves the way for additional chemical modifications. A lead optimization process of the tricyclic pyrimido-pyrrolo-oxazine scaffold could lead to further improve the mTOR potency and selectivity of **12b**. Compound **12b** efficiently inhibited mTOR signaling in cells and showed plasma drug exposure after oral dosing that is expected to fully inhibit mTOR *in vivo*. The minimal brain permeability of compounds **7b** and **12b** suggests the tricyclic pyrimido-pyrrolo-oxazine as a novel scaffold for the development of highly selective and potent ATP-competitive mTOR inhibitors to be exploited for the treatment of systemic tumors. PQR620 (**58**) and the tricyclic pyrimido-pyrrolo-oxazine derivatives span along the different therapeutic applications of mTOR inhibitors. PQR620 (**58**) showed an excellent brain penetration and could be exploited in the treatment of neurological disorders. On the contrary, the conformationally restricted compounds have a limited brain uptake and could find an optimal application in the treatment of systemic cancers, with the advantage of avoiding neurological side effects. Our novel scaffold was also characterized for CYP450 related metabolism to assess the substrate specificity towards CYP1A1 and CYP1A2. The tricyclic pyrimido-pyrrolo-oxazines **7b**, **11b** and **12b** were metabolically stable, with compound **12b** showing the lowest turnover in CYP450 reactive phenotyping. On the basis of its remarkable mTOR potency/selectivity, and favorable pharmacokinetic profile, compound **12b** represents a promising starting point for the development of a novel mTOR candidate in oncology.

EXPERIMENTAL SECTION

General Information.

Reagents were purchased at the highest commercial quality from Acros, Sigma-Aldrich or Fluorochem and used without further purification. Solvents were purchased from Acros Organics in AcroSeal® bottles over molecular sieves. Cross coupling reactions were carried out under nitrogen atmosphere in anhydrous solvents, and glassware was oven dried prior to use. Thin layer chromatography (TLC) plates were purchased from Merck KGaA (Polygram SIL / UV254, 0.2 mm silica with fluorescence indicator) and UV light (254 nm) was used to visualize the compounds. Column chromatographic purifications were performed on Merck KGaA silica gel (pore size 60 Å, 230-400 mesh particle size). Alternatively, flash chromatography was performed with Isco CombiFlash Companion systems using prepacked silica gel columns (40−60 μm particle size RediSep). ^{1}H, ^{19}F and ^{13}C NMR spectra were recorded on a Bruker Avance 400 spectrometer. NMR spectra were obtained in deuterated solvents, such as $CDCl_3$, $(CD_3)_2SO$ or CD_3OD. The chemical shift (δ values) are reported in ppm and corrected to the signal of the deuterated solvents (7.26 ppm (^{1}H NMR) and 77.16 ppm (^{13}C NMR) for $CDCl_3$; 2.50 ppm (^{1}H NMR) and 39.52 ppm (^{13}C NMR) for $(CD_3)_2SO$; and 3.31 ppm (^{1}H NMR) and 49.00 ppm (^{13}C NMR) for CD_3OD). ^{19}F NMR spectra are calibrated relative to $CFCl_3$ (δ = 0 ppm) as external standard. When peak multiplicities are reported, the following abbreviations are used: s (singlet), d (doublet), dd (doublet of doublets), t (triplet), td (triplet of doublets), q (quartet), m (multiplet), br (broadened). Coupling constants, when given, are reported in Hertz (Hz). High resolution mass spectra (HRMS) were recorded on a Bruker maxis 4G, high resolution ESI-QTOF. All analysis were carried out in positive ion mode and in MeOH + 0.1 % formic acid as solvent. Sodium formate was used as calibration standard. MALDI-ToF mass spectra were obtained on a Voyager-De™ Pro measured in *m/z*. The chromatographic purity of final compounds was determined by high performance liquid chromatography (HPLC) analyses on an Ultimate 3000SD System from ThermoFisher with LPG-3400SD pump system, ACC-3000 autosampler and column oven, and DAD-3000 diode array detector. An Acclaim-120 C18 reversed-phase column from ThermoFisher was used as stationary phase. Gradient elution (5:95 for 0.2 min, 5:95 → 100:0 over 10 min, 100:0 for 3 min) of the mobile phase consisting of CH_3CN /

MeOH:$H_2O_{(10:90)}$ was used at a flow rate of 0.5 mL/min at 40 °C. The purity of all final compounds was > 95%. Optical Rotations ($[\alpha]_D^{23}$) were measured on a Perkin Elmer Polarimeter 341 (in a cuvette (l = 1 dm)) at 23 °C at 589 nm.

General procedure 1.

A flask was charged with the corresponding boronic acid pinacol ester (1 eq.), *N,N*-dimethylformamide dimethyl acetal (DMF-DMA, 1.3-1.5 eq.) and THF (5 mL). The mixture was stirred at 70 °C overnight. After completion of the reaction monitored by NMR, the solvents were evaporated and the compound was dried under vacuum.

General Procedure 2.

To a solution of the desired morpholine (1.05 eq.) in DCM (approx. 1 ml / 0.6 mmol) at 0 °C, *N,N*-diisopropylethylamine (2.1 eq.) was added, followed by 2,4,6-trichloropyrimidine (1.0 eq.). The reaction mixture was allowed to warm up to r.t. and was stirred overnight. The reaction mixture was washed with aqueous saturated $NaHSO_4$-solution (2 x). The aqueous layer was extracted with DCM and the combined organic layers were dried over Na_2SO_4, filtered and concentrated under reduced pressure. The crude was purified by column chromatography on silica gel.

Using this procedure, both regioisomers were generated and separated by column chromatography. Only the characterization of the desired regioisomer is reported.

General procedure 3.

Under nitrogen atmosphere, a 1.6 M *n*-BuLi solution (1.0 mL, 1.52 mmol, 1.2 eq.) in THF (approx. 1 ml / 1.5 mmol) was cooled down to -78 °C and a solution of the corresponding morpholine (1 eq.) in THF (approx. 1 ml / 0.4 mmol) was added dropwise. The mixture was stirred at -78 °C for 35 min. CuI (0.05 eq) and a solution of the corresponding sulfamidate (1-1.2 eq.) in THF (approx. 1 ml / 0.5 mmol) were added. The mixture was stirred at -78 °C for 15 min, then allowed to warm to r.t. and stirred overnight. The reaction was quenched by addition of water. Conc. HCl and methanol were added, and the mixture was heated at 45 °C for 4-6 hrs. The reaction mixture was cooled down to 0 °C and a 6M

NaOH-solution was added until pH 10. The reaction mixture was stirred at r.t. for 1-16 hrs, then transferred to a separatory funnel. The layers were separated and the aqueous layer was extracted with EtOAc (2 x). The combined organic layers were dried over Na_2SO_4, filtered and concentrated under reduced pressure. The crude product was purified by column chromatography on silica gel.

General procedure 4.

Chloropyrimidine derivative (1.0 eq.) and boronic acid pinacol ester (1.0 eq.) were charged in a flask. Under nitrogen atmosphere, 1,4-dioxane (approx. 1 ml / 0.2 mmol) was added, followed by an aqueous K_3PO_4-solution (2 eq.) and chloro(2-dicyclohexylphosphino-2',4',6'-triisopropyl-1,1'-biphenyl)[2-(2'-amino-1,1'-biphenyl)]-palladium(II) (XPhos Pd G2, 0.05 eq.). The resulting mixture was stirred at 95 °C for 2-16 hrs. After completion of the reaction monitored by TLC, a 3 M aqueous HCl-solution (10 eq.) was added and the mixture was stirred at 60 °C for 3-16 hrs. A 2 M aqueous NaOH-solution was added until pH 9-10. The aqueous layer was extracted with EtOAc (3 x). The combined organic layers were dried over anhydrous Na_2SO_4, filtered and the solvent was evaporated under reduced pressure. The crude product was purified by column chromatography on silica gel.

General procedure 5.

Step 1. The corresponding di-Boc protected bromo derivative **44** or **49** (1.0 eq.), bis(pinacolato)diboron (1.5 eq.) and KOAc (3.0 eq.) were charged into a flask. Under nitrogen atmosphere, 1,4-dioxane (approx. 1 ml / 0.2 mmol) was added, followed by [1,1′-bis(diphenylphosphino)ferrocene]dichloropalladium(II) ($Pd(dppf)Cl_2$, 0.1 eq.). The reaction mixture was stirred at 100 °C for 2 hrs. *Step 2*. After completion of the reaction monitored by TLC, the chloropyrimidine derivative **22b** (200 mg, 0.65 mmol, 1 eq.) and K_3PO_4 (3.0 eq.) in water (approx. 1 ml / 0.3 mmol) and chloro(2-dicyclohexylphosphino-2',4',6'-triisopropyl-1,1'-biphenyl)[2-(2'-amino-1,1'-biphenyl)]-palladium(II) (XPhos Pd G2, 0.05 eq.) were added. The reaction mixture was stirred at 95 °C for 2-16 hrs. A 15% NH_4Cl-solution was added and the aqueous layer was extracted with EtOAc (3 x). The combined organic layers were dried over anhydrous Na_2SO_4, filtered and the solvent was

evaporated under reduced pressure. The crude product was purified by column chromatography on silica gel.

General procedure 6.

To a cold solution (0 °C) of the corresponding Boc-protected compound (1 eq.) in DCM (approx. 1 ml / 0.1 mmol), trifluoroacetic acid (TFA, 40 eq.) was added dropwise. The reaction mixture was allowed to warm up to room temperature and was stirred for 1-3 hr. After completion of the reaction monitored by TLC, a saturated $NaHCO_3$-solution was slowly added. The aqueous layer was extracted with DCM (3 x). The combined organic layers were dried over anhydrous Na_2SO_4, filtered and concentrated under reduced pressure. The crude product was purified by column chromatography on silica gel.

(*S*)-5-(4-morpholino-5a,6,8,9-tetrahydro-5*H*-pyrimido[5',4':4,5]pyrrolo[2,1-*c*][1,4]oxazin-2-yl)pyridin-2-amine (2a) was prepared according to general procedure 4 from (*S*)-2-chloro-4-morpholino-5a,6,8,9-tetrahydro-5*H*-pyrimido[5',4':4,5]pyrrolo[2,1-*c*][1,4]oxazine **20a** (131 mg, 0.44 mmol, 1 eq) and (*E*)-*N*,*N*-dimethyl-*N*'-(5-(4,4,5,5-tetramethyl-1,3,2-dioxaborolan-2-yl)pyridin-2-yl)formimidamide **38** (121 mg, 0.44 mmol, 1 eq.). Purification by column chromatography on silica gel (cyclohexane / ethyl acetate 1:0 → 0:1) gave compound **2a** as a colorless solid (102 mg, 0.29 mmol, 65%). **^{1}H NMR** (400 MHz, DMSO-d_6): δ 8.83 (d, J = 2.3 Hz, 1 H), 8.18 (dd, J = 8.7, 2.3 Hz, 1 H), 6.45 (d, J = 8.6 Hz, 1 H), 6.27 (br s, 2 H), 4.04 (dd, J = 13.5, 2.6 Hz, 1 H), 3.87 (ddt, J = 10.5, 8.8, 4.3 Hz, 1 H), 3.79-3.71 (m, 3 H), 3.68-3.54 (m, 7 H), 3.35-3.28 (m, 1 H), 3.22-3.10 (m, 3 H), 2.63 (dd, J = 15.3, 4.7 Hz, 1 H). **^{13}C{^{1}H} NMR** (101 MHz, DMSO-d_6): δ 167.71 (s, 1 C), 161.20 (s, 1 C), 160.90 (s, 1 C), 158.28 (s, 1 C), 148.91 (s, 1 C), 136.73 (s, 1 C), 122.60 (s, 1 C), 107.34 (s, 1 C), 93.55 (s, 1 C), 70.07 (s, 1 C), 66.64 (s, 2 C), 66.17 (s, 1 C), 56.91 (s, 1 C), 45.90 (s, 2 C), 42.07 (s, 1 C), 29.14 (s, 1 C). **HRMS** (*m/z*): $[M + H]^+$ calc. for $C_{18}H_{23}N_6O_2$ 355.1877; found: 355.1880. **HPLC** (ACN with 0.1% TFA): t_R = 4.98 min (98.7% purity).

(*R*)-5-(4-morpholino-5a,6,8,9-tetrahydro-5*H*-pyrimido[5',4':4,5]pyrrolo[2,1-*c*][1,4]oxazin-2-yl)pyridin-2-amine (2b) was prepared as described for its (*S*)-enantiomer **2a** starting from (*R*)-2-chloro-4-morpholino-5a,6,8,9-tetrahydro-5*H*-pyrimido[5',4':4,5]pyrrolo[2,1-*c*][1,4]oxazine **20b** (150 mg, 0.51 mmol, 1 eq) and boronic acid pinacol ester **38** in a 76% yield. The spectroscopic data are in agreement with those reported for the (*S*)-enantiomer. **HRMS** (*m/z*): $[M + H]^+$ calc. for $C_{18}H_{23}N_6O_2$ 355.1877; found: 355.1883. **HPLC** (ACN with 0.1% TFA): t_R = 4.95 min (97.4% purity).

(*S*)-5-(2-morpholino-5a,6,8,9-tetrahydro-5*H*-pyrimido[5',4':4,5]pyrrolo[2,1-*c*][1,4]oxazin-4-yl)pyridin-2-amine (2c) was prepared according to general procedure 4 from (*S*)-4-chloro-2-morpholino-5a,6,8,9-tetrahydro-5*H*-pyrimido[5',4':4,5]pyrrolo[2,1-*c*][1,4]oxazine **20c** (80 mg, 0.27 mmol, 1 eq) and (*E*)-*N*,*N*-dimethyl-*N*'-(5-(4,4,5,5-tetramethyl-1,3,2-dioxaborolan-2-yl)pyridin-2-yl)formimidamide **38** (81.5 mg, 0.30 mmol, 1.1 eq.). Purification by column chromatography on silica gel (cyclohexane / ethyl acetate 1:0 → 0:1) gave compound **2c** as a colorless solid (45 mg, 0.13 mmol, 47%). **^{1}H NMR** (400 MHz, DMSO-d_6): δ 8.46 (d, J = 2.4 Hz, 1 H), 7.93 (dd, J = 8.7, 2.4 Hz, 1 H), 6.50 (d, J = 8.7 Hz, 1 H), 6.31 (br s, 2 H), 3.96-3.89 (m, 2 H), 3.81-3.75 (m, 2 H), 3.69-3.61 (m, 8 H), 3.34-3.27 (m, 1 H), 3.24-3.11 (m, 3 H), 2.62 (dd, J = 15.9, 4.5 Hz, 1 H). **^{13}C{^{1}H} NMR** (101 MHz, DMSO-d_6): δ 166.88 (s, 1 C), 161.13 (s, 1 C), 160.00 (s, 1 C), 152.84 (s, 1 C), 147.95 (s, 1 C), 136.12 (s, 1 C), 122.01 (s, 1 C), 107.22 (s, 1 C), 102.42 (s, 1 C), 70.07 (s, 1 C), 66.11 (s, 2 C), 65.54 (s, 1 C), 56.92 (s, 1 C), 44.23 (s, 2 C), 41.31 (s, 1 C), 27.75 (s, 1 C). **HRMS** (*m/z*): $[M + H]^+$ calc. for $C_{18}H_{23}N_6O_2$ 355.1877; found: 355.1881. **HPLC** (ACN with 0.1% TFA): t_R = 3.57 min (99.8% purity).

(*R*)-5-(2-morpholino-5a,6,8,9-tetrahydro-5*H*-pyrimido[5',4':4,5]pyrrolo[2,1-*c*][1,4]oxazin-4-yl)pyridin-2-amine (2d) was prepared as described for its (*S*)-enantiomer **2c** starting from (*R*)-4-chloro-2-morpholino-5a,6,8,9-tetrahydro-5*H*-pyrimido[5',4':4,5]pyrrolo[2,1-*c*][1,4]oxazine **20d** (100 mg, 0.34 mmol, 1 eq) and boronic acid pinacol ester **38** in a 57% yield. The spectroscopic data are in agreement with those reported for the (*S*)-enantiomer. **HRMS** (*m/z*): $[M + H]^+$ calc. for $C_{18}H_{23}N_6O_2$ 355.1877; found: 355.1880. **HPLC** (ACN with 0.1% TFA): t_R = 3.61 min (99.2% purity).

(*S*)-5-(4-Morpholino-5a,6,8,9-tetrahydro-5*H*-pyrimido[5',4':4,5]pyrrolo[2,1-*c*][1,4]oxazin-2-yl)-4-(trifluoromethyl)pyridin-2-amine (3a) was prepared according to general procedure 4 from (*S*)-2-chloro-4-morpholino-5a,6,8,9-tetrahydro-5*H*-pyrimido[5',4':4,5]pyrrolo[2,1-*c*][1,4]oxazine **20a** (544 mg, 1.83 mmol, 1.0 eq.) and boronic acid pinacol ester **50** (818 mg, 2.38 mmol, 1.3 eq.) Purification by column chromatography on silica gel (CH_2Cl_2 / methanol 1:0 → 20:1) gave compound **3a** as a colorless solid (503 mg, 1.19 mmol, 65%). **^{1}H NMR** (400 MHz, $CDCl_3$): δ 8.62 (s, 1 H), 6.77 (s, 1 H), 4.75 (br s, 2 H), 4.10 (dd, J = 14.0, 2.5 Hz, 1 H), 4.01-3.93 (m, 1 H), 3.86-3.70 (m, 6 H), 3.70-3.58 (m, 4 H), 3.47 (td, J = 12.0, 2.8 Hz, 1 H), 3.35 (t, J = 11 Hz, 1 H), 3.27-3.17 (m, 2 H), 2.62 (dd, J = 15.0, 4.8 Hz, 1 H). **^{19}F{^{1}H} NMR** (376 MHz, $CDCl_3$): δ − 60.2 (s, 3 F). **^{13}C{^{1}H} NMR** (101 MHz, $CDCl_3$): δ 167.70 (s, 1 C), 161.65 (s, 1 C), 158.91 (s, 1 C), 158.33 (s, 1 C), 152.29 (s, 1 C), 138.0 (q, J = 32 Hz, 1 C), 123.91-123.81 (m, 1 C), 123.1 (q, J = 274 Hz, 1 C), 105.2 (q, J = 5.6 Hz, 1 C), 93.59 (s, 1 C), 70.44 (s, 1 C), 66.96 (s, 2 C), 66.59 (s, 1 C), 56.97 (s, 1 C), 45.94 (s, 2 C), 42.05 (s, 1 C), 29.66 (s, 1 C). **HRMS** (*m/z*): $[M + H]^+$ calc. for $C_{19}H_{22}F_3N_6O_2$ 423.1751; found: 423.1743. **HPLC**: t_R = 6.74 min (97.5% purity). (*S*)-enantiomer: $[\alpha]_D^{20}$ = – 13.2 (c = 2.0, $CHCl_3$).

(*R*)-5-(4-Morpholino-5a,6,8,9-tetrahydro-5*H*-pyrimido[5',4':4,5]pyrrolo[2,1-*c*][1,4]oxazin-2-yl)-4-(trifluoromethyl)pyridin-2-amine (3b) was prepared as described for its (*S*)-enantiomer **50a** starting from (*R*)-2-chloro-4-morpholino-5a,6,8,9-tetrahydro-5*H*-pyrimido[5',4':4,5]pyrrolo[2,1-*c*][1,4]oxazine **20b** (552 mg, 1.86 mmol, 1.0 eq.) and boronic acid pinacol ester **50** (83 mg, 2.42 mmol, 1.3 eq.) in a 62% yield. The spectroscopic data are in agreement with those reported for the (*S*)-enantiomer. **HRMS** (*m/z*): $[M + H]^+$ calc. for $C_{19}H_{22}F_3N_6O_2$ 423.1751; found: 423.1744. **HPLC**: t_R = 6.73 min (98.9% purity). (*R*)-enantiomer: $[\alpha]_D^{20}$ = + 13.5 (c = 1.6, $CHCl_3$).

(*S*)-5-(4-Morpholino-5,5a,6,7,8,9-hexahydropyrimido[5,4-*b*]indolizin-2-yl)-4-(trifluoromethyl)pyridin-2-amine (4a) was prepared according to general procedure 4 from intermediate **51a** (150 mg, 0.51 mmol, 1.0 eq.) and boronic acid pinacol ester **50** (175 mg, 0.51 mmol, 1.0 eq.). Purification by column chromatography on silica gel (cyclohexane / ethyl acetate 1:0 → 3:2) gave compound **4a** as a yellowish solid (90 mg, 0.21 mmol, 42%). **^{1}H NMR** (400 MHz, DMSO): δ 8.42

(s, 1 H), 6.76 (s, 1 H), 6.67 (br s, 2 H), 4.05 (dd, J = 13, 4.2 Hz, 1 H), 3.67-3.49 (m, 9 H), 3.25 (dd, J = 15.0, 9.1 Hz, 1 H), 2.78-2.64 (m, 2 H), 1.83-1.67 (m, 2 H), 1.63-1.55 (m, 1 H), 1.51-1.37 (m, 1 H), 1.37-1.20 (m, 2 H). **^{19}F{^{1}H} NMR** (376 MHz, DMSO): δ − 59.1 (s, 3 F). **^{13}C{^{1}H} NMR** (101 MHz, DMSO): δ 167.2 (s, 1 C), 160.7 (s, 1 C), 160.2 (s, 1 C), 157.5 (s, 1 C), 151.8 (s, 1 C), 135.7 (q, J = 31 Hz, 1 C), 123.3 (q, J = 274 Hz, 1 C), 121.2-121.1 (m, 1 C), 104.1 (q, J = 5.9 Hz, 1 C), 99.3 (s, 1 C), 66.1 (s, 2 C), 58.9 (s, 1 C), 45.5 (s, 2 C), 41.3 (s, 1 C), 33.6 (s, 1 C), 31.5 (s, 1 C), 24.4 (s, 1 C), 23.6 (s, 1 C). **HRMS** (*m/z*): $[M + H]^+$ calc. for $C_{20}H_{24}F_3N_6O$ 421.1958; found: 421.1962. **HPLC**: t_R = 8.44 min (97.8% purity).

(*R*)-5-(4-Morpholino-5,5a,6,7,8,9-hexahydropyrimido[5,4-*b*]indolizin-2-yl)-4-(trifluoromethyl)pyridin-2-amine (4b) was prepared as described for its (*S*)-enantiomer **4a** starting from **51b** (150 mg, 0.51 mmol, 1.0 eq.) and boronic acid pinacol ester **50** (175 mg, 0.51 mmol, 1.0 eq.) in a 47% yield. The spectroscopic data are in agreement with those reported for the (*S*)-enantiomer. **HRMS** (*m/z*): $[M + H]^+$ calc. for $C_{20}H_{24}F_3N_6O$ 421.1958; found: 421.1966. **HPLC**: t_R = 8.45 min (98.7% purity).

(*S*)-5-(4-(piperidin-1-yl)-5a,6,8,9-tetrahydro-5*H*-pyrimido[5',4':4,5]pyrrolo[2,1-*c*][1,4]oxazin-2-yl)-4-(trifluoromethyl)pyridin-2-amine (5a) was prepared as described for its (*R*)-enantiomer **5b** starting from **52a** (100 mg, 0.34 mmol, 1.0 eq.) and boronic acid pinacol ester **50** (128 mg, 0.37 mmol, 1.1 eq.) in a 75% yield. The spectroscopic data agree with those reported for the (*R*)-enantiomer. **HRMS** (*m/z*): $[M + H]^+$ calc. for $C_{20}H_{24}F_3N_6O$ 421.1958; found: 421.1966. **HPLC**: t_R = 8.55 min (98.3% purity).

(*R*)-5-(4-(Piperidin-1-yl)-5a,6,8,9-tetrahydro-5*H*-pyrimido[5',4':4,5]pyrrolo[2,1-*c*][1,4]oxazin-2-yl)-4-(trifluoromethyl)pyridin-2-amine (5b) was prepared according to general procedure 4 from intermediate **52b** (100 mg, 0.34 mmol, 1.0 eq.) and boronic acid pinacol ester **50** (128 mg, 0.38 mmol, 1.1 eq.). Purification by column chromatography on silica gel (cyclohexane / ethyl acetate 1:0 → 3:2) gave compound **5b** as a colorless solid (114 mg, 0.27 mmol, 80%). **^{1}H NMR** (400 MHz, DMSO): δ 8.43 (s, 1 H), 6.76 (s, 1 H), 6.69 (br s, 2 H), 3.95-3.80 (m, 2 H), 3.77-3.67 (m, 2 H), 3.63-3.50 (m, 4 H), 3.29 (td, J = 12.0, 2.4 Hz, 1 H), 3.23-3.14 (m, 2 H), 3.08 (td, J = 13.0, 3.6 Hz, 1 H), 2.61 (dd, J = 15.0, 4.6 Hz, 1 H), 1.64-1.57 (m,. 2 H), 1.53-1.44 (m, 4 H). **^{19}F{^{1}H} NMR** (376 MHz, DMSO): δ − 58.9 (s, 3 F).

^{13}C{^{1}H} NMR (101 MHz, DMSO): δ 167.10 (s, 1 C), 160.88 (s, 1 C), 160.18 (s, 1 C), 157.47 (s, 1 C), 151.81 (s, 1 C), 135.70 (q, J = 31 Hz, 1 C), 123.30 (q, J = 274 Hz, 1 C), 121.16 (s, 1 C), 104.12 (q, J = 5.7 Hz, 1 C), 92.47 (s, 1 C), 69.51 (s, 1 C), 65.62 (s, 1 C), 56.31 (s, 1 C), 45.88 (s, 2 C), 41.61 (s, 1 C), 29.11 (s, 1 C), 25.57 (s, 2 C), 24.43 (s, 1 C). **HRMS** (*m/z*): [M + H]$^{+}$ calc. for $C_{20}H_{24}F_3N_6O$ 421.1958; found: 421.1963. **HPLC**: t_R = 8.55 min (98.9% purity).

5-((*S*)-4-((*S*)-3-methylmorpholino)-5a,6,8,9-tetrahydro-5*H*-pyrimido[5',4':4,5]pyrrolo[2,1-*c*][1,4]oxazin-2-yl)pyridin-2-amine (6a) was prepared according to general procedure 4 from (*S*)-2-chloro-4-((*S*)-3-methylmorpholino)-5a,6,8,9-tetrahydro-5*H*-pyrimido[5',4':4,5]pyrrolo[2,1-*c*][1,4]oxazine **21a** (84 mg, 0.27 mmol, 1 eq) and (*E*)-*N*,*N*-dimethyl-*N*'-(5-(4,4,5,5-tetramethyl-1,3,2-dioxaborolan-2-yl)pyridin-2-yl)formimidamide **38** (275 mg, 0.27 mmol, 1 eq.). Purification by column chromatography on silica gel (cyclohexane / ethyl acetate 1:0 → 0:1) gave compound **6a** as a colorless solid (76 mg, 0.21 mmol, 76%). **^{1}H NMR** (400 MHz, DMSO-d_6): δ 8.82 (d, J = 2.2 Hz, 1 H), 8.17 (dd, J = 8.7, 2.3 Hz, 1 H), 6.45 (dd, J = 8.7, 0.8 Hz, 1 H), 6.28 (br s, 2 H), 4.36-4.30 (m, 1 H), 4.09-4.02 (m, 2 H), 3.93-3.84 (m, 2 H), 3.79-3.63 (m, 4 H), 3.48 (td, J = 11.7, 2.9 Hz, 1 H), 3.35-3.29 (m, 1 H), 3.26-3.10 (m, 4 H), 2.65 (dd, J = 15.3, 4.7 Hz, 1 H), 1.18 (d, J = 6.7 Hz, 3 H). **^{13}C{^{1}H} NMR** (101 MHz, DMSO-d_6): δ 167.63 (s, 1 C), 161.19 (s, 1 C), 160.88 (s, 1 C), 157.80 (s, 1 C), 148.91 (s, 1 C), 136.70 (s, 1 C), 122.69 (s, 1 C), 107.33 (s, 1 C), 93.14 (s, 1 C), 70.86 (s, 1 C), 70.10 (s, 1 C), 66.98 (s, 1 C), 66.17 (s, 1 C), 56.77 (s, 1 C), 47.58 (s, 1 C), 42.02 (s, 1 C), 40.11 (s, 1 C), 29.18 (s, 1 C), 14.23 (s, 1 C). **HRMS** (*m/z*): [M + H]$^{+}$ calc. for $C_{19}H_{25}N_6O_2$ 369.2034; found: 369.2033. **HPLC** (ACN with 0.1% TFA): t_R = 5.39 min (99.2% purity).

5-((*R*)-4-((*S*)-3-methylmorpholino)-5a,6,8,9-tetrahydro-5*H*-pyrimido[5',4':4,5]pyrrolo[2,1-*c*][1,4]oxazin-2-yl)pyridin-2-amine (6b) was prepared as described for its (*S,R*)-enantiomer **7a** starting from (*R*)-2-chloro-4-((*S*)-3-methylmorpholino)-5a,6,8,9-tetrahydro-5*H*-pyrimido[5',4':4,5]pyrrolo[2,1-*c*][1,4]oxazine **21b** (120 mg, 0.39 mmol, 1 eq) and boronic acid pinacol ester **38** in a 64% yield. The spectroscopic data are in agreement with those reported for the (*S,R*)-enantiomer. **HRMS** (*m/z*): [M +

H]$^+$ calc. for $C_{19}H_{25}N_6O_2$ 369.2034; found: 369.2033. **HPLC** (ACN with 0.1% TFA): t_R = 5.37 min (98.9% purity).

5-((*S*)-4-((*R*)-3-methylmorpholino)-5a,6,8,9-tetrahydro-5*H*-pyrimido[5',4':4,5]pyrrolo[2,1-*c*][1,4]oxazin-2-yl)pyridin-2-amine (7a) was prepared according to general procedure 4 from (*S*)-2-chloro-4-((*R*)-3-methylmorpholino)-5a,6,8,9-tetrahydro-5*H*-pyrimido[5',4':4,5]pyrrolo[2,1-*c*][1,4]oxazine **22a** (84 mg, 0.27 mmol, 1 eq) and (*E*)-*N*,*N*-dimethyl-*N*'-(5-(4,4,5,5-tetramethyl-1,3,2-dioxaborolan-2-yl)pyridin-2-yl)formimidamide **38** (75 mg, 0.27 mmol, 1 eq.). Purification by column chromatography on silica gel (cyclohexane / ethyl acetate 1:0 → 0:1) gave compound **7a** as a colorless solid (72 mg, 0.20 mmol, 74%). **^{1}H NMR** (400 MHz, DMSO-d_6): δ 8.82 (d, J = 2.4 Hz, 1 H), 8.17 (dd, J = 8.7, 2.3 Hz, 1 H), 6.45 (d, J = 8.7 Hz, 1 H), 6.27 (br s, 2 H), 4.35-4.30 (m, 1 H), 4.13-4.02 (m, 2 H), 3.92-3.81 (m, 2 H), 3.79-3.72 (m, 2 H), 3.69-3.61 (m, 2 H), 3.48 (td, J = 11.8, 2.9 Hz, 1 H), 3.36-3.29 (m, 1 H), 3.25-3.09 (m, 4 H), 2.57 (dd, J = 15.3, 4.7 Hz, 1 H), 1.21 (d, J = 6.7 Hz, 3 H). **^{13}C{^{1}H} NMR** (101 MHz, DMSO-d_6): δ 167.25 (s, 1 C), 160.73 (s, 1 C), 160.40 (s, 1 C), 157.20 (s, 1 C), 148.43 (s, 1 C), 136.23 (s, 1 C), 122.22 (s, 1 C), 106.87 (s, 1 C), 92.50 (s, 1 C), 70.41 (s, 1 C), 69.53 (s, 1 C), 66.53 (s, 1 C), 65.68 (s, 1 C), 56.38 (s, 1 C), 47.12 (s, 1 C), 41.64 (s, 1 C), 28.84 (s, 1 C), 13.88 (s, 1 C). **HRMS** (*m/z*): [M + H]$^+$ calc. for $C_{19}H_{25}N_6O_2$ 369.2034; found: 369.2034. **HPLC** (ACN with 0.1% TFA): t_R = 5.42 min (99.3% purity).

5-((*R*)-4-((*R*)-3-methylmorpholino)-5a,6,8,9-tetrahydro-5*H*-pyrimido[5',4':4,5]pyrrolo[2,1-*c*][1,4]oxazin-2-yl)pyridin-2-amine (7b) was prepared as described for its (*S,S*)-enantiomer **6a** starting from (*R*)-2-chloro-4-((*R*)-3-methylmorpholino)-5a,6,8,9-tetrahydro-5*H*-pyrimido[5',4':4,5]pyrrolo[2,1-*c*][1,4]oxazine **22b** (150 mg, 0.48 mmol, 1 eq) and boronic acid pinacol ester **38** in a 49% yield. The spectroscopic data are in agreement with those reported for the (*S,S*)-enantiomer. **HRMS** (*m/z*): [M + H]$^+$ calc. for $C_{19}H_{25}N_6O_2$ 369.2034; found: 369.2035. **HPLC** (ACN with 0.1% TFA): t_R = 5.35 min (99.6% purity).

5-[(9*S*)-6-{8-oxa-3-azabicyclo[3.2.1]octan-3-yl}-11-oxa-1,3,5-triazatricyclo[7.4.0.0^{2,7}]trideca-2(7),3,5-trien-4-yl]pyridin-2-amine (8a) was prepared according to general procedure 4 from (9*S*)-4-chloro-6-{8-oxa-3-azabicyclo[3.2.1]octan-3-yl}-11-oxa-1,3,5-triazatricyclo[7.4.0.0^{2,7}]trideca-2(7),3,5-triene **23a** (150 mg, 0.46 mmol, 1 eq) and (*E*)-*N*,*N*-dimethyl-*N*'-(5-(4,4,5,5-tetramethyl-1,3,2-dioxaborolan-2-yl)pyridin-2-yl)formimidamide **38** (128 mg, 0.46 mmol, 1 eq.). Purification by column chromatography on silica gel (cyclohexane / ethyl acetate 1:0 → 0:1) gave compound **8a** as a colorless solid (118 mg, 0.31 mmol, 67%). **^{1}H NMR** (400 MHz, DMSO-d_6): δ 8.81 (dd, J = 2.3, 0.8 Hz, 1 H), 8.15 (dd, J = 8.6, 2.3 Hz, 1 H), 6.44 (dd, J = 8.7, 0.8 Hz, 1 H), 6.26 (br s, 2 H), 4.38-4.34 (m, 2 H), 4.09-3.95 (m, 3 H), 3.87-3.80 (m, 1 H), 3.77-3.69 (m, 2 H), 3.34-3.27 (m, 1 H), 3.22-3.05 (m, 5 H), 2.63 (dd, J = 15.3, 4.8 Hz, 1 H), 1.84-1.74 (m, 4 H). **^{13}C{^{1}H} NMR** (101 MHz, DMSO-d_6): δ 167.09 (s, 1 C), 160.72 (s, 1 C), 160.25 (s, 1 C), 158.61 (s, 1 C), 148.43 (s, 1 C), 136.26 (s, 1 C), 122.22 (s, 1 C), 106.86 (s, 1 C), 92.56 (s, 1 C), 73.16 (s, 1 C), 73.15 (s, 1 C), 69.60 (s, 1 C), 65.70 (s, 1 C), 56.38 (s, 1 C), 50.70 (s, 1 C), 50.48 (s, 1 C), 41.59 (s, 1 C), 28.84 (s, 1 C), 27.56 (s, 1 C), 27.52 (s, 1 C). **HRMS** (*m/z*): [M + H]$^+$ calc. for $C_{20}H_{25}N_6O_2$ 381.2034; found: 381.2033. **HPLC** (ACN with 0.1% TFA): t_R = 5.34 min (98.2% purity).

5-[(9*R*)-6-{8-oxa-3-azabicyclo[3.2.1]octan-3-yl}-11-oxa-1,3,5-triazatricyclo[7.4.0.0^{2,7}]trideca-2(7),3,5-trien-4-yl]pyridin-2-amine (8b) was prepared as described for its (*S*)-enantiomer **8a** starting from (9*R*)-4-chloro-6-{8-oxa-3-azabicyclo[3.2.1]octan-3-yl}-11-oxa-1,3,5-triazatricyclo[7.4.0.0^{2,7}]trideca-2(7),3,5-triene **23b** (200 mg, 0.62 mmol, 1 eq) and boronic acid pinacol ester **38** in a 86% yield. The spectroscopic data agree with those reported for the (*S*)-enantiomer. **HRMS** (*m/z*): [M + H]$^+$ calc. for $C_{20}H_{25}N_6O_2$ 381.2034; found: 381.2036. **HPLC** (ACN with 0.1% TFA): t_R = 5.17 min (96.4% purity).

5-[(9*S*)-6-{3-oxa-8-azabicyclo[3.2.1]octan-8-yl}-11-oxa-1,3,5-triazatricyclo[7.4.0.0^{2,7}]trideca-2(7),3,5-trien-4-yl]pyridin-2-amine (9a) was prepared according to general procedure 4 from (9*S*)-4-chloro-6-{3-oxa-8-azabicyclo[3.2.1]octan-8-yl}-11-oxa-1,3,5-triazatricyclo[7.4.0.0^{2,7}]trideca-2(7),3,5-triene **24a** (150 mg, 0.46 mmol, 1 eq) and (*E*)-*N*,*N*-dimethyl-*N*'-(5-(4,4,5,5-tetramethyl-1,3,2-

dioxaborolan-2-yl)pyridin-2-yl)formimidamide **38** (128 mg, 0.46 mmol, 1 eq.). Purification by column chromatography on silica gel (cyclohexane / ethyl acetate 1:0 → 0:1) gave compound **9a** as a colorless solid (122 mg, 0.32 mmol, 69%). **^{1}H NMR** (400 MHz, $CDCl_3$): δ 9.04 (d, J = 2.2 Hz, 1 H), 8.35 (dd, J = 8.6, 2.2 Hz, 1 H), 6.50 (d, J = 8.6 Hz, 1 H), 4.61-4.51 (m, 4 H), 4.20 (dd, J = 13.4, 2.8 Hz, 1 H), 4.01-3.93 (m, 1 H), 3.88-3.77 (m, 4 H), 3.58 (d, J = 10.7 Hz, 2 H), 3.50 (td, J = 11.7, 3.0 Hz, 1 H), 3.36-3.23 (m, 2 H), 3.09 (dd, J = 14.9, 9.5 Hz, 1 H), 2.48 (dd, J = 14.9, 4.9 Hz, 1 H), 2.12-1.97 (m, 4 H). **^{13}C{^{1}H} NMR** (101 MHz, DMSO-d_6): δ 166.92 (s, 1 C), 160.96 (s, 1 C), 160.72 (s, 1 C), 155.76 (s, 1 C), 148.43 (s, 1 C), 136.26 (s, 1 C), 122.23 (s, 1 C), 106.86 (s, 1 C), 93.44 (s, 1 C), 70.42 (s, 1 C), 70.38 (s, 1 C), 69.71 (s, 1 C), 65.74 (s, 1 C), 56.46 (s, 1 C), 55.11 (s, 1 C), 55.04 (s, 1 C), 41.51 (s, 1 C), 28.03 (s, 1 C), 26.52 (s, 1 C), 26.45 (s, 1 C). **HRMS** (*m/z*): $[M + H]^+$ calc. for $C_{20}H_{25}N_6O_2$ 381.2034; found: 381.2036. **HPLC** (ACN with 0.1% TFA): t_R = 5.39 min (97.2% purity).

5-[(9*R*)-6-{3-oxa-8-azabicyclo[3.2.1]octan-8-yl}-11-oxa-1,3,5-triazatricyclo[7.4.0.0^{2,7}]trideca-2(7),3,5-trien-4-yl]pyridin-2-amine (9b) was prepared as described for its (*S*)-enantiomer **9a** starting from (9*S*)-4-chloro-6-{3-oxa-8-azabicyclo[3.2.1]octan-8-yl}-11-oxa-1,3,5-triazatricyclo[7.4.0.0^{2,7}]trideca-2(7),3,5-triene **24b** (200 mg, 0.62 mmol, 1 eq) and boronic acid pinacol ester **38** in a 88% yield. The spectroscopic data agree with those reported for the (*S*)-enantiomer. **HRMS** (*m/z*): $[M + H]^+$ calc. for $C_{20}H_{25}N_6O_2$ 381.2034; found: 381.2040. **HPLC** (ACN with 0.1% TFA): t_R = 5.35 min (96.7% purity).

(*S*)-5-(4-(3,3-dimethylmorpholino)-5a,6,8,9-tetrahydro-5*H*-pyrimido[5',4':4,5]pyrrolo[2,1-*c*][1,4]oxazin-2-yl)pyridin-2-amine (10a) was prepared according to general procedure 4 from (*S*)-2-chloro-4-(3,3-dimethylmorpholino)-5a,6,8,9-tetrahydro-5*H*-pyrimido[5',4':4,5]pyrrolo[2,1-*c*][1,4]oxazine **25a** (150 mg, 0.46 mmol, 1 eq) and (*E*)-*N*,*N*-dimethyl-*N*'-(5-(4,4,5,5-tetramethyl-1,3,2-dioxaborolan-2-yl)pyridin-2-yl)formimidamide **38** (127 mg, 0.46 mmol, 1 eq.). Purification by column chromatography on silica gel (cyclohexane / ethyl acetate 1:0 → 3:7) gave compound **10a** as a colorless solid (124 mg, 0.32 mmol, 70%). **^{1}H NMR** (400 MHz, $CDCl_3$): δ 8.83 (d, J = 2.2 Hz, 1 H), 8.16 (dd, J = 8.7, 2.3 Hz, 1 H), 6.47 (d, J = 8.7 Hz, 1 H), 6.29 (br s, 2 H), 4.01 (dd, J = 13.4, 2.6 Hz, 1 H), 3.90-

3.83 (m, 1 H), 3.79-3.65 (m, 4 H), 3.36-3.29 (m, 3 H), 3.20-3.04 (m, 4 H), 2.97 (dd, *J* = 16.0, 9.1 Hz, 1 H), 2.40 (dd, *J* = 15.9, 5.0 Hz, 1 H), 1.47 (s, 3 H), 1.43 (s, 3 H). **^{13}C{^{1}H} NMR** (101 MHz, DMSO-d_6): δ 167.29 (s, 1 C), 160.72 (s, 1 C), 160.67 (s, 1 C), 159.98 (s, 1 C), 148.38 (s, 1 C), 136.03 (s, 1 C), 122.33 (s, 1 C), 107.05 (s, 1 C), 101.51 (s, 1 C), 77.82 (s, 1 C), 69.73 (s, 1 C), 67.12 (s, 1 C), 65.57 (s, 1 C), 56.91 (s, 1 C), 53.80 (s, 1 C), 43.68 (s, 1 C), 41.57 (s, 1 C), 27.77 (s, 1 C), 21.74 (s, 1 C), 20.72 (s, 1 C). **HRMS** (*m/z*): $[M + H]^+$ calc. for $C_{20}H_{27}N_6O_2$ 383.2190; found: 383.2192. **HPLC** (ACN with 0.1% TFA): t_R = 5.58 min (98.1% purity).

(*R*)-5-(4-(3,3-dimethylmorpholino)-5a,6,8,9-tetrahydro-5*H*-pyrimido[5',4':4,5]pyrrolo[2,1-*c*][1,4]oxazin-2-yl)pyridin-2-amine (10b) was prepared as described for its (*S*)-enantiomer **10a** starting from (*S*)-2-chloro-4-(3,3-dimethylmorpholino)-5a,6,8,9-tetrahydro-5*H*-pyrimido[5',4':4,5]pyrrolo[2,1-*c*][1,4]oxazine **25b** (150 mg, 0.46 mmol, 1 eq) and boronic acid pinacol ester **38** in a 88% yield. The spectroscopic data agree with those reported for the (*S*)-enantiomer. **HRMS** (*m/z*): $[M + H]^+$ calc. for $C_{20}H_{27}N_6O_2$ 383.2190; found: 383.2193. **HPLC** (ACN with 0.1% TFA): t_R = 5.61 min (99.5% purity).

5-((*R*)-4-((*R*)-3-methylmorpholino)-5a,6,8,9-tetrahydro-5*H*-pyrimido[5',4':4,5]pyrrolo[2,1-*c*][1,4]oxazin-2-yl)pyrimidin-2-amine (11b). Chloropyrimidine derivative **22b** (100 mg, 0.32 mmol, 1.0 eq.) and 2-aminopyridine-5-boronic acid pinacol ester (71.2 mg, 0.32 mmol, 1.0 eq.) were charged in a flask. Under nitrogen atmosphere, 1,4-dioxane (2 mL) was added, followed by K_3PO_4 (137 mg, 0.65 mmol, 2 eq.) aqueous solution (1 mL) and chloro(2-dicyclohexylphosphino-2',4',6'-triisopropyl-1,1'-biphenyl)[2-(2'-amino-1,1'-biphenyl)]-palladium(II) (XPhos Pd G2, 12.7 mg, 0.016 mmol, 0.05 eq.). The resulting mixture was stirred at 95 °C overnight. After completion of the reaction monitored by TLC, a 15% NH_4Cl-solution (15 mL) was added and the aqueous layer was extracted with EtOAc (3 x). The combined organic layers were dried over anhydrous Na_2SO_4, filtered and the solvent was evaporated under reduced pressure. Purification by column chromatography on silica gel (cyclohexane / ethyl acetate 1:0 → 0:1) gave compound **11b** as a colorless solid (100 mg, 0.27 mmol, 84%). **^{1}H NMR** (400 MHz, DMSO-d_6): δ 8.98 (s, 2 H), 7.00 (br s, 2 H), 4.35-4.29 (m, 1 H), 4.07-4.02 (m, 2 H), 3.92-3.85 (m, 2 H), 3.79-3.61 (m, 4 H), 3.46 (td, *J* = 11.7, 2.9 Hz, 1 H), 3.35-3.29 (m, 1 H), 3.26-3.09 (m, 4 H), 2.66

(dd, J = 15.4, 4.8 Hz, 1 H), 1.17 (d, J = 6.7 Hz, 3 H). **^{13}C{^{1}H} NMR** (101 MHz, DMSO-d_6): δ 167.01 (s, 1 C), 164.01 (s, 1 C), 158.80 (s, 1 C), 157.70 (s, 2 C), 157.24 (s, 1 C), 120.30 (s, 1 C), 93.09 (s, 1 C), 70.37 (s, 1 C), 69.66 (s, 1 C), 66.50 (s, 1 C), 65.73 (s, 1 C), 56.28 (s, 1 C), 47.12 (s, 1 C), 41.54 (s, 1 C), 39.63 (s, 1 C), 28.71 (s, 1 C), 13.82 (s, 1 C). **HRMS** (*m/z*): [M + H]$^+$ calc. for $C_{18}H_{24}N_7O_2$ 370.1986; found: 370.1991. **HPLC**: t_R = 6.09 min (98.7% purity).

5-((*R*)-4-((*R*)-3-methylmorpholino)-5a,6,8,9-tetrahydro-5*H*-pyrimido[5',4':4,5]pyrrolo[2,1-*c*][1,4]oxazin-2-yl)pyrazin-2-amine (12b). Chloropyrimidine derivative **22b** (200 mg, 0.65 mmol, 1.0 eq.), **39** (428 mg, 1.94 mmol, 3.0 eq.) and Cs_2CO_3 (421 mg, 1.29 mmol, 2.0 eq.) were charged in a flask. Under nitrogen atmosphere, THF (2 mL) was added, followed by [1,1′-bis(diphenylphosphino)ferrocene]dichloropalladium(II) (Pd(dppf)Cl_2, 47.2 mg, 0.065 mmol, 0.1 eq.). The resulting mixture was stirred at reflux for 6 hrs. After completion of the reaction monitored by TLC, a 15% NH_4Cl-solution (15 mL) was added and the aqueous layer was extracted with EtOAc (3 x). The combined organic layers were dried over anhydrous Na_2SO_4, filtered and the solvent was evaporated under reduced pressure. Purification by column chromatography on silica gel (cyclohexane / ethyl acetate 1:0 → 0:1) gave compound **12b** as a colorless solid (163 mg, 0.44 mmol, 68%). **^{1}H NMR** (400 MHz, DMSO-d_6): δ 8.78 (s, 1 H), 7.91 (s, 1 H), 6.73 (br s, 2 H), 4.36-4.30 (m, 1 H), 4.09-4.00 (m, 2 H), 3.92-3.85 (m, 2 H), 3.78-3.61 (m, 4 H), 3.46 (td, J = 11.7, 2.9 Hz, 1 H), 3.29-3.09 (m, 5 H), 2.67 (dd, J = 15.4, 4.6 Hz, 1 H), 1.17 (d, J = 6.7 Hz, 3 H). **^{13}C{^{1}H} NMR** (101 MHz, DMSO-d_6): δ 167.44 (s, 1 C), 160.37 (s, 1 C), 157.39 (s, 1 C), 155.84 (s, 1 C), 142.83 (s, 1 C), 138.67 (s, 1 C), 130.87 (s, 1 C), 93.51 (s, 1 C), 70.37 (s, 1 C), 69.64 (s, 1 C), 66.52 (s, 1 C), 65.73 (s, 1 C), 56.27 (s, 1 C), 47.11 (s, 1 C), 41.60 (s, 1 C), 39.65 (s, 1 C), 28.71 (s, 1 C), 13.84 (s, 1 C). **HRMS** (*m/z*): [M + H]$^+$ calc. for $C_{18}H_{24}N_7O_2$ 370.1986; found: 370.1986. **HPLC**: t_R = 5.53 min (98.1% purity).

4-methyl-5-((*R*)-4-((*R*)-3-methylmorpholino)-5a,6,8,9-tetrahydro-5*H*-pyrimido[5',4':4,5]pyrrolo[2,1-*c*][1,4]oxazin-2-yl)pyridin-2-amine (13b). *Step 1*. (*E*)-*N*'-(5-bromo-4-methylpyridin-2-yl)-*N*,*N*-dimethylformimidamide **40** (281 mg, 1.16 mmol, 3.0 eq.), 2-dicyclohexylphosphino-2′,4′,6′-triisopropylbiphenyl (XPhos, 55.4 mg, 0.12 mmol, 0.3 eq.), KOAc (342

mg, 3.48 mmol, 9.0 eq.) and bis(pinacolato)diboron (312 mg, 3.48 mmol, 9.0 eq.) were charged into a flask. Under nitrogen atmosphere, EtOH (11.6 mL) was added ant the reaction mixture was heated at 80 °C. Chloro(2-dicyclohexylphosphino-2',4',6'-triisopropyl-1,1'-biphenyl)[2-(2'-amino-1,1'-biphenyl)]-palladium(II) (XPhos Pd G2, 45.7 mg, 0.058 mmol, 0.15 eq.) was added and the reaction mixture was stirred at 80 °C for 2 hrs. *Step 2.* Then, the mixture was allowed to cool down to room temperature. The chloropyrimidine derivative **22b** (120 mg, 0.39 mmol, 1.0 eq.), 1,4-dioxane (2 mL) and a 1.8M aqueous K_2CO_3-solution (650 µL, 1,16 mmol, 3.0 eq.) were added. The reaction mixture was stirred at 95 °C for 3 hrs. *Step 3.* After completion of the reaction, the mixture was allowed to cool down to room temperature, a 3M HCl-solution (1.3 mL, 3.87 mmol, 10.0 eq.) was added and the reaction mixture was stirred at 80 °C overnight. A 2M aqueous NaOH-solution (15 mL) was added until pH 9-10. The aqueous layer was extracted with EtOAc (3 x). The combined organic layers were dried over anhydrous Na_2SO_4, filtered and the solvent was evaporated under reduced pressure. Purification by column chromatography on silica gel (cyclohexane / ethyl acetate 1:0 → 0:1) gave compound **13b** as a colorless solid (46 mg, 0.12 mmol, 31%). **^{1}H NMR** (400 MHz, $CDCl_3$): δ 8.64 (s, 1 H), 6.35 (s, 1 H), 4.57 (br s, 2 H), 4.34-4.27 (m, 1 H), 4.13 (dd, J = 13.4, 2.4 Hz, 1 H), 4.04-3.93 (m, 3 H), 3.85-3.71 (m, 4 H), 3.59 (td, J = 11.8, 2.9 Hz, 1 H), 3.47 (td, J = 11.7, 2.9 Hz, 1 H), 3.39-3.30 (m, 2 H), 3.28-3.17 (m, 2 H), 2.62 (dd, J = 14.9, 4.8 Hz, 1 H), 2.54 (s, 3 H), 1.28 (d, J = 6.8 Hz, 3 H). **^{13}C{^{1}H} NMR** (101 MHz, $CDCl_3$): δ 167.57 (s, 1 C), 163.28 (s, 1 C), 158.42 (s, 1 C), 158.08 (s, 1 C), 150.47 (s, 1 C), 148.84 (s, 1 C), 126.18 (s, 1 C), 109.96 (s, 1 C), 92.79 (s, 1 C), 71.23 (s, 1 C), 70.57 (s, 1 C), 67.42 (s, 1 C), 66.68 (s, 1 C), 56.89 (s, 1 C), 48.07 (s, 1 C), 42.08 (s, 1 C), 40.43 (s, 1 C), 29.78 (s, 1 C), 22.04 (s, 1 C), 14.26 (s, 1 C). **HRMS** (*m/z*): $[M + H]^+$ calc. for $C_{18}H_{23}N_6O_2$ 383.2190; found: 383.2191. **HPLC** (ACN with 0.1% TFA): t_R = 5.18 min (96.7% purity).

3-methyl-5-((*R*)-4-((*R*)-3-methylmorpholino)-5a,6,8,9-tetrahydro-5*H*-pyrimido[5',4':4,5]pyrrolo[2,1-*c*][1,4]oxazin-2-yl)pyridin-2-amine (14b) was prepared according to general procedure 4 from (*R*)-2-chloro-4-((*R*)-3-methylmorpholino)-5a,6,8,9-tetrahydro-5*H*-pyrimido[5',4':4,5]pyrrolo[2,1-*c*][1,4]oxazine **22b** (120 mg, 0.39 mmol, 1 eq) and (*E*)-*N*,*N*-dimethyl-*N*'-(3-methyl-5-(4,4,5,5-tetramethyl-1,3,2-dioxaborolan-2-yl)pyridin-2-yl)formimidamide **41** (112 mg,

0.39 mmol, 1 eq.). Purification by column chromatography on silica gel (cyclohexane / ethyl acetate 1:0 → 0:1) gave compound **14b** as a colorless solid (98 mg, 0.26 mmol, 66%). **^{1}H NMR** (400 MHz, DMSO-d_6): δ 8.70 (d, J = 2.1 Hz, 1 H), 8.01 (s, 1 H), 6.05 (br s, 2 H), 4.34-4.28 (m, 1 H), 4.09-4.02 (m, 2 H), 3.92-3.83 (m, 2 H), 3.78-3.62 (m, 4 H), 3.47 (td, J = 11.8, 2.9 Hz, 1 H), 3.30-3.28 (m, 1 H), 3.26-3.09 (m, 4 H), 2.64 (dd, J = 15.3, 4.7 Hz, 1 H), 2.08 (s, 3 H), 1.17 (d, J = 6.7 Hz, 3 H). **^{13}C{^{1}H} NMR** (101 MHz, DMSO-d_6): δ 167.15 (s, 1 C), 160.53 (s, 1 C), 159.35 (s, 1 C), 157.36 (s, 1 C), 145.97 (s, 1 C), 135.92 (s, 1 C), 122.83 (s, 1 C), 114.54 (s, 1 C), 92.65 (s, 1 C), 70.41 (s, 1 C), 69.67 (s, 1 C), 66.54 (s, 1 C), 65.74 (s, 1 C), 56.29 (s, 1 C), 47.14 (s, 1 C), 41.57 (s, 1 C), 39.63 (s, 1 C), 28.74 (s, 1 C), 17.20 (s, 1 C), 13.77 (s, 1 C). **HRMS** (*m/z*): $[M + H]^+$ calc. for $C_{18}H_{23}N_6O_2$ 383.2190; found: 383.2191. **HPLC** (ACN with 0.1% TFA): t_R = 5.67 min (99.2% purity).

4-methoxy-5-((*R*)-4-((*R*)-3-methylmorpholino)-5a,6,8,9-tetrahydro-5*H*-pyrimido[5',4':4,5]pyrrolo[2,1-*c*][1,4]oxazin-2-yl)pyridin-2-amine (15b). *Step 1*. (tert-butyl (5-bromo-4-methoxypyridin-2-yl)carbamate **42** (200 mg, 0.66 mmol, 1.0 eq.), 2-dicyclohexylphosphino-2′,4′,6′-triisopropylbiphenyl (XPhos, 31.5 mg, 0.066 mmol, 0.1 eq.), KOAc (194 mg, 1.98 mmol, 3.0 eq.) and bis(pinacolato)diboron (178 mg, 1.98 mmol, 3.0 eq.) were charged into a flask. Under nitrogen atmosphere, EtOH (6.6 mL) was added and the reaction mixture was heated at 60 °C. Chloro(2-dicyclohexylphosphino-2',4',6'-triisopropyl-1,1'-biphenyl)[2-(2'-amino-1,1'-biphenyl)]-palladium(II) (XPhos Pd G2, 26 mg, 0.033 mmol, 0.05 eq.) was added and the reaction mixture was stirred at 80 °C for 3 hrs. *Step 2.* Then, the mixture was allowed to cool down to room temperature. The chloropyrimidine derivative **22b** (102 mg, 0.33 mmol, 0.5 eq.) and K_3PO_4 (210 mg, 0.99 mmol, 1.5 eq.) in water (1.7 mL) were added. The reaction mixture was stirred at 80 °C for 3.5 hrs. *Step 3.* After completion of the reaction monitored by TLC, a 15% NH_4Cl-solution (10 mL) was added and the aqueous layer was extracted with EtOAc (3 x). The combined organic layers were dried over anhydrous Na_2SO_4, filtered and the solvent was evaporated under reduced pressure. The crude was dissolved in 1,4-dioxane (1.6 mL) and a 3M HCl-solution (0.7 mL, 1.98 mmol, 3.0 eq.) was added and the reaction mixture was stirred at 80 °C for 3 hrs. A 2M aqueous NaOH-solution was added until pH 9-10. The aqueous layer was extracted with EtOAc (3 x). The combined organic layers were dried over anhydrous

Na_2SO_4, filtered and the solvent was evaporated under reduced pressure. Purification by column chromatography on silica gel (cyclohexane / ethyl acetate 1:0 → 0:1) gave compound **15b** as a colorless solid (58 mg, 0.15 mmol, 44%). **^{1}H NMR** (400 MHz, DMSO-d_6): δ 8.18 (s, 1 H), 6.04 (br s, 2 H), 6.02 (s, 1 H), 4.32-4.26 (m, 1 H), 4.00-3.90 (m, 2 H), 3.89-3.81 (m, 1 H), 3.75-3.69 (m, 2 H), 3.71 (s, 3 H), 3.67-3.58 (m, 2 H), 3.44 (td, J = 11.7, 2.9 Hz, 1 H), 3.30-3.25 (m, 2 H), 3.21-3.05 (m, 4 H), 2.64 (dd, J = 15.3, 4.7 Hz, 1 H), 1.16 (d, J = 6.7 Hz, 3 H). **^{13}C{^{1}H} NMR** (101 MHz, DMSO-d_6): δ 167.05 (s, 1 C), 164.76 (s, 1 C), 161.73 (s, 1 C), 160.96 (s,1 C), 157.24 (s, 1 C), 150.54 (s, 1 C), 115.28 (s, 1 C), 92.45 (s, 1 C), 89.20 (s, 1 C), 70.45 (s, 1 C), 69.60 (s, 1 C), 66.51 (s, 1 C), 65.66 (s, 1 C), 56.24 (s, 1 C), 54.84 (s, 1 C), 47.03 (s, 1 C), 41.59 (s, 1 C), 39.70 (s, 1 C), 28.69 (s, 1 C), 13.76 (s, 1 C). **HRMS** (*m/z*): [M + H]$^+$ calc. for $C_{20}H_{27}N_6O_3$ 399.2139; found: 399.2145. **HPLC** (ACN with 0.1% TFA): t_R = 4.28 min (95.3% purity).

4-(dimethoxymethyl)-5-((*R*)-4-((*R*)-3-methylmorpholino)-5a,6,8,9-tetrahydro-5*H*-pyrimido[5',4':4,5]pyrrolo[2,1-*c*][1,4]oxazin-2-yl)pyridin-2-amine (16b). was prepared according to general procedure 6 from **18b** (169 mg, 0.26 mmol, 1 eq.). Purification by column chromatography on silica gel (cyclohexane / ethyl acetate 1:0 → 0:1) gave compound **16b** as a colorless solid (88 mg, 0.20 mmol, 76%). **^{1}H NMR** (400 MHz, DMSO-d_6): δ 8.41 (s, 1 H), 6.66 (s, 1 H), 6.45 (s, 1 H), 6.24 (br s, 2 H), 4.33-4.26 (m, 1 H), 3.99-3.94 (m, 2 H), 3.92-3.84 (m, 2 H), 3.79-3.72 (m, 2 H), 3.69-3.61 (m, 2 H), 3.46 (td, J = 11.7, 2.8 Hz, 1 H), 3.35-3.26 (m, 2 H), 3.24-3.10 (m, 3 H), 3.22 (s, 3 H), 3.16 (s, 3 H), 2.68 (dd, J = 15.3, 4.9 Hz, 1 H), 1.19 (d, J = 6.7 Hz, 3 H). **^{13}C{^{1}H} NMR** (101 MHz, DMSO-d_6): δ 166.97 (s, 1 C), 162.33 (s, 1 C), 159.98 (s, 1 C), 157.32 (s, 1 C), 150.47 (s, 1 C), 145.81 (s, 1 C), 122.14 (s, 1 C), 104.47 (s, 1 C), 99.62 (s, 1 C), 92.62 (s, 1 C), 70.39 (s, 1 C), 69.65 (s, 1 C), 66.49 (s, 1 C), 65.68 (s, 1 C), 56.33 (s, 1 C), 53.71 (s, 1 C), 53.26 (s, 1 C), 47.11 (s, 1 C), 41.68 (s, 1 C), 39.79 (s, 1 C), 28.74 (s, 1 C), 13.88 (s, 1 C). **HRMS** (*m/z*): [M + H]$^+$ calc. for $C_{22}H_{31}N_6O_4$ 443.2401; found: 443.2405. **HPLC** (ACN with 0.1% TFA): t_R = 5.19 min (99.5% purity).

4-(dimethoxymethyl)-5-((*R*)-4-((*R*)-3-methylmorpholino)-5a,6,8,9-tetrahydro-5*H*-pyrimido[5',4':4,5]pyrrolo[2,1-*c*][1,4]oxazin-2-yl)pyrimidin-2-amine (17b) was prepared according to general procedure 6 from **19b** (234 mg, 0.36 mmol, 1 eq.). Purification by column chromatography on silica gel (cyclohexane / ethyl acetate 1:0 → 0:1) gave compound **17b** as a colorless solid (122 mg, 0.28 mmol, 76%). **^{1}H NMR** (400 MHz, DMSO-d_6): δ 8.72 (s, 1 H), 6.97 (br s, 2 H), 6.36 (s, 1 H), 4.33-4.27 (m, 1 H), 4.01-3.85 (m, 4 H), 3.79-3.72 (m, 2 H), 3.68-3.60 (m, 2 H), 3.46 (td, J = 11.7, 2.8 Hz, 1 H), 3.36-3.29 (m, 1 H), 3.27 (s, 3 H), 3.25 (s, 3 H), 3.26-3.10 (m, 4 H), 2.68 (dd, J = 15.4, 4.9 Hz, 1 H), 1.18 (d, J = 6.7 Hz, 3 H). **^{13}C{^{1}H} NMR** (101 MHz, DMSO-d_6): δ 166.95 (s, 1 C), 162.97 (s, 1 C), 162.76 (s, 1 C), 160.70 (s, 1 C), 160.57 (s, 1 C), 157.25 (s, 1 C), 120.35 (s, 1 C), 99.37 (s, 1 C), 92.84 (s, 1 C), 70.35 (s, 1 C), 69.66 (s, 1 C), 66.48 (s, 1 C), 65.69 (s, 1 C), 56.33 (s, 1 C), 53.94 (s, 1 C), 53.71 (s, 1 C), 47.13 (s, 1 C), 41.65 (s, 1 C), 39.68 (s, 1 C), 28.70 (s, 1 C), 13.96 (s, 1 C). **HRMS** (*m/z*): $[M + H]^+$ calc. for $C_{21}H_{30}N_7O_4$ 444.2354; found: 444.2358. **HPLC**: t_R = 5.88 min (98.3% purity).

tert-butyl N-[(tert-butoxy)carbonyl]-N-[4-(dimethoxymethyl)-5-[(9*R*)-6-[(3*R*)-3-methylmorpholin-4-yl]-11-oxa-1,3,5-triazatricyclo[7.4.0.0^{2,7}]trideca-2(7),3,5-trien-4-yl]pyridin-2-yl]carbamate (18b) was prepared according to general procedure 5 from **44** (289 mg, 0.65 mmol, 1.0 eq.) and **22b** (200 mg, 0.65 mmol, 1 eq.). Purification by column chromatography on silica gel (cyclohexane / ethyl acetate 1:0 → 1:1) gave compound **18b** as a colorless solid (174 mg, 0.27 mmol, 42%). The product is a mixture of mono- and di-Boc protected derivative and was used for the next step without further purification. **MALDI-MS**: *m/z* = 643.813 ($[M + H]^+$); 543.329 ($[M – Boc + H]^+$).

tert-butyl *N*-[(tert-butoxy)carbonyl]-*N*-[4-(dimethoxymethyl)-5-[(9*R*)-6-[(3*R*)-3-methylmorpholin-4-yl]-11-oxa-1,3,5-triazatricyclo[7.4.0.0^{2,7}]trideca-2(7),3,5-trien-4-yl]pyrimidin-2-yl]carbamate (19b) was prepared according to general procedure 5 from **49** (289 mg, 0.65 mmol, 1.0 eq.) and **22b** (200 mg, 0.65 mmol, 1 eq.). Purification by column chromatography on silica gel (cyclohexane / ethyl acetate 1:0 → 1:1) gave compound **19b** as a yellowish solid (240 mg, 0.37 mmol, 57%). **^{1}H NMR** (400 MHz, DMSO-d_6): δ 9.20 (s, 1 H), 6.36 (s, 1 H), 4.36-4.30 (m, 1 H), 4.05-3.08 (m, 4 H), 3.81-3.76 (m, 2 H), 3.70-3.62 (m, 2 H), 3.47 (td, J = 11.7, 2.9 Hz, 1 H), 3.33 (s, 3

H), 3.28 (s, 3 H), 3.39-3.14 (m, 5 H), 2.76 (dd, *J* = 15.6, 5.0 Hz, 1 H), 1.42 (s, 18 H), 1.21 (d, *J* = 6.8 Hz, 3 H). **MALDI-MS**: *m/z* = 644.445 ($[M + H]^+$).

(*S*)-2-chloro-4-morpholino-5a,6,8,9-tetrahydro-5*H*-pyrimido[5',4':4,5]pyrrolo[2,1-*c*][1,4]oxazine (20a) was prepared according to general procedure 3 from 4-(2,6-dichloropyrimidin-4-yl)morpholine **26** (653 mg, 2.79 mmol, 1 eq.) and (*R*)-tetrahydro-3*H*-[1,2,3]oxathiazolo[4,3-*c*][1,4]oxazine 1,1-dioxide **33b** (500 mg, 2.79 mmol, 1 eq.). Purification by column chromatography (cyclohexane / EtOAc 2:1 → 1:1) gave compound **20a** as a colorless solid (550 mg, 1.85 mmol, 66%). **^{1}H NMR** (400 MHz, $CDCl_3$): δ 4.01 (dd, *J* = 13.5, 2.9 Hz, 1 H), 3.95-3.87 (m, 1 H), 3.79-3.72 (m, 2 H), 3.68-3.65 (m, 4 H), 3.59-3.49 (m, 4 H), 3.38 (td, *J* = 11.7, 2.9 Hz, 1 H), 3.23 (t, *J* = 11.0 Hz, 1H), 3.18-3.09 (m, 2 H), 2.50 (dd, *J* = 15.0, 5.1 Hz, 1 H). **^{13}C{^{1}H} NMR** (101 MHz, $CDCl_3$): δ 167.84 (s, 1 C), 158.32 (s, 1 C), 158.24 (s, 1 C), 93.08 (s, 1 C), 70.49 (s, 1 C), 66.73 (s, 2 C), 66.58 (s, 1 C), 57.32 (s, 1 C), 45.81 (s, 2 C), 42.15 (s, 1 C), 29.06 (s, 1 C). **MALDI-MS**: *m/z* = 297.301 ($[M + H]^+$). **HPLC**: t_R = 6.36 min (97.7% purity). (*S*)-enantiomer: $[\alpha_D]$ = + 4.0 ($CHCl_3$, c = 1.2).

(*R*)-2-chloro-4-morpholino-5a,6,8,9-tetrahydro-5*H*-pyrimido[5',4':4,5]pyrrolo[2,1-*c*][1,4]oxazine (20b) was prepared as described for its (*S*)-enantiomer **20a** starting from (*S*)-tetrahydro-3*H*-[1,2,3]oxathiazolo[4,3-*c*][1,4]oxazine 1,1-dioxide **33a** (506 mg, 2.16 mmol, 1 eq.) in 73% yield. The spectroscopic data are in agreement with those reported for the (*S*)-enantiomer. **HPLC**: t_R = 6.35 min (98.0% purity). (*R*)-enantiomer: $[\alpha_D]$ = - 3.3 ($CHCl_3$, c = 1.5).

(*S*)-4-chloro-2-morpholino-5a,6,8,9-tetrahydro-5*H*-pyrimido[5',4':4,5]pyrrolo[2,1-*c*][1,4]oxazine (20c). was prepared according to general procedure 3 from 4-(4,6-dichloropyrimidin-2-yl)morpholine **32** (298 mg, 1.27 mmol, 1 eq) and (*R*)-tetrahydro-3*H*-[1,2,3]oxathiazolo[4,3-*c*][1,4]oxazine 1,1-dioxide **33b** (228 mg, 1.27 mmol, 1 eq.). Purification by column chromatography (cyclohexane / EtOAc 2:1 → 1:1) gave compound **20c** as a colorless solid (286 mg, 0.96 mmol, 76%). **^{1}H NMR** (400 MHz, $CDCl_3$): δ 4.02-3.94 (m, 2 H), 3.89-3.87 (m, 1 H), 3.86-3.84 (m, 1 H), 3.75-3.70 (m, 8 H), 3.44 (td, *J* = 11.7, 3.0 Hz, 1 H), 3.26 (t, *J* = 11.0 Hz, 1 H), 3.25-3.19 (m, 1 H), 2.99 (dd, *J* = 16.1, 9.4 Hz, 1 H), 2.42 (dd, *J* = 16.1, 5.0 Hz, 1 H). **^{13}C{^{1}H} NMR** (101 MHz, $CDCl_3$): δ 166.64 (s, 1

C), 161.92 (s, 1 C), 151.94 (s, 1 C), 104.19 (s, 1 C), 71.07 (s, 1 C), 66.83 (s, 2 C), 66.40 (s, 1 C), 57.11 (s, 1 C), 44.54 (s, 2 C), 41.79 (s, 1 C), 26.35 (s, 1 C). **MALDI-MS**: *m/z* = 297.030 ($[M + H]^+$). (*S*)-enantiomer: $[\alpha_D]$ = - 61.0 ($CHCl_3$, c = 1.1).

(*R*)-4-chloro-2-morpholino-5a,6,8,9-tetrahydro-5*H*-pyrimido[5',4':4,5]pyrrolo[2,1-*c*][1,4]oxazine (20d) was prepared as described for its (*S*)-enantiomer **20c** starting from (*R*)-tetrahydro-3*H*-[1,2,3]oxathiazolo[4,3-*c*][1,4]oxazine 1,1-dioxide **33a** (281 mg, 1.57 mmol, 1 eq.) in 24% yield. The spectroscopic data are in agreement with those reported for the (*S*)-enantiomer. (*R*)-enantiomer: $[\alpha_D]$ = + 56.2 ($CHCl_3$, c = 1.4).

(*S*)-2-chloro-4-((*S*)-3-methylmorpholino)-5a,6,8,9-tetrahydro-5*H*-pyrimido[5',4':4,5]pyrrolo[2,1-*c*][1,4]oxazine (21a) was prepared according to general procedure 3 from (*S*)-4-(2,6-dichloropyrimidin-4-yl)-3-methylmorpholine **27** (3.68 g, 14.92 mmol, 1 eq.) and (*R*)-tetrahydro-3*H*-[1,2,3]oxathiazolo[4,3-*c*][1,4]oxazine 1,1-dioxide **33b** (2.67 g, 14.92 mmol, 1 eq.). Purification by column chromatography (cyclohexane / ethyl acetate 1:0 → 3:2) gave compound **21a** as a yellowish solid (853 mg, 2.75 mmol, 18%). **^{1}H NMR** (400 MHz, DMSO-d_6): δ 4.23-4.18 (m, 1 H), 3.97-3.73 (m, 6 H), 3.66-3.57 (m, 2 H), 3.42 (td, *J* = 11.8, 3.0 Hz, 1 H), 3.34-3.29 (m, 1 H), 3.24-3.08 (m, 4 H), 2.68 (dd, *J* = 15.4, 5.1 Hz, 1 H), 1.17 (d, *J* = 6.7 Hz, 3 H). **^{13}C{^{1}H} NMR** (101 MHz, DMSO-d_6): δ 167.87 (s, 1 C), 157.71 (s, 1 C), 157.48 (s, 1 C), 93.25 (s, 1 C), 70.13 (s, 1 C), 69.64 (s, 1 C), 66.27 (s, 1 C), 65.69 (s, 1 C), 56.71 (s, 1 C), 47.18 (s, 1 C), 41.55 (s, 1 C), 39.67 (s, 1 C), 28.07 (s, 1 C), 14.10 (s, 1 C). **MALDI-MS**: *m/z* = 311.109 ($[M + H]^+$). **HPLC**: t_R = 7.03 min (96.5% purity).

(*R*)-2-chloro-4-((*S*)-3-methylmorpholino)-5a,6,8,9-tetrahydro-5*H*-pyrimido[5',4':4,5]pyrrolo[2,1-*c*][1,4]oxazine (21b) was prepared as described for its (*S,R*)-enantiomer **22a** starting from (*S*)-tetrahydro-3*H*-[1,2,3]oxathiazolo[4,3-*c*][1,4]oxazine 1,1-dioxide **33a** (1.0 g, 5.58 mmol, 1 eq.) in 24% yield. The spectroscopic data are in agreement with those reported for the (*S,R*)-enantiomer.

(*S*)-2-chloro-4-((*R*)-3-methylmorpholino)-5a,6,8,9-tetrahydro-5*H*-pyrimido[5',4':4,5]pyrrolo[2,1-*c*][1,4]oxazine (22a) was prepared according to general procedure 3 from (*R*)-4-(2,6-dichloropyrimidin-4-yl)-3-methylmorpholine **28** (1.15 g, 4.65 mmol, 1 eq.) and (*R*)-tetrahydro-3*H*-[1,2,3]oxathiazolo[4,3-*c*][1,4]oxazine 1,1-dioxide **33b** (833 mg, 4.65 mmol, 1 eq.). Purification by column chromatography (cyclohexane / ethyl acetate 1:0 → 4:1) gave compound **22a** as a yellowish solid (1.05 g, 3.39 mmol, 73%). **^{1}H NMR** (400 MHz, DMSO-d_6): δ 4.20-4.14 (m, 1 H), 3.93-3.72 (m, 6 H), 3.63 (d, J = 11.1 Hz, 1 H), 3.56 (dd, J = 11.5, 3.1 Hz, 1 H), 3.41 (td, J = 11.8, 2.9 Hz, 1 H), 3.34-3.27 (m, 1 H), 3.25-3.06 (m, 4 H), 2.57 (dd, J = 15.4, 5.0 Hz, 1 H), 1.18 (d, J = 6.8 Hz, 3 H). **^{13}C{^{1}H} NMR** (101 MHz, DMSO-d_6): δ 167.96 (s, 1 C), 157.72 (s, 1 C), 157.40 (s, 1 C), 93.14 (s, 1 C), 70.15 (s, 1 C), 69.55 (s, 1 C), 66.29 (s, 1 C), 65.66 (s, 1 C), 56.76 (s, 1 C), 47.23 (s, 1 C), 41.62 (s, 1 C), 39.56 (s, 1 C), 28.18 (s, 1 C), 14.21 (s, 1 C). **MALDI-MS**: *m/z* = 311.085 ([M + H]$^+$). **HPLC**: t_R = 7.15 min (98.9% purity).

(*R*)-2-chloro-4-((*R*)-3-methylmorpholino)-5a,6,8,9-tetrahydro-5*H*-pyrimido[5',4':4,5]pyrrolo[2,1-*c*][1,4]oxazine (22b) was prepared as described for its (*S,S*)-enantiomer **21a** starting from (*S*)-tetrahydro-3*H*-[1,2,3]oxathiazolo[4,3-*c*][1,4]oxazine 1,1-dioxide **33a** (1.0 g, 5.58 mmol, 1 eq.) in 55% yield. The spectroscopic data are in agreement with those reported for the (*S,S*)-enantiomer. **HPLC**: t_R = 7.24 min (99.6% purity).

(9*S*)-4-chloro-6-{8-oxa-3-azabicyclo[3.2.1]octan-3-yl}-11-oxa-1,3,5-triazatricyclo[7.4.0.0^{2,7}]trideca-2(7),3,5-triene (23a) was prepared according to general procedure 3 from 3-(2,6-dichloropyrimidin-4-yl)-8-oxa-3-azabicyclo[3.2.1]octane **29** (1.21 g, 4.65 mmol, 1 eq.) and (*R*)-tetrahydro-3*H*-[1,2,3]oxathiazolo[4,3-*c*][1,4]oxazine 1,1-dioxide **33b** (1 g, 5.58 mmol, 1.2 eq.). Purification by column chromatography (cyclohexane / ethyl acetate 1:0 → 3:2) gave compound **23a** as a yellowish solid (1.06 g, 3.28 mmol, 71%). **^{1}H NMR** (400 MHz, DMSO-d_6): δ 4.36-4.31 (m, 2 H), 3.92-3.71 (m, 6 H), 3.32-3.27 (m, 1 H), 3.24-3.19 (m, 2 H), 3.16-3.03 (m, 3 H), 2.65 (dd, J = 15.4, 5.0 Hz, 1 H), 1.83-1.69 (m, 4 H). **^{13}C{^{1}H} NMR** (101 MHz, DMSO-d_6): δ 167.75 (s, 1 C), 158.86 (s, 1 C), 157.52 (s, 1 C), 93.27 (s, 1 C), 72.89 (s, 1 C), 72.88 (s, 1 C), 69.59 (s, 1 C), 65.67 (s, 1 C), 56.75 (s, 1

C), 50.61 (s, 1 C), 50.42 (s, 1 C), 41.55 (s, 1 C), 28.20 (s, 1 C), 27.37 (s, 1 C), 27.34 (s, 1 C). **MALDI-MS**: *m/z* = 323.162 ([M + H]$^+$). **HPLC**: t_R = 6.98 min (99.8% purity).

(9*R*)-4-chloro-6-{8-oxa-3-azabicyclo[3.2.1]octan-3-yl}-11-oxa-1,3,5-triazatricyclo[7.4.0.0^{2,7}]trideca-2(7),3,5-triene (23b) was prepared as described for its (*S*)-enantiomer **23a** starting from (*S*)-tetrahydro-3*H*-[1,2,3]oxathiazolo[4,3-*c*][1,4]oxazine 1,1-dioxide **33a** (2.0 g, 11.17 mmol, 1 eq.) in 40% yield. The spectroscopic data are in agreement with those reported for the (*S*)-enantiomer.

(9*S*)-4-chloro-6-{3-oxa-8-azabicyclo[3.2.1]octan-8-yl}-11-oxa-1,3,5-triazatricyclo[7.4.0.0^{2,7}]trideca-2(7),3,5-triene (24a) was prepared according to general procedure 3 from 8-(2,6-dichloropyrimidin-4-yl)-3-oxa-8-azabicyclo[3.2.1]octane **30** (1.21 g, 4.65 mmol, 1 eq.) and (*R*)-tetrahydro-3*H*-[1,2,3]oxathiazolo[4,3-*c*][1,4]oxazine 1,1-dioxide **33b** (1 g, 5.58 mmol, 1.2 eq.). Purification by column chromatography (cyclohexane / ethyl acetate 1:0 → 3:2) gave compound **24a** as a colorless solid (893 mg, 2.77 mmol, 59%). **^{1}H NMR** (400 MHz, DMSO-d_6): δ 4.38-4.33 (m, 2 H), 3.94-3.89 (m, 1 H), 3.80-3.71 (m, 3 H), 3.59 (dd, *J* = 10.8, 5.8 Hz, 2 H), 3.50 (d, *J* = 10.8 Hz, 2 H), 3.36-3.29 (m, 1 H), 3.23 (t, *J* = 11.0 Hz, 1 H), 3.14-3.03 (m, 2 H), 2.54-2.48 (m, 1 H), 1.93-1.85 (m, 4 H). **MALDI-MS**: *m/z* = 323.111 ([M + H]$^+$). **HPLC**: t_R = 7.04 min (95.5% purity). ^{13}C NMR spectroscopic data are not available due to insufficient solubility in standard deuterated solvents.

(9*S*)-4-chloro-6-{3-oxa-8-azabicyclo[3.2.1]octan-8-yl}-11-oxa-1,3,5-triazatricyclo[7.4.0.0^{2,7}]trideca-2(7),3,5-triene (24b) was prepared as described for its (*S*)-enantiomer **24a** starting from (*S*)-tetrahydro-3*H*-[1,2,3]oxathiazolo[4,3-*c*][1,4]oxazine 1,1-dioxide **33a** (2.0 g, 11.17 mmol, 1 eq.) in 26% yield. The spectroscopic data are in agreement with those reported for the (*S*)-enantiomer.

(*S*)-2-chloro-4-(3,3-dimethylmorpholino)-5a,6,8,9-tetrahydro-5*H*-pyrimido[5',4':4,5]pyrrolo[2,1-*c*][1,4]oxazine (25a) was prepared according to general procedure 3 from 4-(2,6-dichloropyrimidin-4-yl)-3,3-dimethylmorpholine **31** (1.21 g, 4.65 mmol, 1 eq.) and (*R*)-

tetrahydro-3*H*-[1,2,3]oxathiazolo[4,3-*c*][1,4]oxazine 1,1-dioxide **33b** (1 g, 5.58 mmol, 1.2 eq.). Purification by column chromatography (cyclohexane / ethyl acetate 1:0 → 4:1) gave compound **25a** as a colorless solid (922 mg, 2.84 mmol, 61%). **^{1}H NMR** (400 MHz, DMSO-d_6): δ 3.95-3.88 (m, 1 H), 3.81-3.73 (m, 3 H), 3.72-3.62 (m, 2 H), 3.35-3.27 (m, 4 H), 3.22-3.07 (m, 4 H), 2.99 (dd, J = 16.1, 9.5 Hz, 1 H), 2.42 (dd, J = 16.1, 5.3 Hz, 1 H), 1.36 (s, 3 H), 1.33 (s, 3 H). **^{13}C{^{1}H} NMR** (101 MHz, DMSO-d_6): δ 168.01 (s, 1 C), 160.49 (s, 1 C), 156.25 (s, 1 C), 102.21 (s, 1 C), 77.30 (s, 1 C), 69.71 (s, 1 C), 66.75 (s, 1 C), 65.51 (s, 1 C), 57.21 (s, 1 C), 54.29 (s, 1 C), 43.33 (s, 1 C), 41.56 (s, 1 C), 27.39 (s, 1 C), 21.71 (s, 1 C), 20.86 (s, 1 C). **MALDI-MS**: *m/z* = 325.036 ([M + H]$^+$). **HPLC**: t_R = 8.19 min (99.1% purity).

(*R*)-2-chloro-4-(3,3-dimethylmorpholino)-5a,6,8,9-tetrahydro-5*H*-pyrimido[5',4':4,5]pyrrolo[2,1-*c*][1,4]oxazine (25b) was prepared as described for its (*S*)-enantiomer **25a** starting from (*S*)-tetrahydro-3*H*-[1,2,3]oxathiazolo[4,3-*c*][1,4]oxazine 1,1-dioxide **33a** (1.64 g, 9.16 mmol, 1.2 eq.) in 66% yield. The spectroscopic data are in agreement with those reported for the (*S*)-enantiomer.

4-(2,6-dichloropyrimidin-4-yl)morpholine (26) were prepared according to literature.[32]

(*S*)-4-(2,6-dichloropyrimidin-4-yl)-3-methylmorpholine (27) was prepared according to general procedure 2 from (*S*)-3-methylmorpholine (1.3 mL, 11.46 mmol, 1.05 eq) and 2,4,6-trichloropyrimidine (1.25 ml, 10.92 mmol, 1.0 eq.). Purification by column chromatography on silica gel (cyclohexane / ethyl acetate 3:1) gave compound **27** as a colorless solid (1.96 g, 7.90 mmol, 72%). **^{1}H NMR** (400 MHz, DMSO-d_6): δ 6.95 (s, 1 H), 4.49 (qd, J = 6.8, 2.9 Hz, 1 H), 4.13 (dd, J = 13.7, 2.8 Hz, 1 H), 3.90 (dd, J = 11.5, 3.8 Hz, 1 H), 3.69 (d, J = 11.5 Hz, 1 H), 3.56 (dd, J = 11.6, 3.2 Hz, 1 H), 3.44-3.37 (m, 1 H), 3.25-3.18 (m, 1 H), 1.21 (d, J = 6.8 Hz, 3 H). The spectroscopic data are in agreement with those reported for the (*R*)-enantiomer.

(*R*)-4-(2,6-dichloropyrimidin-4-yl)-3-methylmorpholine (28) was prepared according to general procedure 2 from (*R*)-3-methylmorpholine (4 g, 39.54 mmol, 1.05 eq) and 2,4,6-trichloropyrimidine (4.55 ml, 39.54 mmol, 1.0 eq.). Purification by column chromatography on silica gel (cyclohexane / ethyl acetate 1:0 → 3:2) gave compound **28** as a colorless solid (6.94 g, 28.10 mmol, 71%). **^{1}H NMR** (400 MHz, DMSO-d_6): δ 7.00 (s, 1 H), 4.46-4.32 (m, 1 H), 4.10-3.97 (m, 1 H), 3.91 (ddt, J = 11.5, 4.0, 1.1 Hz, 1 H), 3.70 (d, J = 11.6 Hz, 1 H), 3.57 (dd, J = 11.7, 3.0 Hz, 1 H), 3.43 (td, J = 11.9, 3.0 Hz, 1 H), 3.21 (td, J = 13.0, 3.8 Hz, 1 H), 1.21 (d, J = 6.7 Hz, 3 H). **^{13}C{^{1}H} NMR** (101 MHz, $CDCl_3$): δ 163.06 (s, 1 C), 160.71 (s, 1 C), 160.06 (s, 1 C), 99.90 (s, 1 C), 70.70 (s, 1 C), 66.56 (s, 1 C), 47.94 (s, 1 C), 39.72 (s, 1 C), 14.09 (s, 1 C). The spectroscopic data are in agreement with those reported for the (*S*)-enantiomer.

3-(2,6-dichloropyrimidin-4-yl)-8-oxa-3-azabicyclo[3.2.1]octane (29) was prepared according to general procedure 2 from 8-oxa-3-azabicyclo[3.2.1]octane.HCl (2.5 g, 16.70 mmol, 1.05 eq) and 2,4,6-trichloropyrimidine (1.83 ml, 15.90 mmol, 1.0 eq.). Purification by column chromatography on silica gel (cyclohexane / ethyl acetate 1:0 → 4:1) gave compound **29** as a colorless solid (3.57 g, 13.73 mmol, 86%). **^{1}H NMR** (400 MHz, DMSO-d_6): δ 6.94 (s, 1 H), 4.47-4.36 (m, 2 H), 4.25-4.04 (m, 1 H), 3.82-3.60 (m, 1 H), 3.26-2.95 (m, 2 H), 1.90-1.74 (m, 2 H), 1.73-1.55 (m, 2 H). **^{13}C{^{1}H} NMR** (101 MHz, $CDCl_3$): δ 164.65 (s, 1 C), 160.53 (s, 1 C), 159.83 (s, 1 C), 99.79 (s, 1 C), 73.33 (s, 2 C), 50.30 (s, 2 C), 27.79 (s, 2 C).

8-(2,6-dichloropyrimidin-4-yl)-3-oxa-8-azabicyclo[3.2.1]octane (30) was prepared according to general procedure 2 from 3-oxa-8-azabicyclo[3.2.1]octane.HCl (2.5 g, 16.70 mmol, 1.05 eq) and 2,4,6-trichloropyrimidine (1.83 ml, 15.90 mmol, 1.0 eq.). Purification by column chromatography on silica gel (cyclohexane / ethyl acetate 1:0 → 4:1) gave compound **30** as a colorless solid (3.33 g, 12.81 mmol, 80%). **^{1}H NMR** (400 MHz, DMSO-d_6): δ 6.98 (s, 1 H), 4.68-4.62 (m, 1 H), 4.52-4.45 (m, 1 H), 3.61-3.53 (m, 4 H), 2.02-1.87 (m, 4 H). **^{13}C{^{1}H} NMR** (101 MHz, DMSO-d_6): δ 160.52 (s, 1 C), 159.36 (s, 1 C), 159.22 (s, 1 C), 102.25 (s, 1 C), 71.21 (s, 2 C), 55.97 (s, 1 C), 55.71 (s, 1 C), 26.95 (s, 1 C), 26.17 (s, 1 C).

4-(2,6-dichloropyrimidin-4-yl)-3,3-dimethylmorpholine (31) was prepared according to general procedure 2 from 3,3-dimethylmorpholine (4.0 g, 34.73 mmol, 1.05 eq) and 2,4,6-trichloropyrimidine (3.8 ml, 33.08 mmol, 1.0 eq.). Purification by column chromatography on silica gel (cyclohexane / ethyl acetate 1:0 → 9:1) gave compound **31** as a colorless solid (4.19 g, 15.99 mmol, 46%). **^{1}H NMR** (400 MHz, DMSO-d_6): δ 7.04 (s, 1 H), 3.81 (t, J = 5.5 Hz, 2 H), 3.59 (t, J = 5.7 Hz, 2 H), 3.46 (s, 2 H), 1.44 (s, 6 H). **^{13}C{^{1}H} NMR** (101 MHz, DMSO-d_6): δ 165.40 (s, 1 C), 159.38 (s, 1 C), 157.59 (s, 1 C), 104.26 (s, 1 C), 75.62 (s, 1 C), 65.76 (s, 1 C), 57.14 (s, 1 C), 42.65 (s, 1 C), 22.57 (s, 2 C).

4-(4,6-dichloropyrimidin-2-yl)morpholine (32) were prepared according to literature.[32]

(*S*)-tetrahydro-3*H*-[1,2,3]oxathiazolo[4,3-*c*][1,4]oxazine 1,1-dioxide (33a) was prepared as described for its (*R*)-enantiomer **33b** starting from (*R*)-Morpholin-3-ylmethanol **34b** (0.685 g, 5.85 mmol, 1 eq.) in 64% yield. The spectroscopic data are in agreement with those reported for the (*R*)-enantiomer. (*S*)-enantiomer: $[\alpha_D]$ = + 53.8 ($CHCl_3$, c = 0.75).

(*R*)-tetrahydro-3*H*-[1,2,3]oxathiazolo[4,3-*c*][1,4]oxazine 1,1-dioxide (33b). A solution of thionyl chloride (2.8 g, 1.7 mL, 23.3 mmol, 1.95 eq.) in DCM (1.7 mL) was added dropwise to a cooled (-5 °C) solution of imidazole (4.9 g, 71.7 mmol, 6 eq.) in DCM (30 mL), and the temperature was kept at -5 °C. The cooling bath was removed and the reaction mixture was stirred for 45 min while allowing it to warm to r.t. The mixture was cooled down to -10 °C and a solution of **34a** (1.4 g, 11.9 mmol, 1 eq.) in DCM (12 mL) was added dropwise. The mixture was stirred at 0 °C for 2 hrs. Water (30 mL) was added and the layers were separated. The organic layer was washed with half-concentrated brine (30 mL) and cooled to 5 °C. A $NaIO_4$-solution (7.7 g, 35.9 mmol) in water (75 mL) was added, followed by RuO_2-H_2O (16 mg). The mixture was allowed to warm up to r.t. and stirred at r.t. overnight. The layers were separated and the organic layer was filtered through a silica gel column eluting with DCM. The solvent was removed under reduced pressure to give compound **33b** (1.1 g, 61.4 mmol, 52%) as a colorless solid. **^{1}H NMR** (400 MHz, $CDCl_3$): δ 4.59 (dd, J = 8.1, 6.4 Hz, 1 H), 4.31 (dd, J = 9.3, 8.1 Hz, 1 H), 4.02 (dd, J = 11.6, 3.4 Hz, 1 H), 3.88 (dt, J = 11.9, 3.6 Hz, 1 H), 3.85-3.79 (m, 1 H), 3.74 (ddd, J = 11.9, 8.9, 3.1 Hz, 1 H), 3.61 (dd, J = 11.6, 7.8 Hz, 1 H), 3.39-3.33 (m, 1 H), 3.15 (ddd, J = 12.2, 8.9, 3.4 Hz,

1 H). **^{13}C{^{1}H} NMR** (101 MHz, $CDCl_3$): δ 69.85 (s, 1 C), 66.52 (s, 1 C), 64.65 (s, 1 C), 54.21 (s, 1 C), 43.43 (s, 1 C). **MALDI-MS**: *m/z* = 180.032 ($[M + H]^+$). (*R*)-enantiomer: $[\alpha_D]$ = - 42.8 ($CHCl_3$, c = 0.65).

(*S*)-Morpholin-3-ylmethanol (34a). A solution of **35a** (14 g, 67.4 mmol) in methanol (200 mL) was placed in a Parr® apparatus and degassed with Argon. Palladium on carbon (10 wt %, 1.5 g) was added and the mixture was stirred under H_2 at 2.8 bar for 48 hrs. The resulting mixture was filtered through celite, washed with MeOH and concentrated under reduced pressure to give compound **34a** (8.0 g, 68.3 mmol, 99%) as a colourless oil. **^{1}H NMR** (400 MHz, $CDCl_3$): δ 3.81-3.80 (m, 1 H), 3.79-3.76 (m, 1 H), 3.60-3.47 (m, 4 H), 3.38-3.32 (m, 1 H), 3.00-2.91 (m, 4 H). The spectroscopic data are consistent with previous literature reports.[41]

(*R*)-Morpholin-3-ylmethanol (34b) was prepared as described for its (*S*)-enantiomer **34a** starting from (*R*)-(4-Benzylmorpholin-3-yl)methanol **35b** (5.2 g, 25.1 mmol, 1 eq.) in 96% yield. The spectroscopic data are in agreement with those reported for the (*S*)-enantiomer.

(*S*)-(4-Benzylmorpholin-3-yl)methanol (35a). To a stirred solution of **36b** (20.6 g, 87.5 mmol, 1 eq.) in THF (320 mL), triethylamine (10.6 g, 14.7 mL, 105.1 mmol) was added. The solution was cooled to 0°C and borane-dimethylsulfide complex (10M in THF, 50 mL, 524.0 mmol) was slowly added. The reaction mixture was heated up to 65 °C for 5 h. After cooling to r.t., the reaction was quenched by addition of water (60 mL). The reaction mixture was stirred at r.t. overnight. The organic solvents were removed under reduced pressure and the residue was diluted with aqueous NaOH solution (20% v/v 2 x). The aqueous layer was extracted with EtOAc (2 x) and the organic layer was washed with an aqueous 1M HCl-solution (2 x). The combined aqueous fractions were then basified to pH 14 by addition of solid NaOH, and re-extracted with EtOAc (3 x). The combined organic layers were dried over Na_2SO_4, filtered and concentrated under reduce pressure to give compound **35a** (15.0 g, 72.4 mmol, 82%) as a clear oil. **^{1}H NMR** (400 MHz, $CDCl_3$): δ 7.53-7.26 (m, 5 H), 4.13 (d, *J* = 13.3 Hz, 1 H), 3.96 (dd, *J* = 11.5, 4.5 Hz, 1 H), 3.84 (ddd, *J* = 11.5, 3.8, 1.1 Hz, 1 H), 3.75 (td, *J* = 3.3, 1.1 Hz, 1 H), 3.73 (td, *J* = 3.3, 1.1 Hz, 1 H), 3.67 (dd, *J* = 11.6, 9.2 Hz, 1 H), 3.56-3.49 (m, 2 H), 2.73 (dt, *J* = 12.0, 2.9 Hz, 1 H),

2.59-2.54 (m, 1 H), 2.52 (br s, 1 H), 2.34 (ddd, J = 12.0, 10.0, 3.3 Hz, 1 H). The spectroscopic data are consistent with previous literature reports.[41]

(*R*)-(4-Benzylmorpholin-3-yl)methanol (35b) was prepared as described for its (*S*)-enantiomer **35a** starting from (*S*)-4-Benzyl-5-oxomorpholine-3-carboxylic acid **36a** (7.4 g, 31.5 mmol, 1 eq.) in 81% yield. The spectroscopic data are in agreement with those reported for the (*S*)-enantiomer.

(*S*)-4-Benzyl-5-oxomorpholine-3-carboxylic acid (36a) was prepared as described for its (*R*)-enantiomer **36b** starting from *N*-benzyl-*S*-serine **37a** (12.2 g, 62.5 mmol, 1 eq.) in 51% yield. The spectroscopic data agree with those reported for the (*R*)-enantiomer.

(*R*)-4-Benzyl-5-oxomorpholine-3-carboxylic acid (36b). To a solution of *N*-benzyl-*R*-serine **37b** (25.6 g, 131.1 mmol, 1 eq.) and K_2CO_3 (36.2 g, 262.2 mmol, 2 eq.) in THF/water (150 mL/150 mL) at 0 °C, a chloroacetyl chloride (17.8 g, 12.5 mL, 157.4 mmol, 1.2 eq.) solution in THF (13 mL) was added dropwise. The mixture was stirred at 0 °C for 1 hr. Solid NaOH (15.72 g, 393 mmol, 3 eq.) was added and the mixture was stirred at 5 °C for 2 hrs. After completion of the reaction, cyclohexane was added and vigorously stirred. The layers were separated and the basic aqueous layer was acidified to pH 1 with conc. HCl. The mixture was kept in the fridge overnight and the solid was filtered off, washed with cold water and dried under vacuum to give compound **36b** (21.8 g, 92.7 mmol, 71%) as a colorless solid. **^{1}H NMR** (400 MHz, DMSO-d_6): δ 7.37-7.26 (m, 5 H), 5.26 (d, J = 15.4 Hz, 1 H), 4.19-4.12 (m, 3 H), 3.96-3.90 (m, 2 H), 3.83 (d, J= 15.4 Hz, 1 H). The spectroscopic data are consistent with previous literature reports.[41]

***N*-Benzyl-(*S*)-serine (37a)** was prepared as described for its (*R*) enantiomer **37b** starting from (*S*)-serine (29.5 g, 280.7 mmol, 1 eq.) in 63% yield. The spectroscopic data are in agreement with those reported for the (*R*) enantiomer.

***N*-Benzyl-(*R*)-serine (37b)**. To a stirred solution of (*R*)-serine (25 g, 237.9 mmol, 1 eq.) in aqueous 2 M NaOH (120 mL), benzaldehyde (24.7 g, 24.5 mL, 233.1 mmol, 1 eq.) was added. The reaction

mixture was stirred at r.t. for 30 minutes before cooling to 5°C. $NaBH_4$ (2.7 g, 71.4 mmol, 0.3 eq.) was added portionwise while keeping the temperature below 10 °C. After addition, the reaction mixture was allowed to warm up to r.t. and stirred 1 h. Additional benzaldehyde (24.7 g, 24.5 mL, 233.1 mmol, 1 eq.) was added and the reaction mixture was stirred at r.t. for 30 minutes. The reaction mixture was cooled to 5°C and further $NaBH_4$ (2.7 g, 71.4 mmol, 0.3 eq.) was added portionwise while a temperature of 5-10°C was maintained. After completion of the addition and the reaction mixture stirred at r.t. for 2 h. The reaction mixture was then extracted with ether (3 x) and the aqueous phase was cooled down to 0 °C and acidified to pH 5 with conc. HCl. The resulting white precipitate was filtered off, washed with water and dried under reduced pressure to give compound **37b** (25.8 g, 132.2 mmol, 55%). **^{1}H NMR** (400 MHz, DMSO-d_6): δ 7.45-7.30 (m, 5 H), 4.04-3.92 (m, 2 H), 3.70-3.61 (m, 3 H), 3.17 (t, J = 5.8 Hz, 1 H). The spectroscopic data are consistent with previous literature reports.[41]

(*E*)-*N*,*N*-dimethyl-*N*'-(5-(4,4,5,5-tetramethyl-1,3,2-dioxaborolan-2-yl)pyridin-2-yl)formimidamide (38) was prepared according to general procedure 1 from 2-aminopyridine-5-boronic acid pinacol ester (500 mg, 2.27 mmol, 1 eq.), and *N*,*N*-dimethylformamide dimethyl acetal (DMF-DMA, 395 µL, 2.95 mmol, 1.3 eq.). Compound **38** was obtained as a beige solid (538 mg, 1.96 mmol, 86%). **^{1}H NMR** (400 MHz, DMSO-d_6): δ 8.57 (s, 1 H), 8.41 (dd, J = 2.0, 0.9 Hz, 1 H), 7.75 (dd, J = 8.1, 2.0 Hz, 1 H), 6.78 (dd, J = 8.0, 0.9 Hz, 1 H), 3.11 (s, 3 H), 3.00 (s, 3 H), 1.29 (s, 12 H).

5-(4,4,5,5-tetramethyl-1,3,2-dioxaborolan-2-yl)pyrazin-2-amine (39). 2-Amino-5-bromopyrazine (1.50 g, 8.77 mmol, 1 eq.), bis(pinacolato)diboron (3.29 g, 12.95 mmol, 1.5 eq.) and KOAc (2.53 g, 25.82 mmol, 3.0 eq.) were charged in a flask. Under nitrogen atmosphere, 1,4-dioxane (20 mL) and [1,1′-bis(diphenylphosphino)ferrocene]dichloropalladium(II) ($Pd(dppf)Cl_2$, 605 mg, 0.86 mmol, 0.1 eq.) were added. The reaction mixture was stirred at 105 °C for 3.5 hrs. After completion of the reaction monitored by TLC, the mixture was filtered through celite and the solvents were evaporated under reduced pressure. Methyl *t*-butyl ether (MTBE) was added and the solid was filtered off. Compound **39** was obtained as a light brownish solid (1.23 g, 5.57 mmol, 64%). **^{1}H NMR** (400 MHz, DMSO-d_6): δ 8.11 (d, J = 1.5 Hz, 1 H), 7.99 (d, J = 1.5 Hz, 1 H), 6.81 (br s, 2 H), 1.27 (s, 12 H).

(*E*)-*N*'-(5-bromo-4-methylpyridin-2-yl)-*N*,*N*-dimethylformimidamide (40) was prepared according to general procedure 1 from 5-bromo-4-methylpyridin-2-amine (8.06 g, 43.10 mmol, 1 eq.), and DMF-DMA (6.92 mL, 51.70 mmol, 1.2 eq.). Compound **40** was obtained as a beige solid (7.6 g, 31.52 mmol, 73%). **^{1}H NMR** (400 MHz, DMSO-d_6): δ 8.69 (s, 1 H), 8.54 (s, 1 H), 7.14 (s, 1 H), 3.38 (s, 3 H), 3.37 (s, 3 H), 2.62 (s, 3 H).

(*E*)-*N*,*N*-dimethyl-*N*'-(3-methyl-5-(4,4,5,5-tetramethyl-1,3,2-dioxaborolan-2-yl)pyridin-2-yl)formimidamide (41) was prepared according to general procedure 1 from 3-methyl-5-(4,4,5,5-tetramethyl-1,3,2-dioxaborolan-2-yl)pyridin-2-amine (500 mg, 2.13 mmol, 1 eq.), and DMF-DMA (430 µL, 3.20 mmol, 1.5 eq.). Compound **41** was obtained as a brownish solid (407 mg, 1.41 mmol, 66%). **^{1}H NMR** (400 MHz, DMSO-d_6): δ 8.51 (s, 1 H), 8.26 (s, 1 H), 7.62 (s, 1 H), 3.11 (s, 3 H), 3.03 (s, 3 H), 2.19 (s, 3 H), 1.28 (s, 12 H).

tert-butyl (5-bromo-4-methoxypyridin-2-yl)carbamate (42). To a solution of Boc anhydride (Boc_2O, 4.73 g, 21.67 mmol, 2.2 eq.) in THF (20 mL) at 0 °C, 5-bromo-4-methoxypyridin-2-amine (2.0 g, 9.85 mmol, 1 eq.) was added. Then, 4-Dimethylaminopyridine (DMAP, 241 mg, 1.97 mmol, 0.2 eq.) was added portionwise. The reaction mixture was stirred overnight while allowed to warm up to room temperature. After completion of the reaction monitored by TLC, the solvent was evaporated and DCM (200 mL) was added. The organic layer was washed with NH_4Cl 15% solution (2 x) and the combined aqueous layers were extracted with DCM (1 x). The combined organic layers were dried over anhydrous Na_2SO_4, filtered and concentrated under reduced pressure. Purification by column chromatography (cyclohexane / EtOAc 1:0 → 1:4) gave compound **42** as a colorless solid (767 mg, 2.53 mmol, 26%). **^{1}H NMR** (400 MHz, DMSO-d_6): δ 9.97 (s, 1 H), 8.22 (s, 1 H), 7.61 (s, 1 H), 3.92 (s, 3 H), 1.48 (s, 9 H).

5-bromo-4-(dimethoxymethyl)pyridin-2-amine (43). To a solution of 4-(dimethoxymethyl)pyridin-2-amine (2.0 g, 11.89 mmol, 1.0 eq.) in 2-methyltetrahydrofuran (24 mL) at 0 °C, N-bromosuccinimide (NBS, 2.23 g, 12.48 mmol, 1.05 eq.) was added portionwise. The reaction mixture was stirred at 0 °C for 1 hr and, then, at r.t. overnight. After completion of the reaction monitored by TLC, the reaction mixture was washed with a Na_2CO_3 8% solution (3 x). The combined aqueous

layers were extracted with 2-methyltetrahydrofuran (1 x). The combined organic layers were dried over anhydrous Na_2SO_4, filtered and concentrated under reduced pressure. Purification by column chromatography (cyclohexane / EtOAc 1:0 → 4:1) gave compound **43** as a beige solid (2.585 g, 10.46 mmol, 88%). **^{1}H NMR** (400 MHz, DMSO-d_6): δ 7.98 (s, 1 H), 6.65 (s, 1 H), 6.24 (br s, 2 H), 5.28 (s, 1 H), 3.29 (s, 6 H).

tert-butyl *N*-[5-bromo-4-(dimethoxymethyl)pyridin-2-yl]-*N*-[(tert-butoxy)carbonyl]carbamate (44) and tert-butyl *N*-[5-bromo-4-(dimethoxymethyl)pyridin-2-yl]carbamate (45). To a solution of Boc anhydride (Boc_2O, 5.02 g, 22.98 mmol, 2.2 eq.) in THF (26 mL) at 0 °C, 5-bromo-4-(dimethoxymethyl)pyridin-2-amine **43** (2.58 g, 10.44 mmol, 1 eq.) was added. Then, 4-Dimethylaminopyridine (DMAP, 256 mg, 2.09 mmol, 0.2 eq.) was added portionwise. The reaction mixture was stirred overnight while allowed to warm up to room temperature. After completion of the reaction monitored by TLC, the reaction mixture was washed with NH_4Cl 15% solution (2 x) and the organic layer was dried over anhydrous Na_2SO_4, filtered and concentrated under reduced pressure. Purification by column chromatography (cyclohexane / EtOAc 1:0 → 0:1) gave compound **44** as a yellowish oil (1.286 g, 2.87 mmol, 27%) and **45** as a white solid (2.154 g, 6.21 mmol, 59%). **44 ^{1}H NMR** (400 MHz, DMSO-d_6): δ 8.66 (s, 1 H), 7.45 (s, 1 H), 5.51 (s, 1 H), 3.33 (s, 6 H), 1.40 (s, 18 H). **45 ^{1}H NMR** (400 MHz, DMSO-d_6): δ 8.70 (s, 1 H), 7.51 (s, 1 H), 5.51 (s, 1 H), 3.33 (s, 6 H), 1.38 (s, 9 H).

(*E*)-4-(dimethylamino)-1,1-dimethoxybut-3-en-2-one (46) was prepared as previously reported in literature.[46] A solution of methylglyoxal dimethyl acetal (26 mL, 211.6 mmol, 1.0 eq.) and DMF-DMA (37 ml, 275.1 mmol, 1.3 eq.) was stirred at 100 °C overnight. The reaction mixture was concentrated under reduced pressure. Compound **46** was obtained as a brown oil (35.7 g, 206.1 mmol, 75%) and used for the next step without further purification.

4-(dimethoxymethyl)pyrimidin-2-amine (47). Compound **46** (35.7 g, 206.1 mmol, 1.0 eq.) was dissolved in ethanol (780 mL). Potassium carbonate (71.2 g, 512.3 mmol, 2.5 eq.) and guanidine hydrochloride (23.6 g, 247.3 mmol, 1.2 eq.) were added and the resulting suspension heated to reflux

overnight. After completion of the reaction monitored by TLC, ethanol was evaporated under reduced pressure. The residue was stirred with water for 6 hrs, filtered and dried under vacuum to afford compound **47**. The filtrate was extracted with dichloromethane (3 x) and the combined organic layers were dried over anhydrous Na_2SO_4 sodium sulfate and concentrated under reduced pressure to give compound **47** as a brown solid (24.8 g, 146.6 mmol, 71%). **^{1}H NMR** (400 MHz, $CDCl_3$): δ 8.34 (d, J = 5.0 Hz, 1 H), 6.84 (d, J = 5.0 Hz, 1 H), 5.28 (br s, 1 H), 5.14 (s, 1 H), 4.76 (br s, 1 H), 3.39 (s, 6 H).

5-bromo-4-(dimethoxymethyl)pyrimidin-2-amine (48). To a solution of 4-(dimethoxymethyl)pyrimidin-2-amine **47** (5.0 g, 29.58 mmol, 1.0 eq.) in ACN (150 mL), NBS (5.53 g, 31.06 mmol, 1.05 eq.) was added portion wise. The reaction mixture was stirred at 70 °C overnight. After completion of the reaction monitored by TLC, ACN was evaporated. The solid was dissolve in DCM (250 mL) and the organic layer was washed with a Na_2CO_3 8% solution (3 x). The organic layer was dried over anhydrous Na_2SO_4, filtered and concentrated under reduced pressure. The product was recrystallized from dichloromethane / heptanes to obtain compound **48** as a beige solid (6.50 g, 26.20 mmol, 89%). **^{1}H NMR** (400 MHz, DMSO-d_6): δ 8.34 (s, 1 H), 7.02 (br s, 2 H), 5.27 (s, 1 H), 3.35 (s, 6 H).

tert-butyl *N*-[5-bromo-4-(dimethoxymethyl)pyrimidin-2-yl]-*N*-[(tert-butoxy)carbonyl]carbamate (49). To a solution of Boc anhydride (Boc_2O, 12.59 g, 57.66 mmol, 2.2 eq.) in THF (65 mL) at 0 °C, 5-bromo-4-(dimethoxymethyl)pyrimidin-2-amine **48** (6.50 g, 26.21 mmol, 1 eq.) was added. Then, DMAP (640 mg, 5.24 mmol, 0.2 eq.) was added portionwise. The reaction mixture was stirred overnight while allowed to warm up to room temperature. After completion of the reaction monitored by TLC, the reaction mixture was washed with a 0.1M HCl-solution (2 x) and the organic layer was dried over anhydrous Na_2SO_4, filtered and concentrated under reduced pressure. Recrystallization from heptanes gave compound **49** as a beige solid (10.71 g, 23.91 mmol, 91%). **^{1}H NMR** (400 MHz, DMSO-d_6): δ 9.12 (s, 1 H), 5.54 (s, 1 H), 3.39 (s, 6 H), 1.40 (s, 18 H).

(*E*)-*N*,*N*-dimethyl-*N*'-(5-(4,4,5,5-tetramethyl-1,3,2-dioxaborolan-2-yl)-4-(trifluoromethyl)pyridin-2-yl)formimidamide (50) were prepared according to literature.[33]

(*S*)-4-(2-Chloro-5,5a,6,7,8,9-hexahydropyrimido[5,4-*b*]indolizin-4-yl)morpholine (51a) was prepared as described for its (*R*)-enantiomer **51b** starting from (*S*)-hexahydro-[1,2,3]oxathiazolo[3,4-*a*]pyridine 1,1-dioxide **53a** (507 mg, 2.86 mmol, 1.2 eq.) in 43% yield. The spectroscopic data are in agreement with those reported for the (*R*)-enantiomer.

(*R*)-4-(2-Chloro-5,5a,6,7,8,9-hexahydropyrimido[5,4-*b*]indolizin-4-yl)morpholine (51b) was prepared according to general procedure 3 from 4-(2,6-dichloropyrimidin-4-yl)morpholine (702 mg, 3.00 mmol, 1.0 eq.) and (*R*)-hexahydro-[1,2,3]oxathiazolo[3,4-*a*]pyridine 1,1-dioxide **53b** (638 mg, 3.60 mmol, 1.2 eq). Purification by column chromatography on silica gel (cyclohexane / ethyl acetate 1:0 → 9:1) gave compound **51b** as a colorless solid (324 mg, 1.10 mmol, 36%). **^{1}H NMR** (400 MHz, $CDCl_3$): δ 3.91 (dd, J = 13.0, 4.2 Hz, 1 H), 3.68-3.57 (m, 5 H), 3.52-3.44 (m, 4 H), 3.24 (dd, J = 15.0, 9.5 Hz, 1 H), 2.75 (td, J = 13.0, 3.2 Hz, 1 H), 2.66 (dd, J = 15.0, 6.4 Hz, 1 H), 1.82-1.67 (m, 2 H), 1.63-1.55 (m, 1 H), 1.50-1.36 (m, 1 H), 1.35-1.20 (m, 2 H). **^{13}C{^{1}H} NMR** (101 MHz, DMSO): δ 167.84 (s, 1 C), 157.66-157.53 (m, 2 C), 93.32 (s, 1 C), 65.99 (s, 2 C), 59.15 (s, 1 C), 45.34 (s, 2 C), 41.29 (s, 1 C), 32.60 (s, 1 C), 31.62 (s, 1 C), 24.43 (s, 1 C), 23.35 (s, 1 C). **MALDI-MS**: m/z = 295.267 ($[M + H]^+$).

(*S*)-2-Chloro-4-(piperidin-1-yl)-5a,6,8,9-tetrahydro-5*H*-pyrimido[5',4':4,5]pyrrolo[2,1-*c*][1,4]oxazine (52a) was prepared as described for its (*R*)-enantiomer **52b** starting from (*R*)-tetrahydro-3*H*-[1,2,3]oxathiazolo[4,3-*c*][1,4]oxazine 1,1-dioxide **33b** in 70% yield. The spectroscopic data are in agreement with those reported for the (*R*)-enantiomer.

(*R*)-2-Chloro-4-(piperidin-1-yl)-5a,6,8,9-tetrahydro-5*H*-pyrimido[5',4':4,5]pyrrolo[2,1-*c*][1,4]oxazine (52b) was prepared according to general procedure 3 from dichloropyrimidine **54** (200 mg, 0.86 mmol, 1.0 eq.) and (*S*)-tetrahydro-3*H*-[1,2,3]oxathiazolo[4,3-*c*][1,4]oxazine 1,1-dioxide **33a** (185 mg, 1.03 mmol, 1.2 eq). Purification by column chromatography on silica gel (cyclohexane / ethyl acetate 1:0 → 9:1) gave compound **52b** as a colorless solid (168 mg, 0.57 mmol, 66%). **^{1}H NMR** (400

MHz, $CDCl_3$): δ 4.03-3.88 (m, 2 H), 3.79 (ddd, J = 16.0, 11.0, 3.8 Hz, 2 H), 3.60-3.53 (m, 4 H), 3.44 (td, J = 12.0, 2.9 Hz, 1 H), 3.29 (t, J = 11.0 Hz, 1 H), 3.22-3.12 (m, 2 H), 2.54 (dd, J = 15.0, 5.0 Hz, 1 H), 1.69-1.61 (m, 2 H), 1.61-1.53 (m, 4 H). **$^{13}C\{^1H\}$ NMR** (101 MHz, $CDCl_3$): δ 168.44 (s, 1 C), 158.98 (s, 1 C), 158.49 (s, 1 C), 92.49 (s, 1 C), 70.55 (s, 1 C), 66.72 (s, 1 C), 57.32 (s, 1 C), 46.69 (s, 2 C), 42.11 (s, 1 C), 29.55 (s, 1 C), 26.16 (s, 2 C), 24.84 (s, 1 C). **MALDI-MS**: m/z = 295.082 ($[M + H]^+$).

(*S*)-Hexahydro-[1,2,3]oxathiazolo[3,4-*a*]pyridine 1,1-dioxide (53a) was prepared as described for its (*R*)-enantiomer **53b** in a 74% yield. **^1H NMR** (400 MHz, $CDCl_3$): δ 4.57 (dd, J = 7.7, 5.8 Hz, 1 H), 4.18 (dd, J = 9.9, 7.8 Hz, 1 H), 3.59-3.51 (m, 1 H), 3.50-3.40 (m, 1 H), 2.76 (ddd, J = 12.0, 11.0, 3.1 Hz, 1 H), 1.96-1.86 (m, 2 H), 1.86-1.78 (m, 1 H), 1.69-1.57 (m, 1 H), 1.50-1.27 (m, 2 H). The spectroscopic data are consistent with those reported in literature.[47]

(*R*)-Hexahydro-[1,2,3]oxathiazolo[3,4-*a*]pyridine 1,1-dioxide (53b). *Step 1.* To a solution of imidazole (1.77 g, 26.0 mmol, 6.0 eq.) in DCM (18 ml), a solution of $SOCl_2$ (610 µL, 8.36 mmol, 1.9 eq.) in DCM (6 ml) was added dropwise. The resulting colorless suspension was stirred at r.t. for 1 hr. Then, a solution of (*R*)-piperidin-2-ylmethanol (500 mg, 4.34 mmol, 1.0 eq.) in DCM (800 µL) was added dropwise at – 10 °C. The reaction mixture was allowed to warm up to r.t. and stirred at r.t. for 1.5 hrs. After completion of the reaction monitored by TLC, deionized H_2O (35 ml) was added and the layers were separated. The organic layer was washed with brine (15 ml) and used in the next step. *Step 2.* Under vigorous stirring, a solution of RuO_2-H_2O (5.80 mg, 43.6 µmol, 0.01 eq.) and $NaIO_4$ (2.38 g, 11.1 mmol, 2.6 eq.) in deionized H_2O (24 ml) was added. The reaction mixture was stirred at r.t. for 30 min. After completion of the reaction, the layers were separated and the organic layer was filtered through a pad of silica gel (12 g) (eluent: DCM). The solvent was evaporated to give compound **53b** as a colorless liquid (638 mg, 3.60 mmol, 83%). **^1H NMR** (400 MHz, $CDCl_3$): δ 4.57 (dd, J = 7.8, 5.8 Hz, 1 H), 4.18 (dd, J = 9.9, 7.7 Hz, 1 H), 3.59-3.52 (m, 1 H), 3.50-3.40 (m, 1 H), 2.76 (ddd, J = 12.0, 11.0, 3.1 Hz, 1 H), 1.96-1.86 (m, 2 H), 1.86-1.78 (m, 1 H), 1.69-1.56 (m, 1 H), 1.51-1.27 (m, 2 H).

2,4-dichloro-6-(piperidin-1-yl)pyrimidine (54) were prepared according to general procedure 2 from 2,4,6-trichloropyrimidine (627 µL, 5.45 mmol, 1.0 eq.) and piperidine (566 µL, 5.72 mmol, 1.0 eq.). Purification by column chromatography on silica gel (cyclohexane / ethyl acetate 1:0 → 4:1) gave compound **54** as a colorless solid (849 mg, 3.66 mmol, 67%). **^{1}H NMR** (400 MHz, $CDCl_3$): δ 6.39 (s, 1 H), 3.79-3.36 (m, 4 H), 1.74-1.66 (m, 2 H), 1.66-1.57 (m, 4 H). **^{13}C{^{1}H} NMR** (101 MHz, $CDCl_3$): δ 162.82 (s, 1 C), 160.31 (s, 1 C), 160.02 (s, 1 C), 99.66 (s, 1 C), 45.81 (br s, 2 C), 25.61 (s, 2 C), 24.41 (s, 1 C).

Structure modeling of PI3K and mTOR kinase complexes.

The coordinates of PIKiN3 in PI3Kγ complex (PDB code 5JHB, resolution of 2.48 Å), CNX-1351 in PI3Kα (PDB code 3ZIM, resolution of 2.85 Å), and mTOR kinase bound to PI103 (PDB code 4JT6; 3.6 Å) were used as starting points to dock molecules into the ATP-binding sites. Ligands in crystal structures were manually replaced using Maestro 11.1 and energy minimization was carried out. Further measurements and figures were generated in Maestro 11.1 and Chimera UCSF.

Determination of inhibitor dissociation constants.

Dissociation constants of compounds (K_i) for p110α and mTOR were determined by commercial LanthaScreen (Life Technologies) and evaluated as described in Ref. 33. Briefly, AlexaFluor647-labeled Kinase Tracer314 (#PV6087) with a K_d of 2.2 nM was used at 20 nM for p110α, and at a final concentration of 10 nM for mTOR (K_d of 19 nM). Recombinant N-terminally $(His)_6$-tagged p110α was detected with biotinylated anti-$(His)_6$-tag antibody (2 nM, #PV6089) and LanthaScreen Eu-Steptavidin (2 nM, #PV5899); N-terminal GST fused to truncated mTOR (amino acids 1360-2549; #PR8683B) was detected with a LanthaScreen Eu-labelled anti-GST antibody (2 nM, #PV5594). The p110α assay buffer was composed of 50 mM HEPES pH 7.5, 10 mM $MgCl_2$, 1 mM EGTA, and 0.01% (v/v) Brij-35, and the mTOR assay buffer contained 50 mM HEPES; 5 mM $MgCl_2$; 1mM EGTA; 0.01% Pluronic F-127. Further details and calculations are explained in Ref. 32.

Kinome profiling.

The inhibitory capacity and selectivity of compound was determined using the ScanMax platform provided by DiscoverX.[48] In short binding of immobilized ligand to DNA-tagged kinases was competed with 10 μM compound. The amount of kinase bound to the immobilized ligand was measured by quantitative PCR of the respective DNA tags and is given as percentage of control. Binding constants of compounds for kinases of interest were determined by competing the immobilized ligand kinase interactions with an 11-point 3-fold serial dilution of compound starting from 30 μM and subsequent

quantitative PCR of DNA tags. Binding constants were calculated by a standard dose-response curve using the Hill equation (with Hill Slope set to -1):

Response = Background + (Signal - Background)/(1 + 10^([lg Kd - lg dose] * HillSlope))

Selectivity cores[49] were calculated as

S = Number of hits / Number of tested kinases (excluding mutant variants),

where S35, S10, S1 were calculated using %Ctrl as a potency threshold (35, 10, 1%); for example

S(35) = (number of non-mutant kinases with %Ctrl <35)/(number of non-mutant kinases tested).

Cellular PI3K and mTOR signaling.

Downstream signals emerging from mTORC2 (phosphorylation of Ser473 of PKB/Akt; rabbit polyclonal antibody from Cell Signaling Technology (CST), #4058) and mTORC1 (phosphorylation of Ser235/236 on the ribosomal protein S6; rabbit monoclonal antibody from CST, #4856) were measured in In-Cell Western assays plating $2x10^4$ A2058 cells/well in 96-well plates (Cell Carrier, Perkin Elmer) for 24 h (37°C, 5%CO_2), before exposing cells for 1 h to inhibitors or DMSO. Then, cells were fixed (4% PFA in PBS for 30 min at RT), blocked (1% BSA/0.1% Triton X-100/5% goat serum in PBS for 30 min, RT), and stained with CST primary antibodies (1:500). Tubulin staining (mouse anti-α-tubulin, 1:2000, Sigma #T9026) was assessed as internal standard. Secondary antibody [IRDye680-conjugated goat anti-mouse, and IRDye800-conjugated goat anti-rabbit antibodies (LICOR # 926-68070 and # 926-32211), both 1:500] fluorescence was detected on an Odyssey CLx infrared imaging scanner (LICOR). Remaining phospho-protein signals were normalized to cellular tubulin and related to DMSO controls. ICW anaylsis and determination of IC_{50} were done as described in Ref. 33.

Pharmacokinetic studies.

Male Sprague Dawley rats (8 weeks old at delivery) were purchased from Janvier Labs (France). The animals were housed in a temperature-controlled room (20-24°C) and maintained in a 12h light/12h dark cycle. Food and water were available *ad libitum* throughout the duration of the study. Formulations

of compound **7b** and **12b** were prepared by weighing the test items into glass vials and dissolving them by addition of Captisol (40% w/w in water) and water for injection in a proportion of 50% and 35% of the final desired volume. The pH was adjusted to 3 with 0.2M HCl and finally, the volume was completed with water for injection. The formulations were stirred continuously until application to the animals. At each time point (30 min, 2, 4 and 8 hours), three rats were anesthetized with isoflurane and 1 ml blood was collected, via heart puncture, in tubes containing lithium-heparin. After blood sampling, the rats were euthanized and brain, liver and skin were collected. Blood samples were stored on dry ice until centrifugation at 6000 rpm (10 min, 4°C). Plasma supernatants and tissue samples were kept at -80°C until being assayed. The calibration standards and quality controls were prepared in duplicates. A volume of 50 µl of unknown samples, zero samples and blanks were spiked with 6 µl DMSO. After 10 min of equilibration, a volume of 100 µl acetonitrile containing the internal standard (Diazepam, 300 ng/ml) was added to each calibration standard, QC, zero sample and unknown sample, while a volume of 100 µl plain acetonitrile was added to all blanks. Samples were vigorously shaken and centrifuged for 10 minutes at 6000 g and 20°C. The particle free supernatant was diluted 1+1 with water. An aliquot was transferred to 200 µl sampler vials and subsequently subjected to LC-MS. The HPLC system consisted of an Accela U-HPLC pump and an Accela auto sampler (Thermo Fisher Scientific, USA). Mass spectrometry was performed on an Exactive mass spectrometer (orbitrap technology with accurate mass) equipped with a heated electrospray (H-ESI 2) interface (Thermo Fisher Scientific, USA) connected to a PC running the standard software Xcalibur 2.1.

Ethic statement: all experimental procedures were approved by and conducted in accordance with the regulations of the local Animal Welfare authorities (Landesamt für Gesundheit und Verbraucherschutz, Abteilung Lebensmittel- und Veterinärwesen, Saarbrücken).

Hepatocyte stability assay.

Primary hepatocytes from mouse (CD-1), rat (Sprague-Dawley, SD), dog (Beagle), and human were used. Assays were performed using cryopreserved hepatocytes in suspension. Hepatocytes were thawed according to the instructions of the supplier before seeding in 48-well cell culture plates at a density of 200,000 cells / well in 225 µl incubation medium consisting of WME (Williams Medium E)

supplemented with 2 mM L-glutamine and 25 mM HEPES. Stock solution of compound **11b** was prepared with 10 mM in DMSO. A working solution was obtained by dilution of the stock solution in DMSO (first step) and in incubation medium (second step) resulting in a concentration of 10-fold higher strength (50 µM) than the final intended test concentration (5 µM) and a solvent content of 5% DMSO.

Positive control incubations were performed using 7-ethoxycoumarin as substrate. A 10 mM stock solution in acetonitrile (ACN) was further diluted in ACN (first step) and in incubation medium (second step) to give a working solution in 10% ACN and of 10-fold higher strength than the final intended incubation concentration (5 µM). To 225 µl of cell suspension, 25 µl of the 10-fold concentrated working solution of test or reference item was added, resulting in a final test concentration of 5 µM for compound **11b** or 7-ethoxycoumarin, respectively, with final solvent concentrations of 0.5% DMSO (**11b**) or 1% ACN (7-ethoxycoumarin). For analysis, samples were taken after 0, 15, 60, 90 and 180 min of incubation for **11b** and after 0, 60 and 180 min for reference item. The sample preparation was performed afterwards by protein precipitation using ACN (200 µl cell suspension plus 200 µl ACN/ISTD3). After centrifugation (5 minutes, 4,800 x g), the particle-free supernatants were diluted with one volume water and were analyzed by LC-MS. Negative controls were performed to exclude non-metabolic degradation processes; i.e. the finding that the concentrations remained stable over the investigated time suggests that the decrease of the parent compound was mainly due to metabolism. Negative control incubations were performed in line with all experiments using incubation medium in absence of hepatocytes.

For quantitative analysis of compound **11b** in samples from primary human hepatocytes, the HPLC system consisted of a LC pump Surveyor Plus and an auto sampler Surveyor Plus (Thermo-Fisher, USA). Mass spectrometry was performed on a TSQ Quantum Discovery Max triple quadrupole mass spectrometer equipped with an electro-spray ion source (ESI) (Thermo Fisher Scientific, USA) connected to a PC running the standard software Xcalibur 2.0.7.

CYP reactive phenotyping with human recombinant CYP1A1 and CYP1A2 isoenzymes.

Human recombinant isoenzymes from insect cells infected by baculovirus and containing cDNA of a single human CYP isoenzyme (Supersomes™, Corning) were used. The test item stock solutions were

diluted in DMSO/H2O (1:8, v/v) to obtain 50-fold concentrated working solutions (solvent content 12.5% DMSO/87.5% H_2O) for CYP1A1 and CYP1A2. The test compound concentration applied in the CYP reactive phenotyping assay was 1 µM in presence of 0.25% DMSO. The assays were performed in duplicate using human recombinant enzymes systems from Corning (BD Gentest P450 High Throughput Inhibitor Screening Kits). The cofactor-mix, containing the NADP+-regenerating system, was prepared according to the instructions of the manufacturer. For CYP1A1 and CYP1A2, 4 µl of the 50-fold concentrated working solution was added to 96 µl cofactor-mix. Cofactor mix and test item were pipetted into the respective wells of a pre-warmed 96-well-plate and pre-warmed for 10 minutes on a shaker with fitted heating block. The reactions were initiated by addition of 100 µl pre-warmed enzyme-mix. By default, the final protein concentration of all CYP isoenzymes was 25 pmol/ml. Incubations with a final volume of 200 µl were performed at 37°C. After 0 and 60 minutes (30 minutes for positive control substrates), the reactions were stopped by the addition of 200 µl stop solution, i.e. ACN containing the internal standard. Two control groups were run in parallel for every assay: positive controls (PC, n=2) using specific probe substrates for each CYP isoform as reference compounds (CYP1A1 = Melatonin and CYP1A2 = Phenacetin) to prove the quality of the enzyme activity of the used batches as well as a negative control (NC, n=2), which were performed without cofactors and glucose-6-phosphate-dehydrogenase to ensure that the potential loss of parent compound is due to CYP-mediated metabolism.

For quantitative analysis of compound **7b**, **11b** and **12b**, LC-MS systems were used: (i) LC-MS: Accela U-HPLC pump and an Accela auto sampler (Thermo Fisher Scientific, USA) connected to an Exactive mass spectrometer (Orbitrap with accurate mass (Thermo Fisher Scientific, USA)); data handling with the standard software Xcalibur 2.1; (ii) LC-HRMS: Accela U-HPLC pump and an Accela Open auto sampler (Thermo Fisher Scientific, USA) connected to an Q-Exactive mass spectrometer (Orbitrap); data handling with the standard software Xcalibur 2.2. (iii) LC-MS: Surveyor MS Plus HPLC (Thermo Electron) HPLC system connected to a TSQ Quantum Discovery Max (Thermo Electron) triple quadrupole mass spectrometer equipped with an electrospray (ESI) or APCI interface (Thermo Fisher Scientific, USA); connected to a PC running the standard software Xcalibur 2.0.7.

The pump flow rate was set to 600 µl/min and the analytes were separated on a Kinetex Phenyl-Hexyl analytical column 2.6 µm, 50x2.1 mm (Phenomenex, Germany).

Metabolite identification of compound 11b.

CYP1A1 and CYP1A2 incubates were screened for the presence of potential metabolites using LC-HRMS Q-Exactive (Thermo Scientific) instrument, combining high-performance quadrupole precursor selection with high resolution (up to 140,000) and accurate mass detection (Orbitrap™). The full scan accurate mass analysis of suspected metabolites was confirmed or refused using three primary tools: (i) screening for prototypical Phase I metabolites, (ii) predictive chemical formula and corresponding mass error analysis, and (iii) confirmation by product ion scan. The putative metabolites were identified based on the test item fragmentation pattern of compound **11b** and its corresponding characteristic fragments.

ASSOCIATED CONTENT

Supporting Information

Supporting information is available at http://pubs.acs.org

Synthesis of Bromo Derivative **44** (Scheme S1); Synthesis of Bromo Derivative **49** (Scheme S2); Synthesis of Compounds **3a-5a** and **3b-5b** (Scheme S3); Plasma Concentration of **7b** after a Single p.o. Dose of 5 mg/kg in Rats (Table S1); Brain Concentration of **7b** after a Single p.o. Dose of 5 mg/kg in Rats (Table S2); Plasma Concentration of **12b** after a Single p.o. Dose of 5 mg/kg in Rats (Table S3); Brain Concentration of **12b** after a Single p.o. Dose of 5 mg/kg in Rats (Table S4); Stability of Compound **11b** (5 μM) in Primary Mouse, Rat, Dog and Human Hepatocytes (n = 2) (Table S5); CYP1A1 and CYP1A2 Metabolites Identification of **11b** (Table S6); Proposed Metabolic Pathway for CYP-Dependent Metabolism of **11b** (Figure S1); Chromatogram of Compound **11b** Incubated with CYP1A1 (60 min) (Figure S2); Chromatogram of Compound **11b** Incubated with CYP1A1 (0 min) (Figure S3); Chromatogram of Compound **11b** Incubated with CYP1A2 (60 min) (Figure S4); Chromatogram of Compound **11b** Incubated with CYP1A2 (0 min) (Figure S5); Final Compounds SAR Studies: Activity Data and Standard Errors (SEM) (Table S7); Compounds for Modelling: Activity Data and Standard Errors (SEM) (Table S8); TREEspot Data Visualization of KINOMEScan Interactions of compound **12b**, PQR620 and INK128 (Figure S6); Selectivity Profile Calculated from KinomeScan Data (Table S9); Kinase Interactions (KINOMEscan data) (Table S10); 1H NMR Spectra; 13C{1H} NMR Spectra; NSI-HRMS Spectra; HPLC Chromatograms; Final Compounds (Chemical Structures); Intermediates (Chemical Structures).

Molecular formula strings (CSV)

Compound **3a**-PI3Kγ (PDB)

Compound **2a**-mTOR (PDB)

Compound **2b**-mTOR (PDB)

Compound **2a**-PI3Kα (PDB)

Compound **2b**-PI3Kα (PDB)

Accession Codes

PDB code 5JHB was used for docking of compound **3a** into PI3Kγ. PDB code 4JT6 was used for docking of compounds **2a** and **2b** into mTOR kinase. PDB code 3ZIM was used for docking of compounds **2a** and **2b** into PI3Kα.

AUTHOR INFORMATION

Corresponding Author

Matthias P. Wymann, Phone: +41 61 207 5046. Fax: +41 61 207 3566.

E-mail: Matthias.Wymann@UniBas.CH

Notes: conflicts of interest

ADA, FB, PHe, PHi, and DF are current or past employees of PIQUR Therapeutics AG, Basel; and PHe, DF, and MPW are shareholders of PIQUR Therapeutics AG.

The manuscript was written through contributions of all authors. All authors have given approval to the final version of the manuscript.

ACKNOWLEGEMENTS

We thank A. Pfaltz, J. Füglistaler, C. Meyer, J. Schwarte, and E. Teillet for advice, discussions and contributions to synthetic efforts; and S. Bünger for technical assistance.

Funding Sources

This work was supported by the Swiss Commission for Technology and Innovation (CTI) by PFLS-LS grants 14032.1, 15811.2, and 17241.1; the Stiftung für Krebsbekämpfung grant 341, Swiss National Science Foundation grants 310030_153211 and 316030_133860 (to MPW).

ABBREVIATIONS USED

mTOR, mechanistical (or mammalian) target of Rapamycin; TORC1, mTOR complex 1; TORC2, mTOR complex 2; PI3K: phosphoinositide 3-kinase, PKB, protein kinase B/Akt; S6RP, ribosomal protein S6; S6K, p70 S6 kinase; VPS34, vacuolar protein sorting 34 (the class III PI3K); TORKIs, mTOR kinase inhibitors; PK, pharmacokinetic; TR-FRET, time-resolved Förster resonance energy transfer.

REFERENCES

1. Wymann, M. P.; Schneiter, R., Lipid signalling in disease. *Nat Rev Mol Cell Biol* **2008,** *9* (2), 162-176.
2. Yang, H.; Rudge, D. G.; Koos, J. D.; Vaidialingam, B.; Yang, H. J.; Pavletich, N. P., mTOR kinase structure, mechanism and regulation. *Nature* **2013,** *497* (7448), 217-223.
3. Sarbassov, D. D.; Guertin, D. A.; Ali, S. M.; Sabatini, D. M., Phosphorylation and regulation of Akt/PKB by the rictor-mTOR complex. *Science* **2005,** *307* (5712), 1098-1101.
4. Feng, J.; Park, J.; Cron, P.; Hess, D.; Hemmings, B. A., Identification of a PKB/Akt hydrophobic motif Ser-473 kinase as DNA-dependent protein kinase. *J Biol Chem* **2004,** *279* (39), 41189-41196.
5. Wymann, M. P.; Marone, R., Phosphoinositide 3-kinase in disease: timing, location, and scaffolding. *Current Opinion in Cell Biology* **2005,** *17* (2), 141-149.
6. Bozulic, L.; Hemmings, B. A., PIKKing on PKB: regulation of PKB activity by phosphorylation. *Curr Opin Cell Biol* **2009,** *21* (2), 256-261.
7. Magnuson, B.; Ekim, B.; Fingar, D. C., Regulation and function of ribosomal protein S6 kinase (S6K) within mTOR signalling networks. *Biochem J* **2012,** *441* (1), 1-21.
8. Laplante, M.; Sabatini, D. M., mTOR signaling in growth control and disease. *Cell* **2012,** *149* (2), 274-93.
9. Saxton, R. A.; Sabatini, D. M., mTOR signaling in growth, metabolism, and disease. *Cell* **2017,** *168* (6), 960-976.
10. Vivanco, I.; Sawyers, C. L., The phosphatidylinositol 3-kinase AKT pathway in human cancer. *Nat Rev Cancer* **2002,** *2* (7), 489-501.
11. Marone, R.; Cmiljanovic, V.; Giese, B.; Wymann, M. P., Targeting phosphoinositide 3-kinase: moving towards therapy. *Biochim Biophys Acta* **2008,** *1784* (1), 159-185.
12. Wymann, M., PI3Ks—drug targets in inflammation and cancer. In *Phosphoinositides I: Enzymes of Synthesis and Degradation*, Balla, T.; Wymann, M.; York, J. D., Eds. Springer Netherlands: Dordrecht, **2012**, 111-181.
13. Choi, J.; Chen, J.; Schreiber, S. L.; Clardy, J., Structure of the FKBP1 2-rapamycin complex interacting with the binding domain of human FRAP. *Science* **1996,** *273* (5272), 239-242.
14. Hudes, G.; Carducci, M.; Tomczak, P.; Dutcher, J.; Figlin, R.; Kapoor, A.; Staroslawska, E.; Sosman, J.; McDermott, D.; Bodrogi, I.; Kovacevic, Z.; Lesovoy, V.; Schmidt-Wolf, I. G. H.; Barbarash, O.; Gokmen, E.; O'Toole, T.; Lustgarten, S.; Moore, L.; Motzer, R. J., Temsirolimus, interferon alfa, or both for advanced renal-cell carcinoma. *N Engl J Med* **2007,** *356* (22), 2271-2281.

15. Motzer, R. J.; Escudier, B.; Oudard, S.; Hutson, T. E.; Porta, C.; Bracarda, S.; Grünwald, V.; Thompson, J. A.; Figlin, R. A.; Hollaender, N.; Urbanowitz, G.; Berg, W. J.; Kay, A.; Lebwohl, D.; Ravaud, A., Efficacy of everolimus in advanced renal cell carcinoma: a double-blind, randomised, placebo-controlled phase III trial. *The Lancet* **2008,** *372* (9637), 449-456.
16. Jerusalem, G.; Rorive, A.; Collignon, J., Use of mTOR inhibitors in the treatment of breast cancer: an evaluation of factors that influence patient outcomes. *Breast Cancer (Dove Med Press)* **2014,** *6*, 43-57.
17. André, F.; O'Regan, R.; Ozguroglu, M.; Toi, M.; Xu, B.; Jerusalem, G.; Masuda, N.; Wilks, S.; Arena, F.; Isaacs, C.; Yap, Y.-S.; Papai, Z.; Lang, I.; Armstrong, A.; Lerzo, G.; White, M.; Shen, K.; Litton, J.; Chen, D.; Zhang, Y.; Ali, S.; Taran, T.; Gianni, L., Everolimus for women with trastuzumab-resistant, HER2-positive, advanced breast cancer (BOLERO-3): a randomised, double-blind, placebo-controlled phase 3 trial. *The Lancet Oncology* **2014,** *15* (6), 580-591.
18. Peterson, M. E., Management of adverse events in patients with hormone receptor-positive breast cancer treated with everolimus: observations from a phase III clinical trial. *Supportive care in cancer : official journal of the Multinational Association of Supportive Care in Cancer* **2013,** *21* (8), 2341-2349.
19. Santulli, G.; Totary-Jain, H., Tailoring mTOR-based therapy: molecular evidence and clinical challenges. *Pharmacogenomics* **2013,** *14* (12), 1517-1526.
20. Meng, L. H.; Zheng, X. F., Toward rapamycin analog (rapalog)-based precision cancer therapy. *Acta Pharmacol Sin* **2015,** *36* (10), 1163-1169.
21. Feldman, M. E.; Apsel, B.; Uotila, A.; Loewith, R.; Knight, Z. A.; Ruggero, D.; Shokat, K. M., Active-site inhibitors of mTOR target rapamycin-resistant outputs of mTORC1 and mTORC2. *PLoS Biol* **2009,** *7* (2), e38.
22. Kang, S. A.; Pacold, M. E.; Cervantes, C. L.; Lim, D.; Lou, H. J.; Ottina, K.; Gray, N. S.; Turk, B. E.; Yaffe, M. B.; Sabatini, D. M., mTORC1 phosphorylation sites encode their sensitivity to starvation and rapamycin. *Science* **2013,** *341* (6144), 1236566.
23. Jacinto, E.; Loewith, R.; Schmidt, A.; Lin, S.; Ruegg, M. A.; Hall, A.; Hall, M. N., Mammalian TOR complex 2 controls the actin cytoskeleton and is rapamycin insensitive. *Nat Cell Biol* **2004,** *6* (11), 1122-8.
24. O'Reilly, K. E.; Rojo, F.; She, Q. B.; Solit, D.; Mills, G. B.; Smith, D.; Lane, H.; Hofmann, F.; Hicklin, D. J.; Ludwig, D. L.; Baselga, J.; Rosen, N., mTOR inhibition induces upstream receptor tyrosine kinase signaling and activates Akt. *Cancer Res* **2006,** *66* (3), 1500-1508.
25. Liu, P.; Gan, W.; Chin, Y. R.; Ogura, K.; Guo, J.; Zhang, J.; Wang, B.; Blenis, J.; Cantley, L. C.; Toker, A.; Su, B.; Wei, W., PtdIns(3,4,5)P3-dependent activation of the mTORC2 kinase complex. *Cancer Discov* **2015,** *5* (11), 1194-1209.
26. Nowak, P.; Cole, D. C.; Brooijmans, N.; Bursavich, M. G.; Curran, K. J.; Ellingboe, J. W.; Gibbons, J. J.; Hollander, I.; Hu, Y.; Kaplan, J.; Malwitz, D. J.; Toral-Barza, L.; Verheijen, J. C.; Zask, A.; Zhang, W. G.; Yu, K., Discovery of potent and selective inhibitors of the mammalian target of rapamycin (mTOR) kinase. *J Med Chem* **2009,** *52* (22), 7081-7089.
27. Jin, Z.; Niu, H.; Wang, X.; Zhang, L.; Wang, Q.; Yang, A., Preclinical study of CC223 as a potential anti-ovarian cancer agent. *Oncotarget* **2017,** *8* (35), 58469-58479.
28. Slotkin, E. K.; Patwardhan, P. P.; Vasudeva, S. D.; de Stanchina, E.; Tap, W. D.; Schwartz, G. K., MLN0128, an ATP-competitive mTOR kinase inhibitor with potent in vitro and in vivo antitumor activity, as potential therapy for bone and soft-tissue sarcoma. *Mol Cancer Ther* **2015,** *14* (2), 395-406.

29. Pike, K. G.; Malagu, K.; Hummersone, M. G.; Menear, K. A.; Duggan, H. M.; Gomez, S.; Martin, N. M.; Ruston, L.; Pass, S. L.; Pass, M., Optimization of potent and selective dual mTORC1 and mTORC2 inhibitors: the discovery of AZD8055 and AZD2014. *Bioorg Med Chem Lett* **2013,** *23* (5), 1212-1216.
30. Lee, J. S.; Vo, T. T.; Fruman, D. A., Targeting mTOR for the treatment of B cell malignancies. *Br J Clin Pharmacol* **2016,** *82* (5), 1213-1228.
31. Rageot, D.; Bohnacker, T.; Melone, A.; Langlois, J. B.; Borsari, C.; Hillmann, P.; Sele, A. M.; Beaufils, F.; Zvelebil, M.; Hebeisen, P.; Loscher, W.; Burke, J.; Fabbro, D.; Wymann, M. P., Discovery and preclinical characterization of 5-[4,6-Bis({3-oxa-8-azabicyclo[3.2.1]octan-8-yl})-1,3,5-triazin-2-yl]-4-(difluoro methyl)pyridin-2-amine (PQR620), a highly potent and selective mTORC1/2 inhibitor for cancer and neurological disorders. *J Med Chem* **2018,** *61* (22), 10084-10105.
32. Bohnacker, T.; Prota, A. E.; Beaufils, F.; Burke, J. E.; Melone, A.; Inglis, A. J.; Rageot, D.; Sele, A. M.; Cmiljanovic, V.; Cmiljanovic, N.; Bargsten, K.; Aher, A.; Akhmanova, A.; Diaz, J. F.; Fabbro, D.; Zvelebil, M.; Williams, R. L.; Steinmetz, M. O.; Wymann, M. P., Deconvolution of Buparlisib's mechanism of action defines specific PI3K and tubulin inhibitors for therapeutic intervention. *Nat Commun* **2017,** *8*, 14683.
33. Beaufils, F.; Cmiljanovic, N.; Cmiljanovic, V.; Bohnacker, T.; Melone, A.; Marone, R.; Jackson, E.; Zhang, X.; Sele, A.; Borsari, C.; Mestan, J.; Hebeisen, P.; Hillmann, P.; Giese, B.; Zvelebil, M.; Fabbro, D.; Williams, R. L.; Rageot, D.; Wymann, M. P., 5-(4,6-Dimorpholino-1,3,5-triazin-2-yl)-4-(trifluoromethyl)pyridin-2-amine (PQR309), a potent, brain-penetrant, orally bioavailable, pan-class I PI3K/mTOR inhibitor as clinical candidate in oncology. *J Med Chem* **2017,** *60* (17), 7524-7538.
34. Tarantelli, C.; Gaudio, E.; Arribas, A. J.; Kwee, I.; Hillmann, P.; Rinaldi, A.; Cascione, L.; Spriano, F.; Bernasconi, E.; Guidetti, F.; Carrassa, L.; Pittau, R. B.; Beaufils, F.; Ritschard, R.; Rageot, D.; Sele, A.; Dossena, B.; Rossi, F. M.; Zucchetto, A.; Taborelli, M.; Gattei, V.; Rossi, D.; Stathis, A.; Stussi, G.; Broggini, M.; Wymann, M. P.; Wicki, A.; Zucca, E.; Cmiljanovic, V.; Fabbro, D.; Bertoni, F., PQR309 is a novel dual PI3K/mTOR inhibitor with preclinical antitumor activity in lymphomas as a single agent and in combination therapy. *Clin Cancer Res* **2018,** *24* (1), 120-129.
35. Wicki, A.; Brown, N.; Xyrafas, A.; Bize, V.; Hawle, H.; Berardi, S.; Cmiljanovic, N.; Cmiljanovic, V.; Stumm, M.; Dimitrijevic, S.; Herrmann, R.; Pretre, V.; Ritschard, R.; Tzankov, A.; Hess, V.; Childs, A.; Hierro, C.; Rodon, J.; Hess, D.; Joerger, M.; von Moos, R.; Sessa, C.; Kristeleit, R., First-in human, phase 1, dose-escalation pharmacokinetic and pharmacodynamic study of the oral dual PI3K and mTORC1/2 inhibitor PQR309 in patients with advanced solid tumors (SAKK 67/13). *Eur J Cancer* **2018,** *96*, 6-16.
36. Fang, Z.; Song, Y.; Zhan, P.; Zhang, Q.; Liu, X., Conformational restriction: an effective tactic in 'follow-on'-based drug discovery. *Future Med Chem* **2014,** *6* (8), 885-901.
37. Cmiljanovic, V.; Hebeisen, P.; Jackson, E.; Beaufils, F.; Bohnacker, T.; Wymann, M. P. Conformationally restricted PI3K and mTOR inhibitors. **2015**, WO2015049369.
38. Leroux, F. R.; Manteau, B.; Vors, J. P.; Pazenok, S., Trifluoromethyl ethers--synthesis and properties of an unusual substituent. *Beilstein J Org Chem* **2008,** *4*, 13.
39. Burger, M. T.; Pecchi, S.; Wagman, A.; Ni, Z. J.; Knapp, M.; Hendrickson, T.; Atallah, G.; Pfister, K.; Zhang, Y.; Bartulis, S.; Frazier, K.; Ng, S.; Smith, A.; Verhagen, J.; Haznedar, J.; Huh, K.; Iwanowicz, E.; Xin, X.; Menezes, D.; Merritt, H.; Lee, I.; Wiesmann, M.; Kaufman, S.; Crawford, K.; Chin, M.; Bussiere, D.; Shoemaker, K.; Zaror, I.; Maira, S. M.; Voliva, C. F., Identification of NVP-BKM120 as a

potent, selective, orally bioavailable class I PI3 Kinase inhibitor for treating cancer. *ACS Med Chem Lett* **2011,** *2* (10), 774-779.

40. Rousseau, J. F.; Chekroun, I.; Ferey, V.; Labrosse, J. R., Concise preparation of a stable cyclic sulfamidate intermediate in the synthesis of a enantiopure chiral active diamine derivative. *Organic Process Research & Development* **2015,** *19* (4), 506-513.
41. Brown, G. R.; Foubister, A. J.; Wright, B., Chiral synthesis of 3-substituted morpholines via serine enantiomers and reductions of 5-oxomorpholine-3-carboxylates. *Journal of the Chemical Society, Perkin Transactions 1* **1985**, 2577-2580.
42. Hebeisen, P.; Alker, A.; Buerkler, M., Iterative one pot reactions of a chiral sulfamidate with 2,4,6-trichloropyridine: regiocontrolled synthesis of linear and angular chiral dipyrrolidino pyridines. *Heterocycles* **2012,** *85* (1), 65-72.
43. Zask, A.; Kaplan, J.; Verheijen, J. C.; Richard, D. J.; Curran, K.; Brooijmans, N.; Bennett, E. M.; Toral-Barza, L.; Hollander, I.; Ayral-Kaloustian, S.; Yu, K., Morpholine derivatives greatly enhance the selectivity of mammalian target of rapamycin (mTOR) inhibitors. *J Med Chem* **2009,** *52* (24), 7942-7945.
44. Thomas, V. H.; Bhattachar, S.; Hitchingham, L.; Zocharski, P.; Naath, M.; Surendran, N.; Stoner, C. L.; El-Kattan, A., The road map to oral bioavailability: an industrial perspective. *Expert Opinion on Drug Metabolism & Toxicology* **2006,** *2* (4), 591-608.
45. Mortensen, D. S.; Fultz, K. E.; Xu, S.; Xu, W.; Packard, G.; Khambatta, G.; Gamez, J. C.; Leisten, J.; Zhao, J.; Apuy, J.; Ghoreishi, K.; Hickman, M.; Narla, R. K.; Bissonette, R.; Richardson, S.; Peng, S. X.; Perrin-Ninkovic, S.; Tran, T.; Shi, T.; Yang, W. Q.; Tong, Z.; Cathers, B. E.; Moghaddam, M. F.; Canan, S. S.; Worland, P.; Sankar, S.; Raymon, H. K., CC-223, a potent and selective inhibitor of mTOR kinase: in vitro and in vivo characterization. *Mol Cancer Ther* **2015,** *14* (6), 1295-1305.
46. Nosik, P. S.; Ryabukhin, S. V.; Artamonov, O. S.; Grygorenko, O. O., Synthesis of trans-disubstituted pyrazolylcyclopropane building blocks. *Monatshefte Fur Chemie* **2016,** *147* (9), 1629-1636.
47. Zhang, L.; Luo, S.; Mi, X.; Liu, S.; Qiao, Y.; Xu, H.; Cheng, J. P., Combinatorial synthesis of functionalized chiral and doubly chiral ionic liquids and their applications as asymmetric covalent/non-covalent bifunctional organocatalysts. *Org Biomol Chem* **2008,** *6* (3), 567-576.
48. Fabian, M. A., Biggs, W. H., Treiber, D. K., Atteridge, C. E., Azimioara, M. D., Benedetti, M. G., Carter, T. A., Ciceri, P., Edeen, P. T., Floyd, M., Ford, J. M., Galvin, M., Gerlach, J. L., Grotzfeld, R. M., Herrgard, S., Insko, D. E., Insko, M. A., Lai, A. G., Lélias, J. M., Mehta, S. A., Milanov, Z. V., Velasco, A. M., Wodicka, L. M., Patel, H. K., Zarrinkar, P. P., Lockhart, D. J. A small molecule-kinase interaction map for clinical kinase inhibitors. *Nat Biotechnol* **2005**, *23*, 329-336.
49. Karaman, M. W., Herrgard, S., Treiber, D. K., Gallant, P., Atteridge, C. E., Campbell, B. T., Chan, K. W., Ciceri, P., Davis, M. I., Edeen, P. T., Faraoni, R., Floyd, M., Hunt, J. P., Lockhart, D. J., Milanov, Z. V., Morrison, M. J., Pallares, G., Patel, H. K., Pritchard, S., Wodicka, L. M., Zarrinkar, P. P. A quantitative analysis of kinase inhibitor selectivity. *Nat Biotechnol* **2008**, *26*, 127-132.

For Table of Contents Use Only.